MIT-2073-1
(MITNE-51)

FUEL CYCLE ANALYSIS IN A THORIUM FUELED REACTOR USING BIDIRECTIONAL FUEL MOVEMENT

by
FERDINAND HOFMANN

JUNE 1964

DEPARTMENT OF NUCLEAR ENGINEERING
MASSACHUSETTS INSTITUTE OF TECHNOLOGY
CAMBRIDGE, MASSACHUSETTS

WORK PERFORMED UNDER CONTRACT NO. AT(30-1)-2073
WITH THE
NEW YORK OPERATIONS OFFICE
U. S. ATOMIC ENERGY COMMISSION

DISTRIBUTION

This report is being distributed under the category "Reactor Technology," TID 4500. Additional copies may be obtained from USAEC Division of Technical Information Extension (DTIE), P.O. Box 62, Oak Ridge, Tennessee.

Previous reports on this project:

NYO-2131 MITNE-1
NYO-9715 MITNE-10

LEGAL NOTICE

MIT-2073-1

MITNE-51

FUEL CYCLE ANALYSIS IN A THORIUM FUELED REACTOR USING BIDIRECTIONAL FUEL MOVEMENT

by

Ferdinand Hofmann

DEPARTMENT OF NUCLEAR ENGINEERING

MASSUCHUSETTS INSTITUTE OF TECHNOLOGY

CAMBRIDGE, MASSACHUSETTS

June, 1964

Work performed under Contract No. AT(30-1)-2073

with the

New York Operations Office

U.S. Atomic Energy Commission

PREFACE

This report extends to a reactor fueled with a mixture of U^{233}, U^{235}, and thorium some of the techniques for fuel-cycle analysis which were developed at MIT for reactors fueled with mixtures of U^{235}, plutonium, and U^{238}.

The contents of this report were submitted by the author in partial fulfillment of the requirements for the degree of Master of Science in Nuclear Engineering at the Massachusetts Institute of Technology, in June, 1964.

The author wishes to thank Dr Manson Benedict and Dr. Edward A. Mason for their help and guidance as his thesis supervisors.

He also appreciates the assistance received from Jerry A. Sovka and Max C. Richardson.

The work was performed under Contract AT(30-1)-2073 with the U.S. Atomic Energy Commission. The financial support afforded by that contract is gratefully acknowledged.

This work was done in part at the MIT Computation Center, Cambridge, Massachusetts.

FUEL CYCLE ANALYSIS IN A THORIUM FUELED REACTOR USING BIDIRECTIONAL FUEL MOVEMENT

by

Ferdinand Hofmann

Submitted to the Department of Nuclear Engineering on May 22, 1964 in partial fulfillment of the requirements for the degree of Master of Science.

ABSTRACT

A computer code has been written for an IBM 7090/7094 computer to investigate the equilibrium fuel cycle of a thorium fueled CANDU-type reactor having a radial blanket. The U-233 fuel which is bred in core and blanket is assumed to be recycled continuously (along with all the higher uranium isotopes contained in it). The blanket is fed with pure ThO_2. For a conversion ratio less than unity, a certain amount of U-235 makeup is required to keep the reactor critical. The equilibrium fuel cycle is then characterized by the fact that all nuclides have reached their equilibrium concentrations.

The code has been used to study the effects of five important variables on the performance of the reactor. The five variables are: the blanket thickness, the lattice pitch, the average fuel burnup, the maximum linear power, and the recycle losses.

If all five variables are set equal to the corresponding CANDU design parameters, and a recycle loss of 2.0 % is assumed, an overall conversion ratio of 0.789 results. The maximum possible overall conversion ratio which could be achieved by varying the five parameters is 0.924. This value, however, applies to a reactor with a very low power output and a low fuel burnup. The conversion ratio of a CANDU-type reactor could possibly be raised above unity by adding an axial blanket and decreasing the amount of zirconium in the core (pressure vessel design).

Thesis Supervisor: Dr. Manson Benedict
Title: Professor of Nuclear Engineering

Thesis Supervisor: Dr. Edward A. Mason
Title: Professor of Nuclear Engineering

Table of Contents

List of Figures

List of Tables

I. Introduction and Summary

Although the Th-U^{233} cycle has not been used for power reactors as widely as the U-Pu cycle, its use in the long run will certainly be essential to the conservation of fissionable materials. The main reasons for this are:

1. The total amount of thorium on earth is about three times as large as the total amount of uranium (W2).

2. The nuclear properties of U^{233} allow breeding over a wider neutron energy range than do the properties of Pu^{239} or U^{235}. In fact, the Th-U^{233} cycle is the only known way to breed in a thermal reactor.

The purpose of this study is to analyze some of the characteristics of the Th-U^{233} cycle in a heavy water moderated thermal reactor.

To this end, a computer code has been written, based on the reactor physics model of Shanstrom (S1) and Neill (N1).

1.1. The Reactor

The analysis will be limited to one particular reactor design, namely the CANDU reactor which is being built at the Douglas Point site on the eastern shore of Lake Huron, Ontario, Canada.

CANDU is a pressure tube reactor using natural uranium as a fuel (in the form of UO_2), heavy water as a moderator and coolant, and zirconium as the principal structural material (cladding, pressure tubes, etc.). It is designed for on-load push-through fueling. The fuel in alternate channels moves through the reactor in opposite directions in order to maintain flux symmetry.

All non-fuel materials used in the CANDU reactor have a very low absorption cross section for thermal neutrons. The neutron economy is therefore excellent. It is for this reason that CANDU was chosen as a reference design for this study. The reactor analyzed here differs from the CANDU reactor only in the following three points:

1. A different fuel is used (a mixture of UO_2 and ThO_2 instead of natural UO_2),
2. a radial blanket is added (the blanket channels are fueled with pure ThO_2),
3. the spacing between the channels (pitch) may be different from that used in CANDU.

In addition, the following three parameters are considered as variables:

4. BURNUP, the average fuel burnup in the core (in MWD/tonne),
5. PDNLM, the maximum linear power (in kw per cm of fuel bundle),
6. ROSS, the reprocessing and fabricating losses (%).

Since the fuel composition (item 1. above) is entirely determined by the equilibrium conditions (Chapter II., sect. 10.), we are left with the following five independent variables:

1.2. The Five Variables

1.2.1. BR, the outside radius of the blanket

The incentive for adding a blanket is, of course, the possibility of improving the neutron economy of the system by increasing the number of neutrons captured in fertile material and decreasing the number of neutrons lost through leakage.

In order to keep the number of variables within certain limits, only the outside radius of the blanket (BR) is considered an independent variable. The core radius, the core height, and the outside radius of the reflector are kept constant.

However, the code is written in such a way as to permit variation of all physical dimensions of the reactor.

1.2.2. VFL, the fuel volume fraction in the unit cell

Varying the fuel volume fraction is equivalent to changing the spacing between the fuel channels (i.e., the pitch), because the size and geometry of the fuel channel is fixed.

For higher values of VFL, there will be less moderator in the core, and, consequently, the neutron energy spectrum will be harder.

In the U-Pu cycle, a well-thermalized spectrum is necessary to achieve a high conversion ratio. In the Th-U^{233} cycle, however, this requirement is not as stringent because the decrease in η in the epithermal energy region is much less severe for U^{233} than it is for U^{235} or Pu^{239}.

1.2.3. BURNUP, the average fuel burnup in the core

The average fuel burnup determines the concentration of low-cross-section fission products in the fuel. From the point of view of neutron economy, a low burnup seems to be desirable. From the point of view of fuel reprocessing and fabricating costs, however, a high average burnup is much more attractive.

The maximum allowable burnup depends on the metallurgical properties of the fuel, and is, therefore, a given constant, so that a low ratio of maximum to average burnup is desirable in any case.

In a CANDU-type reactor, this ratio depends on the relative velocities at which the fuel travels through the various channels.

The following three options are available in the code:

1. Constant velocity in all channels (in the core),

2. specified velocity distribution,
3. computed velocity distribution for constant burnup in all channels (in the core).

In all three cases, BURNUP is interpreted as the average burnup of the fuel in the reactor core.

The velocity (and, hence, the burnup) in the blanket channels can be specified by choosing a discharge flux-time (which is assumed constant for all blanket channels).

1.2.4. PDNLM, the maximum linear power

The maximum power per unit length of fuel bundle determines the flux level and, hence, the Pa^{233} concentration in the reactor. Neutron capture in Pa^{233} severely affects the conversion ratio, because each neutron captured in Pa^{233} represents a double loss: not only the neutron, but also a potential U^{233} atom is lost.

Again, for high conversion ratio, a low flux (i.e. a low power density) is desirable, but for low power cost, a high power density is necessary.

1.2.5. ROSS, the reprocessing and fabricating losses

It is assumed that a certain fraction of the fuel which is discharged from the reactor will be lost in reprocessing spent fuel and fabricating new fuel. That fraction is denoted by ROSS. It has a great influence on the equilibrium concentration of the higher isotopes.

Higher uranium isotopes are produced from U^{233} by successive neutron captures. They are removed from the system in two ways:

1. Conversion to Np^{237} followed by separation of Np^{237} from uranium in reprocessing,

2. reprocessing and fabricating losses.

The second of these two processes is usually (e.g., for ROSS = 2%) more effective than the first, so that ROSS actually controls the concentration and, hence, the poisoning effect of the higher isotopes.

The above list of variables is by no means exhaustive. A complete analysis would involve the investigation of at least 20 variables. It is felt, however, that the five parameters considered here represent some of the most important factors which determine the fuel cycle behaviour of a nuclear reactor system operating on the Th-U^{233} cycle.

1.3. Results

As a starting point for the investigation, a "standard" set of variables is defined. This "standard case" is characterized by the following numbers:

Blanket radius, BR	= 255.0 cm
Fuel volume fraction, VFL	= 0.0567
Average burnup in core, BURNUP	= 10,000 MWD/tonne
Maximum linear power, PDNLM	= 8.712 kw/cm
Recycle loss, ROSS	= 2.0 %

All other geometric parameters are kept constant. They are the same as in the CANDU reactor:

Core radius, R	= 225.61 cm
Outside radius of reflector	= 299.70 cm
Core height, CH	= 500.40 cm
Fuel channel geometry	see Appendix 2

It follows that the blanket thickness in the "standard" case is 29.39 cm.

The "standard case" is identical with the CANDU design except for the radial blanket thickness, which is 0 in CANDU.

Table I.1., Effects of the "Five Variables" on Performance of Thorium Fueled CANDU Reactor (Summary)

Radial Blanket Thickness, cm	Volume Fraction Fuel	Average Burnup, MWD/tonne	Maximum Linear Power, kw/cm	% Fuel Loss in Recycle	Transit Time of Fuel (in Core), Full-Power Days	Overall Conversion Ratio	Thermal Power, MW
0*	0.0567*	10,000	8.712*	2.0	497.9	0.7888	752.1
14.39	0.0567	10,000	8.712	2.0	584.6	0.8300	643.7
29.39**	0.0567**	10,000**	8.712**	2.0**	587.3**	0.8430**	639.3**
44.39	0.0567	10,000	8.712	2.0	581.8	0.8476	644.0
29.39	0.0167	10,000	8.712	2.0	633.2	0.8293	174.3
29.39	0.0267	10,000	8.712	2.0	615.3	0.8829	286.3
29.39	0.0367	10,000	8.712	2.0	601.2	0.8852	402.9
29.39	0.0467	10,000	8.712	2.0	594.1	0.8675	519.2
29.39	0.0667	10,000	8.712	2.0	572.2	0.8106	769.1
29.39	0.0567	4,000	8.712	2.0	254.8	0.8395	568.6
29.39	0.0567	6,000	8.712	2.0	372.5	0.8488	603.9
29.39	0.0567	8,000	8.712	2.0	482.6	0.8476	622.0
29.39	0.0567	12,000	8.712	2.0	675.1	0.8353	665.3
29.39	0.0567	10,000	4.712	2.0	1156.7	0.8711	323.7
29.39	0.0567	10,000	6.712	2.0	791.3	0.8560	473.7
29.39	0.0567	10,000	10.712	2.0	455.8	0.8300	820.9
29.39	0.0567	10,000	12.712	2.0	374.8	0.8198	999.5
29.39	0.0567	10,000	8.712	1.0	578.4	0.8411	647.5
29.39	0.0567	10,000	8.712	1.5	583.0	0.8432	643.0
29.39	0.0567	10,000	8.712	2.5	590.1	0.8398	635.2
29.39	0.0567	10,000	8.712	3.0	592.9	0.8363	632.5

* = Values in CANDU design, ** = "Standard case"

A summary of the principal results of all 21 computer runs (which are analyzed in detail in Chap. III.) is presented in Table I.1. The following trends are apparent:

Blanket Thickness

The conversion ratio increases with increasing blanket thickness. This is due to a decrease in the number of neutrons lost through leakage, and a corresponding increse in the number of captures in fertile material. If the blanket thickness is increased beyond ~ 30 cm, the additional gain in conversion ratio is very small.

The blanket thickness also affects the flux shape (see Figs. III.6. and III.8.) and, hence the ratio of maximum to average power density in the core. Since this ratio increases with increasing blanket thickness, and since the maximum power density is fixed (it is determined by the maximum linear power and the fuel volume fraction), the total thermal power decreases with increasing blanket thickness. For the thickest blanket (44.39 cm), the total power in the blanket amounts to 0.104 % of the total power in the core.

Fuel Volume Fraction

As the fuel volume fraction is decreased from the "standard" value (=0.0567), the conversion ratio increases first. This is caused by a softening of the neutron energy

spectrum (see Fig.III.10.) and a corresponding increase in the average η values for U^{233} and U^{235}. Decreasing the fuel volume fraction also increases the mean free path of the neutrons and, hence, the leakage. This second effect, which tends to decrease the conversion ratio, eventually predominates, and, consequently, the conversion ratio goes through a maximum (at VFL = 0.035, Fig.III.2).

The thermal power is roughly proportional to the fuel volume fraction.

Average Burnup

The overall conversion ratio (which includes the recycle losses) is affected in two ways by the average burnup: high burnups tend to lower the conversion ratio due to fission product poisoning, very low burnups also decrease the conversion ratio because the frequency of reprocessing is increased. For a given recycle loss (here 2.0 %), the overall conversion ratio (CR_L) as a function of burnup reaches therefore a maximum (at 7,000 MWD/tonne, Fig.III.3.).

As the average burnup is increased, the total thermal power increases due to a decreasing ratio of maximum to average power density which, in turn, is caused by an increasing amount of flux flattening.

Maximum Linear Power

The conversion ratio steadily decreases as the maximum

linear power is increased. The reason for this is that the Pa^{233} concentration in the core is essentially proportional to the thermal flux (see Fig.III.13.) and, hence, to the power density. Neutron captures in Pa^{233} severely affect the conversion ratio not only because the parasitic absorption is increased, but also because potential fissionable material (U^{233}) is lost.

The total power is roughly proportional to the maximum linear power.

Recycle Loss

The recycle loss affects the performance of the system in two ways: a high loss rate obviously tends to decrease the conversion ratio, on the other hand, for low recycle losses. the higher isotopes build up to very high concentrations so that the conversion ratio is again decreased. The two effects nearly balance each other (Fig.III.5.).

The total thermal power is only slightly affected by the recycle losses.

It is seen from the above discussion that the "five variables" have a considerable influence on the performance, and especially on the conversion ratio, of the system. The question arises therefore as to whether these five parameters could be so chosen that the conversion ratio would be greater than unity.

In order to estimate the combined effects of all the

variables, we may write the conversion ratio as

$$CR = CR_o + f_1(BR) + f_2(VFL) + f_3(BURNUP) + f_4(PDNLM) + f_5(ROSS)$$

where CR_o is the conversion ratio for "standard conditions", and each f expresses the change in conversion ratio caused by changing one of the variables from its standard value, all other variables remaining constant. The maximum conversion ratio is then found simply by taking the maximum of each f.

Applying this treatment to the data given in Table I.1. yields a maximum overall conversion ratio, $CR_{L,max} = 0.924$. The subscript "L" indicates that the recycle losses are taken into account, as in Eq. (2.11.2).

The maximum conversion ratio of the reactor itself (including core and blanket, but not the recycle losses) as defined by Eq. (2.11.1), is found in a similar way. The result is: $CR_{max} = 0.986$.

By making radical changes from the mechanical design of the CANDU reactor, as by eliminating pressure tubes and adding axial blankets, it would be possible to increase the conversion ratio further, thus possibly achieving breeding.

It should be borne in mind, however, that high conversion ratios necessarily require low power densities (as for example half of the CANDU design value) and low fuel burnups (as for example 6000 MWD/tonne), which cannot be tolerated if economic nuclear power is to be produced.

A more detailed discussion of the results is given in Chapters III. and IV.

II. Description of Code

2.1. The Neutron Cycle

A schematic diagram of the neutron cycle is shown in Fig.II.1.

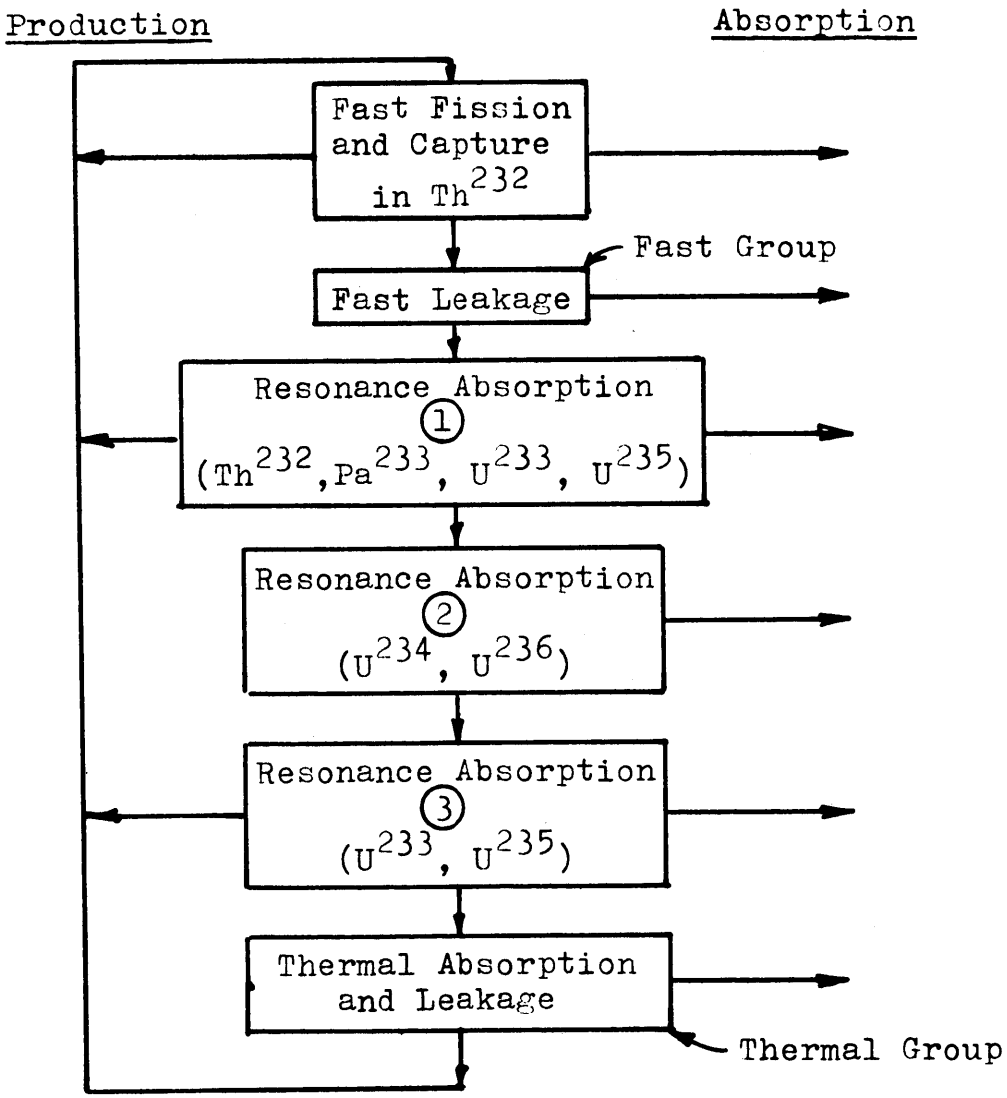

Fig.II.1., The Neutron Cycle

The above model is essentially the same as the one used

by Neill (N1) except that the resonance absorption in U^{233} and U^{235} is now allowed to take place both below and above the resonances in U^{234} and U^{236} ($\sim$ 5 ev). Neill assumed that resonance absorption in the two fissionable nuclides occurred strictly below 5 ev.

2.1.1. Fast Fission and Capture in Th^{232}

The total number of fast neutrons produced per unit time per unit volume is, by definition, equal to the slowing down density q at fission energy. Hence, the number of fast neutrons produced by thermal and resonance fissions must be q/ε.

Considering the fast effect only, we have the following situation:

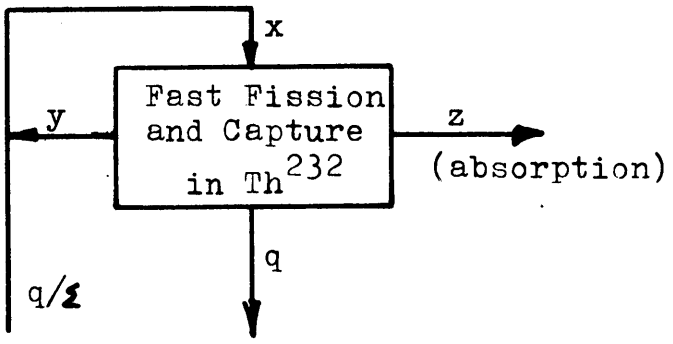

Fig.II.2., The Fast Effect

where $\frac{y}{z} = \eta_1$, $x = \frac{q}{\varepsilon} + y$, $x = q + z$, and η_1 is the number of neutrons produced per fast neutron absorbed in

Th^{232}. Solving for x, y, and z yields

$$x = \frac{q(\varepsilon \eta_1 - 1)}{\varepsilon(\eta_1 - 1)} \qquad (2.1.1)$$

$$y = \frac{\eta_1 \, q(\varepsilon - 1)}{\varepsilon(\eta_1 - 1)} \qquad (2.1.2)$$

$$z = \frac{q(\varepsilon - 1)}{\varepsilon(\eta_1 - 1)} \qquad (2.1.3)$$

2.1.2. The Fast Group

The diffusion equation for the fast group is

$$D_1 \nabla^2 \phi_1 - \Sigma_1 \phi_1 + q = 0 \qquad (2.1.4)$$

The fast leakage is equal to $- D_1 \nabla^2 \phi_1$. For convenience this is written as $q(1 - P_1)$, where P_1 is the fast non-leakage probability. We therefore have the following picture for the fast group:

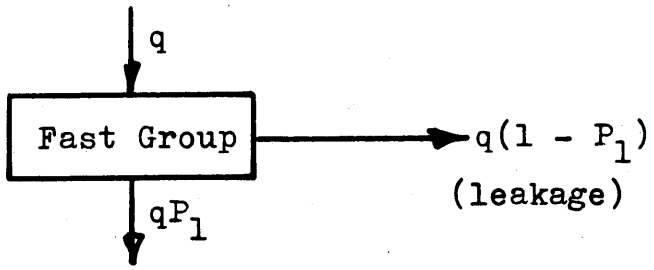

Fig.II.3. The Fast Group

2.1.3. Resonance Region (1)

Here, concurrent resonance absorption takes place in Th^{232}, Pa^{233}, U^{233}, and U^{235}. The effect is a reduction in the slowing down density and a production of resonance fission neutrons. The number of neutrons absorbed is equal to $qP_1(1 - p_1p_2p_7p_9)$, where

p_1 = resonance escape probability for Th^{232}
p_2 = resonance escape probability for Pa^{233}
p_7 = resonance escape probability for U^{233} (above 5 ev)
p_9 = resonance escape probability for U^{235} (above 5 ev)

(For the calculation of these resonance escape probabilities refer to Eq. 2.4.1.)

The number of neutrons produced equals

$$qP_1\left[\langle 1-p\rangle_7 \eta_7 + \langle 1-p\rangle_9 \eta_9\right],$$

where η_7 is the number of fast neutrons produced per neutron absorbed in U^{233} (epithermal neutrons above 5 ev), and η_9 is the same quantity for U^{235}. $\langle 1-p\rangle_7$ and $\langle 1-p\rangle_9$ are defined by Eq.2.4.5.

A schematic diagram of the resonance region (1) is shown in Fig.II.4., on the following page.

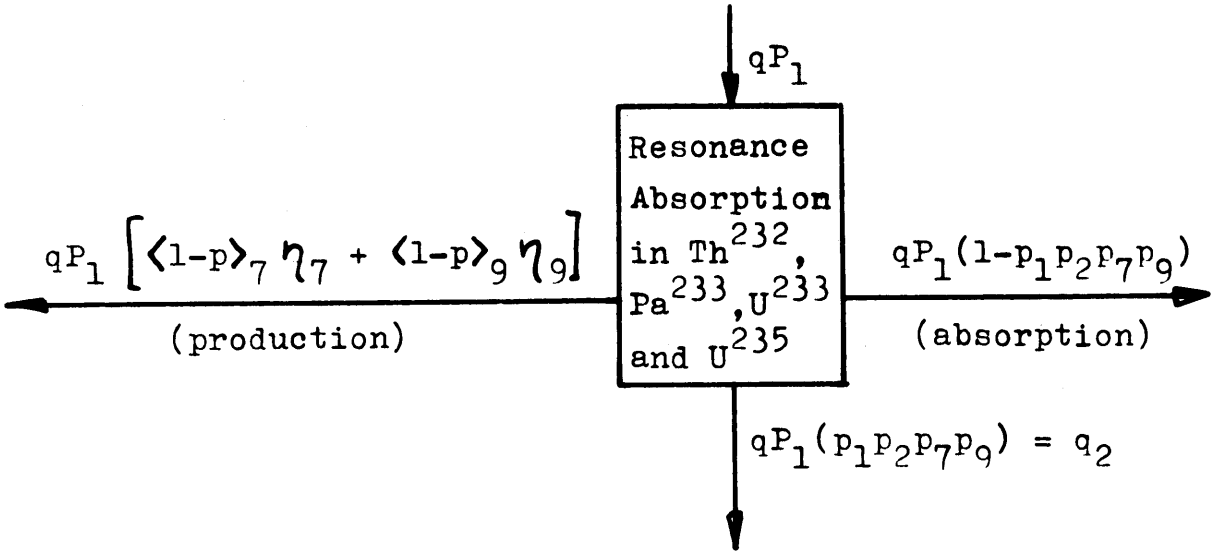

Fig.II.4., The Resonance Region ①

2.1.4. Resonance Region ②

The total number of resonance neutrons absorbed by U^{234} and U^{236} is equal to $q_2(1 - p_4p_6)$, where p_4 and p_6 are the resonance escape probabilities for U^{234} and U^{236}, respectively.

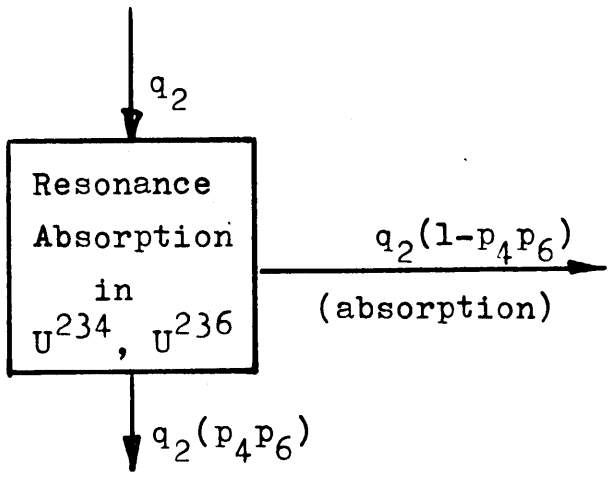

Fig.II.5., The Resonance Region ②

2.1.5. Resonance Region ③

Again, the number of epithermal neutrons lost is given by $q_2\ p_4 p_6 (1 - p_3 p_5)$, where p_3 and p_5 are the resonance escape probabilities for U^{233} and U^{235} (below 5 ev). The net number of neutrons produced is

$q_2\ p_4 p_6 \left[\langle 1-p \rangle_3\ \eta_3 + \langle 1-p \rangle_5\ \eta_5 \right]$, where η_3 and η_5 denote the number of fast neutrons produced per neutron absorbed in U^{233} and U^{235}, respectively (epithermal neutrons below 5 ev). The quantities $\langle 1-p \rangle_3$ and $\langle 1-p \rangle_5$ are defined by Eq. 2.4.5.

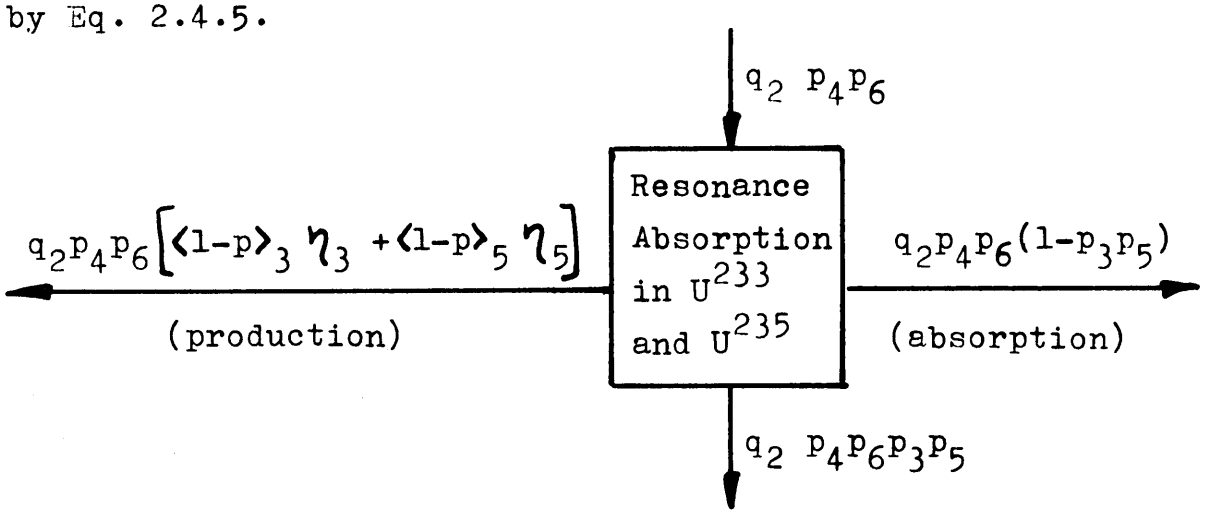

Fig.II.6., The Resonance Region ③

2.1.6. The Thermal Group

The diffusion equation for the thermal group is

$$D \nabla^2 \phi - \Sigma_a \phi + p_T \Sigma_1 \phi_1 = 0 \qquad (2.1.5)$$

where ϕ is the average thermal flux in space (in the unit

cell) and energy (0 to 0.45 ev), p_T is the total resonance escape probability, and the rest of the symbols have their usual meaning.

The source of thermal neutrons is

$$\begin{aligned} p_T \Sigma_1 \phi_1 &= q_2\, p_4 p_6 p_3 p_5 \\ &= q P_1\, p_1 p_2 p_7 p_9\, p_4 p_6 p_3 p_5 \\ &= q P_1\, p_T \end{aligned}$$

The number of fast neutrons produced from thermal fissions is given by $\left[\Sigma_{f3}\nu_3 + \Sigma_{f5}\nu_5\right]\phi$. The thermal group is represented schematically in Fig.II.7.

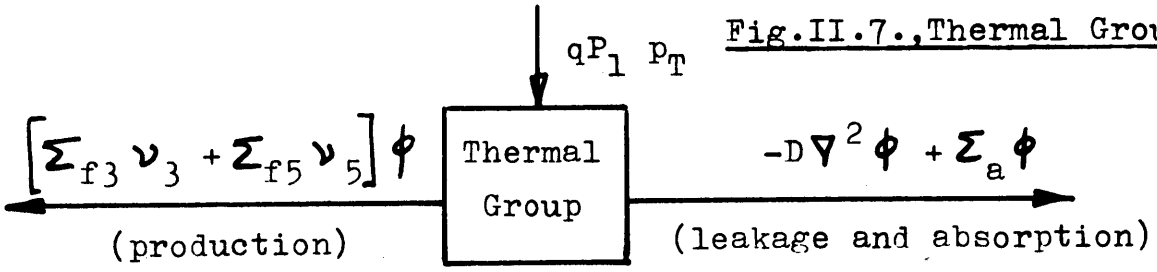

Fig.II.7., Thermal Group

The macroscopic fission cross sections for U^{233} and U^{235}, Σ_{f3} and Σ_{f5}, are averaged over the flux spectrum (refer to section 2.2.).

2.1.7. Neutron Balance

From Fig.II.1. and Fig.II.2. it follows that q/ε must equal the total number of fast neutrons resulting from

thermal and resonance fissions:

$$\frac{q}{\xi} = \left[\Sigma_{f3}\nu_3 + \Sigma_{f5}\nu_5\right]\phi$$
$$+ qP_1\left[\left[\langle 1-p\rangle_7\eta_7+\langle 1-p\rangle_9\eta_9\right]+ p_1p_2p_7p_9p_4p_6\left[\langle 1-p\rangle_3\eta_3+\langle 1-p\rangle_5\eta_5\right]\right]$$

or simply

$$\frac{q}{\xi} = \phi C_{10} + qP_1C_{11} \qquad (2.1.6)$$

(The correct definition of C_{10} and C_{11}, taking into account the flux depression in the fuel, is given in Eqns. (2.6.2), and (2.6.4)).

Combining the last equation with the diffusion equations for the fast and thermal fluxes leads to the"condensed two-group equation" (S1):

$$D\nabla^2\phi + \frac{p_T\tau}{1-C_{11}\xi}\nabla^2\left[\frac{\Sigma_a\phi - D\nabla^2\phi}{p_T}\right] = \left[\Sigma_a - \frac{\xi p_T C_{10}}{1-C_{11}\xi}\right]\phi \qquad (2.1.7)$$

In this equation, all quantities, except ξ, are functions of the spatial coordinates r and z in the reactor. The method of solution is described in section 2.8.

2.2. Neutron Spectrum and Effective Thermal Cross Sections

2.2.1. Microscopic Cross Sections as a Function of Energy

The microscopic cross sections for U^{233}, U^{235}, Np^{237}, Sm^{149}, and Sm^{151} are generated by a series of equations of the Breit-Wigner form:

$$\sigma(E) = \frac{1}{\sqrt{E}} \left\{ a + \sum_{i=1}^{n} \frac{c_i}{b_i + (E - E_i^o)^2} \right\} \quad (2.2.1)$$

The parameters a, b_i, c_i, and E_i^o are taken from Westcott (W1).

The Xe cross section is calculated from a single-level Breit-Wigner formula using Smith's data:(S2)

$$\sigma_{Xe}(E) = \frac{1}{\sqrt{E}} \left\{ \frac{c}{\frac{\Gamma^2}{4} + (E - E^o)^2} \right\} \quad (2.2.2)$$

Here, the variation in the total width Γ is taken into account:

$$\Gamma = \Gamma_a + \Gamma_n^o \sqrt{\frac{E}{E_o}}$$

All other cross sections are assumed to follow the 1/v law. Cross sections at thermal energy (0.0253 ev) are taken from BNL 325 (H4).

2.2.2. The Neutron Spectrum

According to the Wilkins theory (C1, S1) the neutron energy spectrum depends only on the function

$$A(x) = \frac{\Sigma_a(x)}{\overline{\xi \Sigma_s}} \qquad (2.2.3)$$

where $\Sigma_a(x)$ is the total macroscopic absorption cross section of the homogenized unit cell as a function of the normalized velocity $x = v/v_o$, $v_o = 2200$ m/s, and $\overline{\xi \Sigma_s}$ is the slowing down power of the unit cell (assumed constant over the flux spectrum).

The function $\Sigma_a(x)$ is given by

$$\Sigma_a(x) = \frac{\sum_i N_i V_i \sigma_{ai}(x) \psi_i}{\sum_i V_i \psi_i} \qquad (2.2.4)$$

where N_i is the number of atoms per unit volume of the i^{th} component, V_i is the volume of the i^{th} component, $\sigma_{ai}(x)$ is the microscopic cross section of the i^{th} component, and ψ_i is the corresponding disadvantage factor. ψ_i is defined as the average thermal flux in the region containing the i^{th} component devided by the average thermal flux in the unit cell.

The derivation of the Wilkins equation is given by Cohen (C1), and the method of solution is described in de-

tail by Shanstrom (S1).

2.2.3. Effective Cross Sections

Effective thermal cross sections are then obtained by weighting the microscopic cross sections over the Wilkins flux distribution up to the resonance cut-off energy of 0.45 ev (S1), i.e.

$$\sigma_i = \frac{\int_0^{0.45\ ev} \sigma_i(E)\, \frac{d\phi}{dE}\, dE}{\int_0^{0.45\ ev} \frac{d\phi}{dE}\, dE} \qquad (2.2.5)$$

where the denominator represents the "thermal flux", ϕ:

$$\phi = \int_0^{0.45\ ev} \frac{d\phi}{dE}\, dE \qquad (2.2.6)$$

The Wilkins-hardened microscopic cross sections, σ_i, are computed periodically at 6 selected points in the reactor core and blanket (Fig.II.8.). Cross sections at intermediate points are obtained by parabolic interpolation.

Fig.II.8., Six Selected Points for Cross Section Calculations

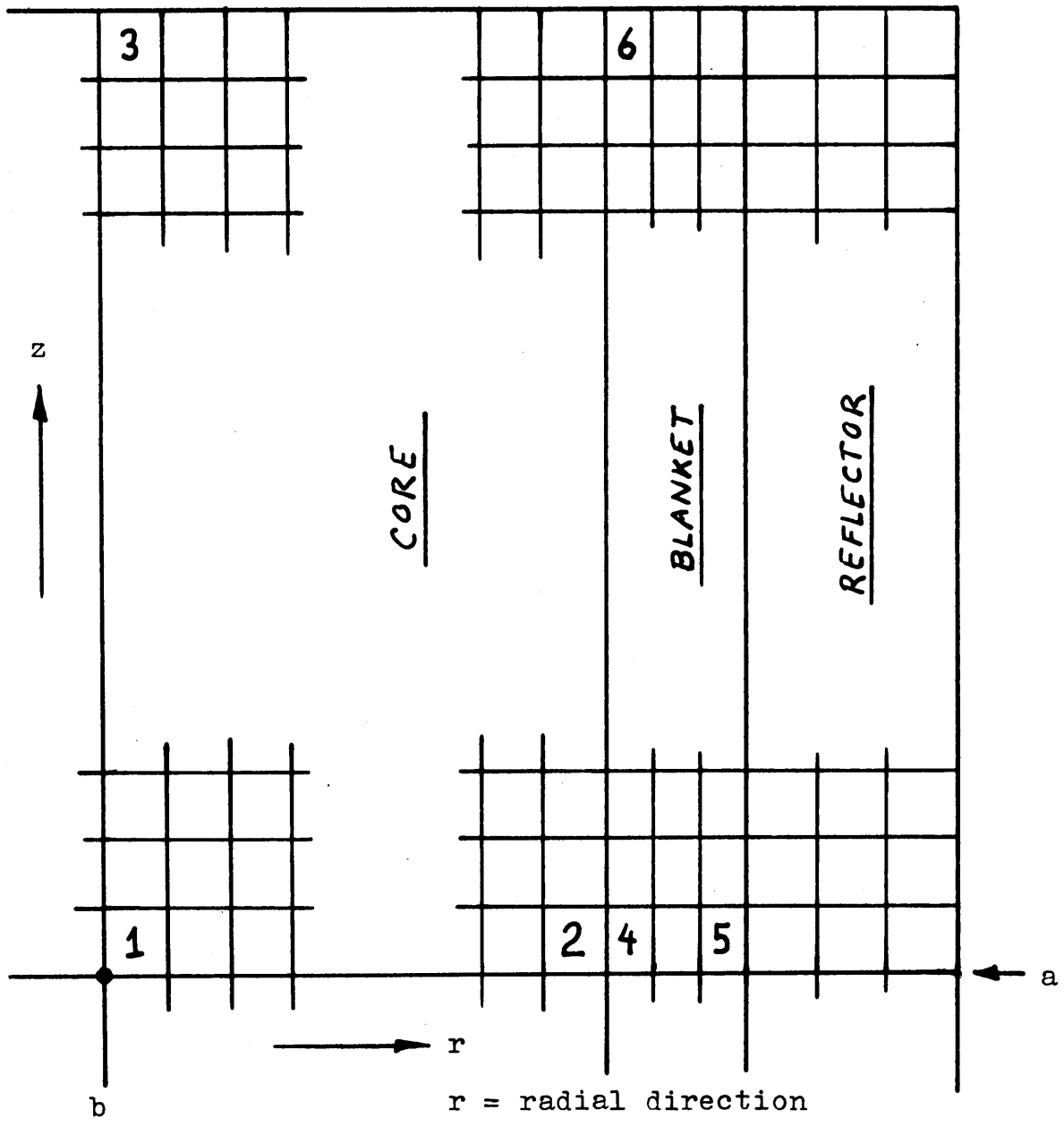

r = radial direction
z = axial direction
a = midplane of reactor
b = centerline

2.3. Nuclear Properties

2.3.1. Disadvantage Factors

For a cylindrical fuel rod surrounded by moderator, the following three disadvantage factors may be defined:

$$\Psi_f = \frac{\text{average flux in the fuel}}{\text{average flux in the unit cell}} \qquad (2.3.1)$$

$$\Psi_s = \frac{\text{flux on the surface of the fuel rod}}{\text{average flux in the unit cell}} \qquad (2.3.2)$$

$$\Psi_m = \frac{\text{average flux in the moderator}}{\text{average flux in the unit cell}} \qquad (2.3.3)$$

If the effect of the cladding on the flux shape is assumed to be small, then the average flux in the cladding will be approximately equal to the flux at the surface of the fuel rod. In this case the three disadvantage factors can be evaluated from diffusion theory (K1) :

The thermal utilization is, by definition, the number of neutrons absorbed in the fuel per neutron absorbed in the unit cell,

$$f = \frac{N_o \sigma_{ao} V_o \bar{\phi}_o}{N_o \sigma_{ao} V_o \bar{\phi}_o + N_1 \sigma_{a1} V_1 \bar{\phi}_1} \qquad (2.3.4)$$

where the subscripts o and 1 refer to fuel and moderator, respectively, and V is the volume.

For a cylindrical cell, f is given by

$$\frac{1}{f} = \frac{N_1 \sigma_{a1} V_1}{N_o \sigma_{ao} V_o} F + E \qquad (2.3.5)$$

where $$F = \frac{\kappa_o r_o}{2} \frac{I_o(\kappa_o r_o)}{I_1(\kappa_o r_o)}$$

$$\approx \frac{\kappa_o r_o}{2} + \frac{16}{(\kappa_o r_o + 4)^2}$$

$$E = \frac{\kappa_1(r_1^2 - r_o^2)}{2r_o} \frac{I_o(\kappa_1 r_o)K_1(\kappa_1 r_1) + K_o(\kappa_1 r_o)I_1(\kappa_1 r_1)}{I_1(\kappa_1 r_1)K_1(\kappa_1 r_o) - K_1(\kappa_1 r_1)I_1(\kappa_1 r_o)}$$

$$\approx 1 + \frac{(\kappa_1 r_1)^2}{2} \left\{ \frac{r_1^2}{r_1^2 - r_o^2} \ln\left(\frac{r_1}{r_o}\right) - \frac{3}{4} + \frac{r_o^2}{4r_1^2} \right\}$$

and r_o is the radius of the fuel rod, r_1 is the radius of the unit cell, κ_o and κ_1 are the reciprocals of the thermal diffusion lengths in the fuel and the moderator, respectively.

It follows that

$$\frac{\bar{\phi}_1}{\bar{\phi}_o} = F + (E - 1) \frac{N_o \sigma_{ao} V_o}{N_1 \sigma_{a1} V_1}$$

The average flux in the cell is defined by

$$\bar{\phi}_{cell} = \frac{\bar{\phi}_o V_o + \bar{\phi}_1 V_1}{V_o + V_1} , \quad V_o + V_1 = V_{cell} ,$$

hence $$\frac{\bar{\phi}_{cell}}{\bar{\phi}_o} = \frac{V_o}{V_{cell}} + \frac{\bar{\phi}_1}{\bar{\phi}_o} \frac{V_1}{V_{cell}} , \quad \text{and}$$

$$\Psi_f = \frac{\bar{\phi}_o}{\bar{\phi}_{cell}} = \frac{1}{\frac{V_o}{V_{cell}} + \left\{ F + (E-1) \frac{N_o \sigma_{ao} V_o}{N_1 \sigma_{a1} V_1} \right\} \frac{V_1}{V_{cell}}} \tag{2.3.6}$$

$$\Psi_s = \frac{\bar{\phi}_s}{\bar{\phi}_{cell}} = \frac{\bar{\phi}_s}{\bar{\phi}_o} \frac{\bar{\phi}_o}{\bar{\phi}_{cell}} = F \Psi_f \tag{2.3.7}$$

$$\Psi_m = \frac{\bar{\phi}_1}{\bar{\phi}_{cell}} = \frac{\bar{\phi}_1}{\bar{\phi}_o} \frac{\bar{\phi}_o}{\bar{\phi}_{cell}} = \left\{ F + (E-1) \frac{N_o \sigma_{ao} V_o}{N_1 \sigma_{a1} V_1} \right\} \Psi_f \tag{2.3.8}$$

In the case of a rod bundle the above formulas do not strictly hold, for several reasons. First, the "rod" is no longer cylindrical. Secondly, the definition of the boundary between the "fuel" and the "moderator" is somewhat arbitrary. We will assume here the so-called "rubber band approximation", where all the materials inside the "rubber band" are considered as "fuel" and the rest is considered as "moderator" (Fig.II.9).

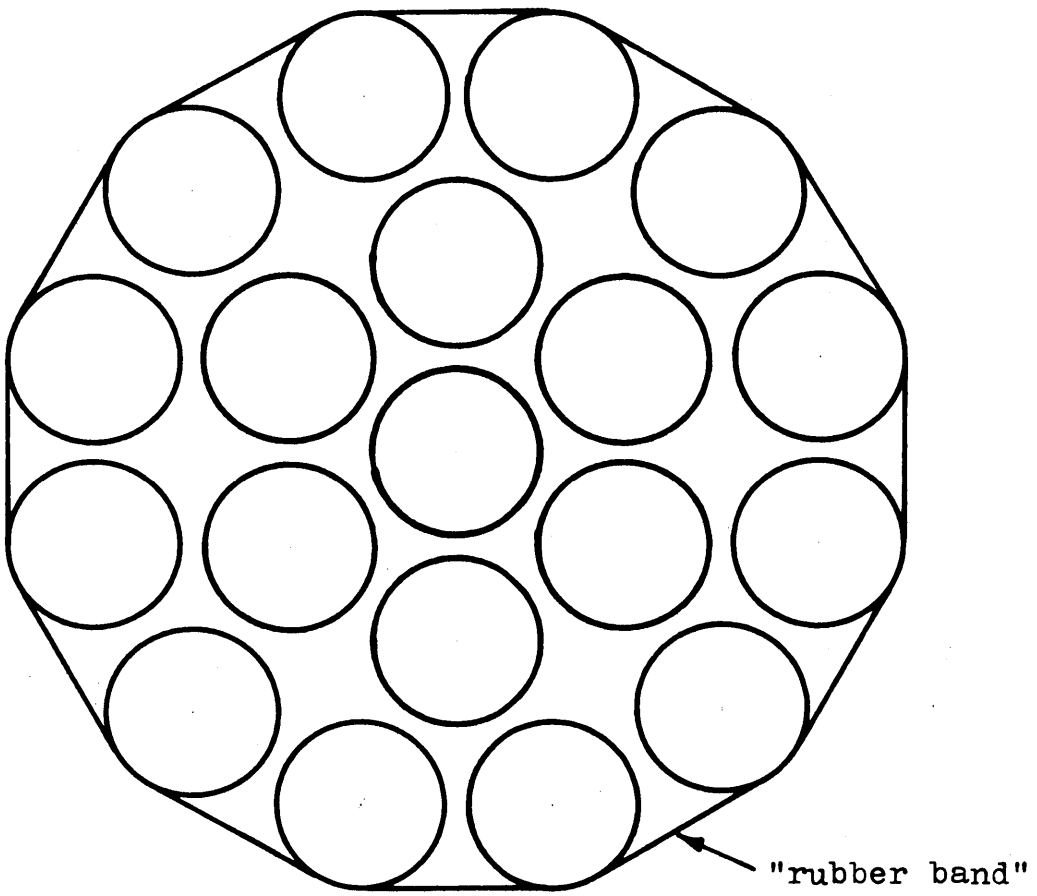

Fig.II.9., The "rubber band approximation"

The radius r_o of the fuel region is obtained by transforming the "rubber band" into a circle of equal area. K_o is calculated by homogenizing all materials in the fuel region and K_1 is calculated in a similar way for the moderator region.

2.3.2. The Fast Effect

For a cylindrical fuel rod surrounded by moderator the fast fission factor is given by (K1) :

$$\varepsilon - 1 = \frac{\sigma_f \left[\nu_f - 1 - \frac{\sigma_r}{\sigma_f}\right]}{\frac{\sigma}{P(a\Sigma)} - \left[\nu_f \sigma_f + \sigma_e\right]} \qquad (2.3.9)$$

where σ_f = fission cross section

ν_f = number of neutr. per fission

σ_r = capture cross section

σ_e = elastic scattering cross sect.

σ = total cross section

Σ = total macroscopic cross sect.

a = radius of rod

$P(a\Sigma)$ = collision probability

σ_f, ν_f, σ_r, σ_e, σ, and Σ represent averages over the flux spectrum above threshold for fast fission.

In the case of a rod bundle (Fig.II.9.), we may again use the "rubber band approximation" to find an equivalent rod radius. In the formula for ε , all microscopic cross sections must be replaced by the macroscopic cross sections of the homogenized "fuel rod" :

$$\varepsilon - 1 = \frac{\Sigma_f \left[\nu_f - 1 - \frac{\Sigma_r}{\Sigma_f} \right]}{\frac{\Sigma}{P(a\Sigma)} - \left[\nu_f \Sigma_f + \Sigma_e \right]} \qquad (2.3.10)$$

Here, Σ_e includes the elastic scattering cross section of all heavy nuclides present in the fuel region. Elastic scattering by light elements, such as H, degrades the neutron energy below fast fission threshold and is therefore treated as inelastic scattering.

The above formula (2.3.10) as applied to the CANDU reactor, yields a value of 1.0247 for ε (see Appendix 3.). The reported value (A1) is 1.0267.

In a thorium fueled reactor, the fast effect is far less significant than it is in a reactor using U^{238} as the fertile material. This is due to the low fast fission cross section of Th^{232} as compared to U^{238}. The value obtained for a thorium fueled CANDU reactor is (Appendix 3.):

$$\varepsilon = 1.0023$$

2.3.3. The Fermi Age

The Fermi age, τ, in a mixture of metal and moderator is given, approximately, by (K1)

$$\overline{\tau} = \tau_{mod} \left[1 + \frac{V_{metal}}{V_{cell}} \right]^2 \qquad (2.3.11)$$

If this formula is applied to the CANDU reference design a value of 147.5 cm^2 is obtained for τ . The value given in (Al) is 151.8 cm^2.

2.3.4. The Diffusion Coefficient for Thermal Neutrons

The diffusion coefficient is calculated from the formula:

$$\overline{D_{th}} = \frac{\sum_i \Psi_i V_i}{3 \sum_i \sigma_{tr,i} N_i V_i \Psi_i} \qquad (2.3.12)$$

where the summation extends over all materials present in the unit cell, and $\sigma_{tr,i}$ is the microscopic transport cross section of the i^{th} nuclide.

2.3.5. The Slowing Down Power

The slowing down power of the non-fuel part of the unit cell is

$$\overline{\xi \Sigma_s} = \frac{\sum_{non-fuel} \xi_i \sigma_{si} N_i V_i}{\sum_{non-fuel} V_i} \qquad (2.3.13)$$

2.3.6. Thermal Absorption in the Non-fuel Region

The unhomogenized macroscopic absorption cross section of the non-fuel region is given by

$$\Sigma_{mod} = \frac{\sum^{non-fuel} N_i \sigma_i \psi_i V_i}{\sum^{non-fuel} V_i \psi_i} \qquad (2.3.14)$$

2.3.7. The Epithermal Scattering Cross Section of the Fuel

The epithermal macroscopic scattering cross section of the fuel region, which will be used in the calculation of the resonance disadvantage factors (sect.2.4.), is evaluated according to the formula

$$\Sigma_{s,fl} = \frac{\sum^{fuel} N_i \sigma_{si} V_i}{\sum^{fuel} V_i} \qquad (2.3.15)$$

where σ_{si} is the epithermal scattering cross section of the i^{th} nuclide.

2.3.8. The Average Temperature of the D_2O

The average D_2O temperature is required for the solution of the Wilkins equation (S1). It is computed from

the average moderator temperature and the average coolant temperature by volume weighting:

$$\overline{T}_{D_2O} = \frac{T_{mod}\ V_{mod} + T_{cool}\ V_{cool}}{V_{mod} + V_{cool}} \qquad (2.3.16)$$

The average moderator temperature, T_{mod}, the moderator volume V_{mod}, the average coolant temperature T_{cool}, and the coolant volume, V_{cool} are given in Appendix 2.

2.4. Resonance Escape Probabilities

2.4.1. The Fuel Region

The resonance escape probability of the m^{th} nuclide in the fuel is given by (S1)

$$p_m = \exp - \left\{ \frac{V_{fl}\ N_m\ RI_m^{\infty}}{\overline{\xi \Sigma_s}\ (1-V_{fl})\ \Psi_{1,m}} \right\} \qquad (2.4.1)$$

where V_{fl} is the volume fraction of the fuel in the unit cell, N_m is the number of atoms of the m^{th} nuclide per unit volume of fuel, RI_m^{∞} is the infinite-dilution resonance integral of the m^{th} nuclide, $\overline{\xi \Sigma_s}$ is the slowing down power of the non-fuel region, and $\Psi_{1,m}$ is the resonance disadvantage factor for the m^{th} nuclide.

The resonance disadvantage factors are obtained, according to the Crowther-Weil technique (S1), from the formula

$$\Psi_{1,m} = 1 + \frac{N_m\ RI_m^{\infty}}{\Sigma_{s,fl}} \qquad (2.4.2)$$

where $\Sigma_{s,fl}$ is the epithermal macroscopic scattering cross section of the fuel region (sect.2.3.7.).

In the case of concurrent resonance absorption in M

different nuclides, the slowing down density is reduced by a factor of

$$p_M = \prod_{m=1}^{M} [p_m] \qquad (2.4.3)$$

and the total number of neutrons absorbed by all M nuclides is

$$q \left[1 - \prod_{m=1}^{M} [p_m] \right] \qquad (2.4.4)$$

As the fractional absorption in the m^{th} nuclide is

$$\frac{\left[\frac{N_m \, RI_m^{\infty}}{\psi_{1,m}} \right]}{\sum_{m=1}^{M} \left[\frac{N_m \, RI_m^{\infty}}{\psi_{1,m}} \right]} ,$$

the number of neutrons absorbed by the m^{th} nuclide is given by

$$q\langle 1-p \rangle_m = q \left[1 - \prod_{m=1}^{M} [p_m] \right] \frac{\left[\frac{N_m \, RI_m^{\infty}}{\psi_{1,m}} \right]}{\sum_{m=1}^{M} \left[\frac{N_m \, RI_m^{\infty}}{\psi_{1,m}} \right]} \qquad (2.4.5)$$

2.4.2. The Non-fuel Region

The resonance absorption rate in the non-fuel materials is proportional to

$$\langle 1-p \rangle_{mod} = 1 - \exp - \left\{ \frac{\sum^{\text{non-fuel}} V_i N_i RI_i}{\S \Sigma_s (1-V_{fl})} \right\}$$

$$\approx \frac{\sum^{\text{non-fuel}} V_i N_i RI_i}{\S \Sigma_s (1-V_{fl})} \qquad (2.4.6)$$

Here, V_i is the volume of the i^{th} component, N_i is the number of atoms per unit volume of pure material, RI is the resonance integral, and the rest of the symbols have the same meaning as in Eq.2.4.1.

In the CANDU reactor, the only significant resonance absorption in the non-fuel region occurs in the zirconium cladding and pressure tubes, so that

$$\langle 1-p \rangle_{mod} \approx \frac{V_{Zr} N_{Zr} RI_{Zr}}{\S \Sigma_s (1-V_{fl})} \qquad (2.4.7)$$

2.5. Concentration Changes

2.5.1. The Nuclide Concentration Equations

Considering only the reactions shown in Fig.II.10., and assuming that all half lives are zero except those of Pa^{233} and Xe^{135}, we obtain the following equations for the nuclide concentrations:

$$\underline{Th^{232}:} \quad \frac{dN_1}{dt} = -N_1\sigma_{a1}\phi - \frac{q}{V_{f1}}\left[P_1\langle 1-p\rangle_1 + \frac{\varepsilon-1}{\varepsilon(\eta_1-1)}\right] \qquad (2.5.1)$$

$$\underline{Pa^{233}:} \quad \frac{dN_2}{dt} = \left[N_1\sigma_{a1}-N_2\sigma_{a2}\right]\phi - \lambda_{Pa}N_2 + \frac{q}{V_{f1}}\left\{P_1\left[\langle 1-p\rangle_1 - \langle 1-p\rangle_2\right] + \frac{\alpha_1(\varepsilon-1)}{(1+\alpha_1)\varepsilon(\eta_1-1)}\right\} \qquad (2.5.2)$$

$$\underline{U^{233}:} \quad \frac{dN_3}{dt} = \lambda_{Pa}N_2 - N_3\sigma_{a3}\phi - \frac{qP_1}{V_{f1}}\left[\langle 1-p\rangle_7 + p_{174}\langle 1-p\rangle_3\right] \qquad (2.5.3)$$

$$\underline{U^{234}:} \quad \frac{dN_4}{dt} = \left[N_3(\sigma_{a3}-\sigma_{f3}) + N_2\sigma_{a2} - N_4\sigma_{a4}\right]\phi + \frac{qP_1}{V_{f1}}\left\{\frac{\langle 1-p\rangle_7\alpha_7}{1+\alpha_7} + \frac{p_{174}\langle 1-p\rangle_3\alpha_3}{1+\alpha_3} + \langle 1-p\rangle_2 - p_{17}\langle 1-p\rangle_4\right\} \qquad (2.5.4)$$

Fig.II.10., Nuclear Reactions

(FP = Fission Products)

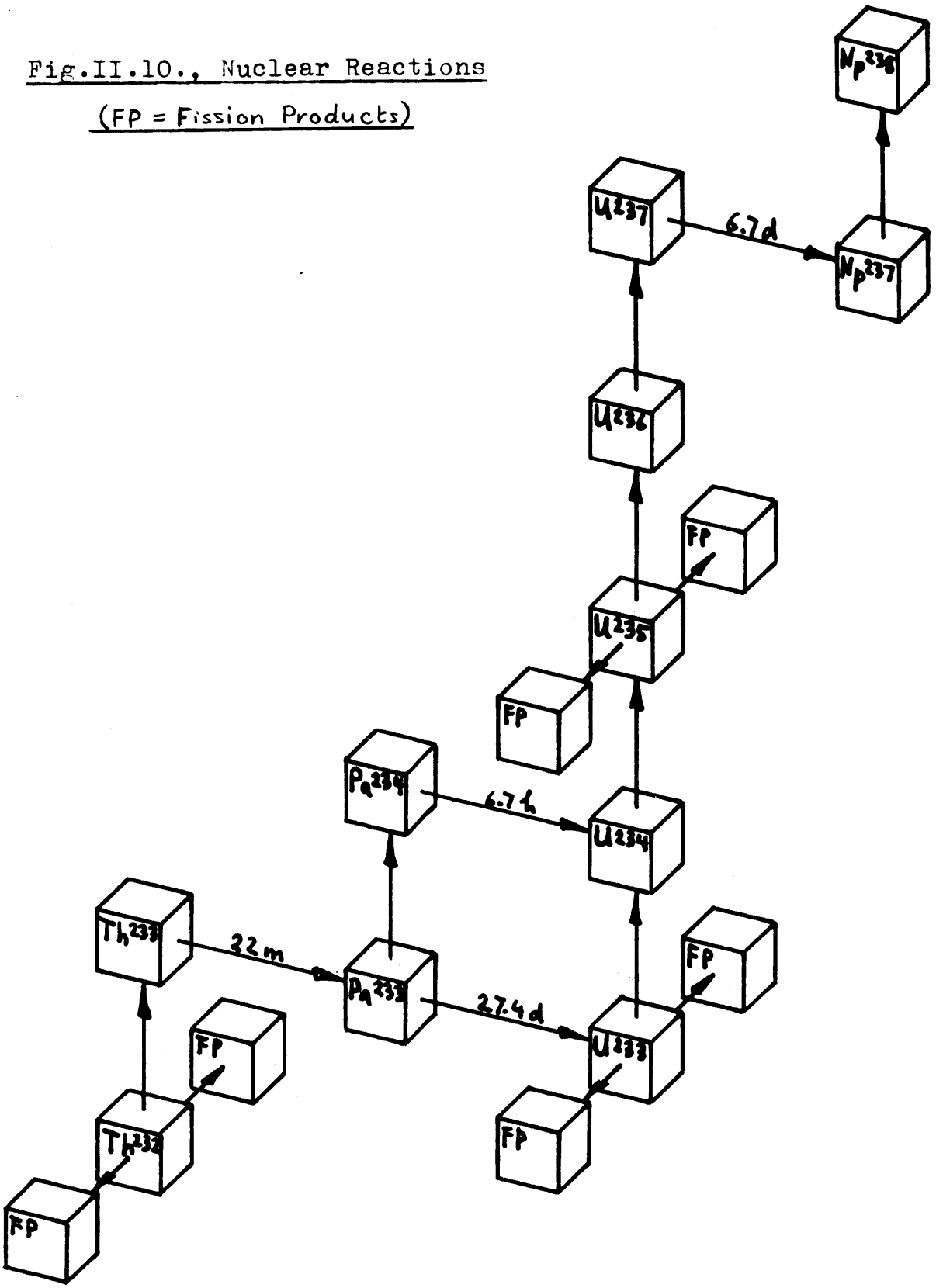

$$\underline{U^{235}:} \quad \frac{dN_5}{dt} = \left[N_4\sigma_{a4} - N_5\sigma_{a5}\right]\phi + \frac{qP_1}{V_{f1}}\left\{p_{17}\langle 1-p\rangle_4 - \langle 1-p\rangle_9 - p_{174}\langle 1-p\rangle_5\right\} \tag{2.5.5}$$

$$\underline{U^{236}:} \quad \frac{dN_6}{dt} = \left[N_5(\sigma_{a5}-\sigma_{f5}) - N_6\sigma_{a6}\right]\phi + \frac{qP_1}{V_{f1}}\left\{\frac{\langle 1-p\rangle_9\alpha_9}{1+\alpha_9} + \frac{p_{174}\langle 1-p\rangle_5\alpha_5}{1+\alpha_5} - p_{17}\langle 1-p\rangle_6\right\} \tag{2.5.6}$$

$$\underline{Np^{237}:} \quad \frac{dN_7}{dt} = \left[N_6\sigma_{a6} - N_7\sigma_{a7}\right]\phi + \frac{qP_1}{V_{f1}}\left[p_{17}\langle 1-p\rangle_6\right] \tag{2.5.7}$$

U^{233} and Th^{232} fissions:

$$\frac{dN_8}{dt} = N_3\sigma_{f3}\phi + \frac{qP_1}{V_{f1}}\left[\frac{\langle 1-p\rangle_7}{1+\alpha_7} + p_{174}\frac{\langle 1-p\rangle_3}{1+\alpha_3}\right] + \frac{q}{V_{f1}}\left[\frac{\varepsilon - 1}{\varepsilon(\eta_1-1)(\alpha_1+1)}\right] \tag{2.5.8}$$

U^{235} fissions:

$$\frac{dN_9}{dt} = N_5\sigma_{f5}\phi + \frac{qP_1}{V_{f1}}\left\{\frac{\langle 1-p\rangle_9}{1+\alpha_9} + p_{174}\frac{\langle 1-p\rangle_5}{1+\alpha_5}\right\} \tag{2.5.9}$$

The equilibrium concentrations of Sm^{149}, Sm^{151}, and Xe^{135} are given by

$\underline{Sm^{149}}$:

$$N_{10} = \frac{1}{\sigma_{10}}\left[N_3\sigma_{f3}y_{S92}+N_5\sigma_{f5}y_{S93}+\frac{q}{\phi V_{f1}}\left[\frac{\varepsilon-1}{\varepsilon(\eta_1-1)(\alpha_1+1)}\right]y_{S91}\right.$$

$$+\frac{qP_1}{\phi V_{f1}}\left\{\left[\frac{\langle 1-p\rangle_7}{1+\alpha_7}+p_{174}\frac{\langle 1-p\rangle_3}{1+\alpha_3}\right]y_{S92}\right.$$

$$\left.\left.+\left[\frac{\langle 1-p\rangle_9}{1+\alpha_9}+p_{174}\frac{\langle 1-p\rangle_5}{1+\alpha_5}\right]y_{S93}\right\}\right] \qquad (2.5.10)$$

$\underline{Sm^{151}}$:

$$N_{11} = \frac{1}{\sigma_{11}}\left[N_3\sigma_{f3}y_{S12}+N_5\sigma_{f5}y_{S13}+\frac{q}{\phi V_{f1}}\left[\frac{\varepsilon-1}{\varepsilon(\eta_1-1)(\alpha_1+1)}\right]y_{S11}\right.$$

$$+\frac{qP_1}{\phi V_{f1}}\left\{\left[\frac{\langle 1-p\rangle_7}{1+\alpha_7}+p_{174}\frac{\langle 1-p\rangle_3}{1+\alpha_3}\right]y_{S12}\right.$$

$$\left.\left.+\left[\frac{\langle 1-p\rangle_9}{1+\alpha_9}+p_{174}\frac{\langle 1-p\rangle_5}{1+\alpha_5}\right]y_{S13}\right\}\right] \qquad (2.5.11)$$

$\underline{Xe^{135}}$:

$$N_{12} = \frac{1}{\sigma_{12}+\frac{\lambda_{Xe}}{\phi}}\left[N_3\sigma_{f3}y_{X2}+N_5\sigma_{f5}y_{X3}+\frac{q}{\phi V_{f1}}\left[\frac{\varepsilon-1}{\varepsilon(\eta_1-1)(\alpha_1+1)}\right]y_{X1}\right.$$

$$+\frac{qP_1}{V_{f1}}\left\{\left[\frac{\langle 1-p\rangle_7}{1+\alpha_7}+p_{174}\frac{\langle 1-p\rangle_3}{1+\alpha_3}\right]y_{X2}\right.$$

$$\left.\left.+\left[\frac{\langle 1-p\rangle_9}{1+\alpha_9}+p_{174}\frac{\langle 1-p\rangle_5}{1+\alpha_5}\right]y_{X3}\right\}\right] \qquad (2.5.12)$$

where the following notation has been used

N = number of atoms per unit volume of fuel

σ = microscopic cross section, averaged over the Wilkins spectrum

P_1 = fast non-leakage probability

η_1 = number of neutrons produced per fast neutron absorbed in Th^{232}

$p_{17} = p_1 p_2 p_7 p_9$

$p_{174} = p_1 p_2 p_7 p_9 p_4 p_6$

y = yield per fission

λ = decay constant

with the subscripts

1 = Th^{232}
2 = Pa^{233}
3 = U^{233}
4 = U^{234}
5 = U^{235}
6 = U^{236}

} for N and σ for p, $\langle 1-p \rangle$, and α : below 5 ev

7 = Np^{237}
8 = fission product pairs from U^{233} and Th^{232}
9 = fission product pairs from U^{235}
10 = Sm^{149}
11 = Sm^{151}
12 = Xe^{135}

} for N and σ

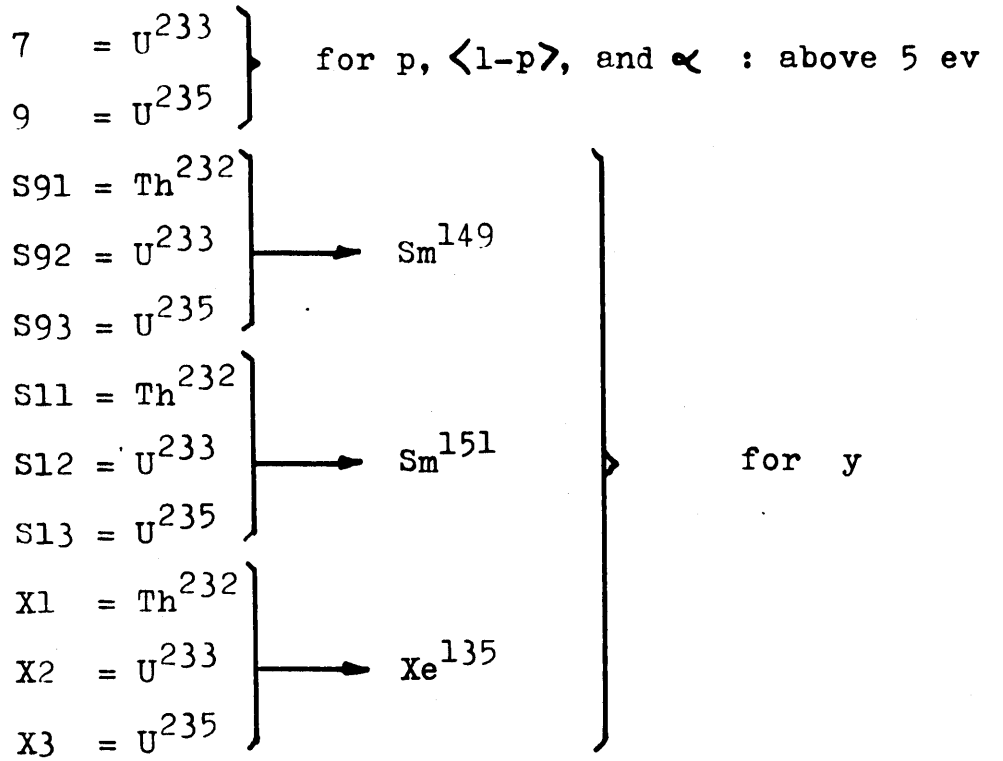

2.5.2. The Method of Solution

Equations (2.5.1) through (2.5.9) are solved numerically by a third order Adams integration technique using a third order Runge-Kutta startup procedure.

Given a differential equation of the form

$$\frac{dy}{dx} = F(x,y)$$

with the initial condition $y(x_o) = y_o$, we first define a number of discrete values of the independent variable, x, by the relation

$$x_k = x_o + kh \tag{2.5.13}$$

where h is a constant. Furthermore $y_k = y(x_k)$ and $F_k = F(x_k, y_k)$. We can now expess the function y at the point x_{k+1} in terms of y_k and F_k, F_{k-1}, F_{k-2}, F_{k-3}, etc., as follows (H1):

$$y_{k+1} = y_k + h\left[F_k + \frac{1}{2}\Delta F_{k-1} + \frac{5}{12}\Delta^2 F_{k-2} + \frac{3}{8}\Delta^3 F_{k-3} + \ldots\right] \tag{2.5.14}$$

where $\Delta F_r = F_{r+1} - F_r$, and $\Delta^n F_r = \Delta^{n-1} F_{r+1} - \Delta^{n-1} F_r$.

This formula, if truncated at $\Delta^n F_{k-n}$, gives the exact solution if, over the interval $(x_k - nh, x_k + h)$, the unknown function is a polynomial of degree n+1.

Retaining first and second differences yields

$$y_{k+1} = y_k + h\left[F_k + \frac{1}{2}\Delta F_{k-1} + \frac{5}{12}\Delta^2 F_{k-2}\right] \quad , \text{ or}$$

$$y_{k+1} = y_k + \frac{h}{12}\left[23F_k - 16F_{k-1} + 5F_{k-2}\right] \tag{2.5.15}$$

which is the third order Adams integration formula.

It is obvious that the Adams method cannot be used for startup. For the first three steps we need a "self-starting"

procedure, such as the Runge-Kutta method. Here, y_{k+1} is expressed in terms of y_k and a number of F's which are evaluated at intermediate points, i.e., between x_k and x_{k+1}, and between y_k and y_{k+1}. The third order formula can be written as (H1):

$$y_{k+1} = y_k + \frac{1}{6}(a_1 + 4a_2 + a_3)$$

where $a_1 = h\ F(x_k, y_k)$

$$a_2 = h\ F\left(\left(x_k + \frac{h}{2}\right), \left(y_k + \frac{a_1}{2}\right)\right)$$

$$a_3 = h\ F((x_k + h), (y_k + 2a_2 - a_1))$$

It is clear that, with the Runge-Kutta method, the function F(x,y) must be evaluated many times for each integration step, whereas with the Adams method, F(x,y) must be evaluated only once for each step.

Since the function F may be very involved, it is obvious that the Adams method requires less computation time than does the R-K method (at the expense of requiring a special start-up procedure, of course).

The above treatment can easily be extended to several simultaneous equations, such as the nuclide concentration equations.

The independent variable is now the time, along with all quantities which are direct functions of time, such as the distance along the fuel channel (the fuel travels through the reactor at a constant velocity), and all nuclear parameters which are functions of position (i.e. the flux, the slowing down density, the fast non-leakage probability, and the Wilkins-hardened microscopic cross sections).

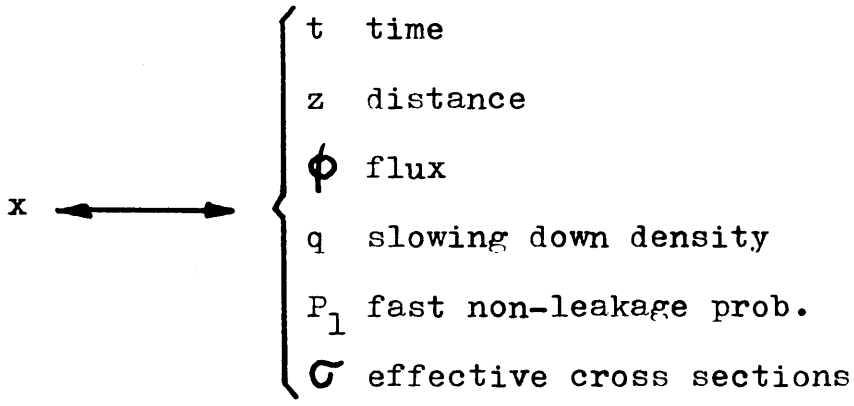

The dependent variables are the nuclide concentrations, and the resonance escape probabilities (which are direct functions of the nuclide concentrations).

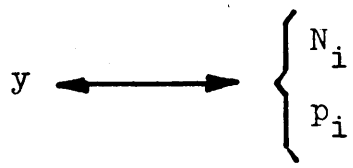

2.6. The Six Homogenized Properties

The six unit cell properties which are used in the solution of the diffusion equation (Eq.2.1.7) and in the calculation of the flux level in the reactor, are

$$\Sigma_a = \Sigma_{FP} \psi_f V_{f1} + \Sigma_{mod} g_w \psi_{mod}(1-V_{f1}) + \frac{qP_1}{\phi} p_T \langle 1-p \rangle_{mod} + \left[\sum_{i=1}^{7} N_i \sigma_i + \sum_{i=10}^{12} N_i \sigma_i \right] \psi_f V_{f1} \qquad (2.6.1)$$

$$C_{10} = \left[N_3 \sigma_{f3} \nu_3 + N_5 \sigma_{f5} \nu_5 \right] \psi_f V_{f1} \qquad (2.6.2)$$

$$C_{53} = \left[N_3 \sigma_{f3} + N_5 \sigma_{f5} \right] \psi_f V_{f1} \qquad (2.6.3)$$

$$C_{11} = \nu_3 \left[\frac{\langle 1-p \rangle_7}{1+\alpha_7} + p_{174} \frac{\langle 1-p \rangle_3}{1+\alpha_3} \right] + \nu_5 \left[\frac{\langle 1-p \rangle_9}{1+\alpha_9} + p_{174} \frac{\langle 1-p \rangle_5}{1+\alpha_5} \right] \qquad (2.6.4)$$

$$C_{54} = \left[\frac{\langle 1-p \rangle_7}{1+\alpha_7} + p_{174} \frac{\langle 1-p \rangle_3}{1+\alpha_3} \right] + \left[\frac{\langle 1-p \rangle_9}{1+\alpha_9} + p_{174} \frac{\langle 1-p \rangle_5}{1+\alpha_5} \right] \qquad (2.6.5)$$

$$p_T = p_1 p_2 p_7 p_9 p_4 p_6 p_3 p_5 \qquad (2.6.6)$$

where g_w is the ratio of the effective to the 2200 m/s

cross section for any nuclide whose cross section varies as 1/v. Σ_{FP} is the macroscopic fission product cross section of the fuel (see sect.2.7.)

2.7. Fission Product Poisoning

If a batch of fission products is irradiated, the average 2200 m/s cross section per fission product pair is given as a function of the 2200 m/s flux-time, θ_2, by

$$\sigma_{FP2} = y_1\sigma_1 e^{-\sigma_1\theta_2} + y_2\sigma_2 e^{-\sigma_2\theta_2} + y_3\sigma_3 e^{-\sigma_3\theta_2} \qquad (2.7.1)$$

where the quantities y_i and σ_i are the yields and cross sections of three pseudo fission products (C3).

If the fission products build up in the fuel under irradiation, the total macroscopic fission product cross section, at 2200 m/s flux-time θ_2, is given by

$$\Sigma_{FP2} = \int_0^{\theta_2} \sigma_{FP2}(\theta_2 - \theta_2') \frac{dN_{FP}'}{d\theta_2'} d\theta_2' \qquad (2.7.2)$$

where $\frac{dN_{FP}'}{d\theta_2'}$ is the number of fission products produced per unit flux time at θ_2'.

Fig.II.11., The Fuel Channel

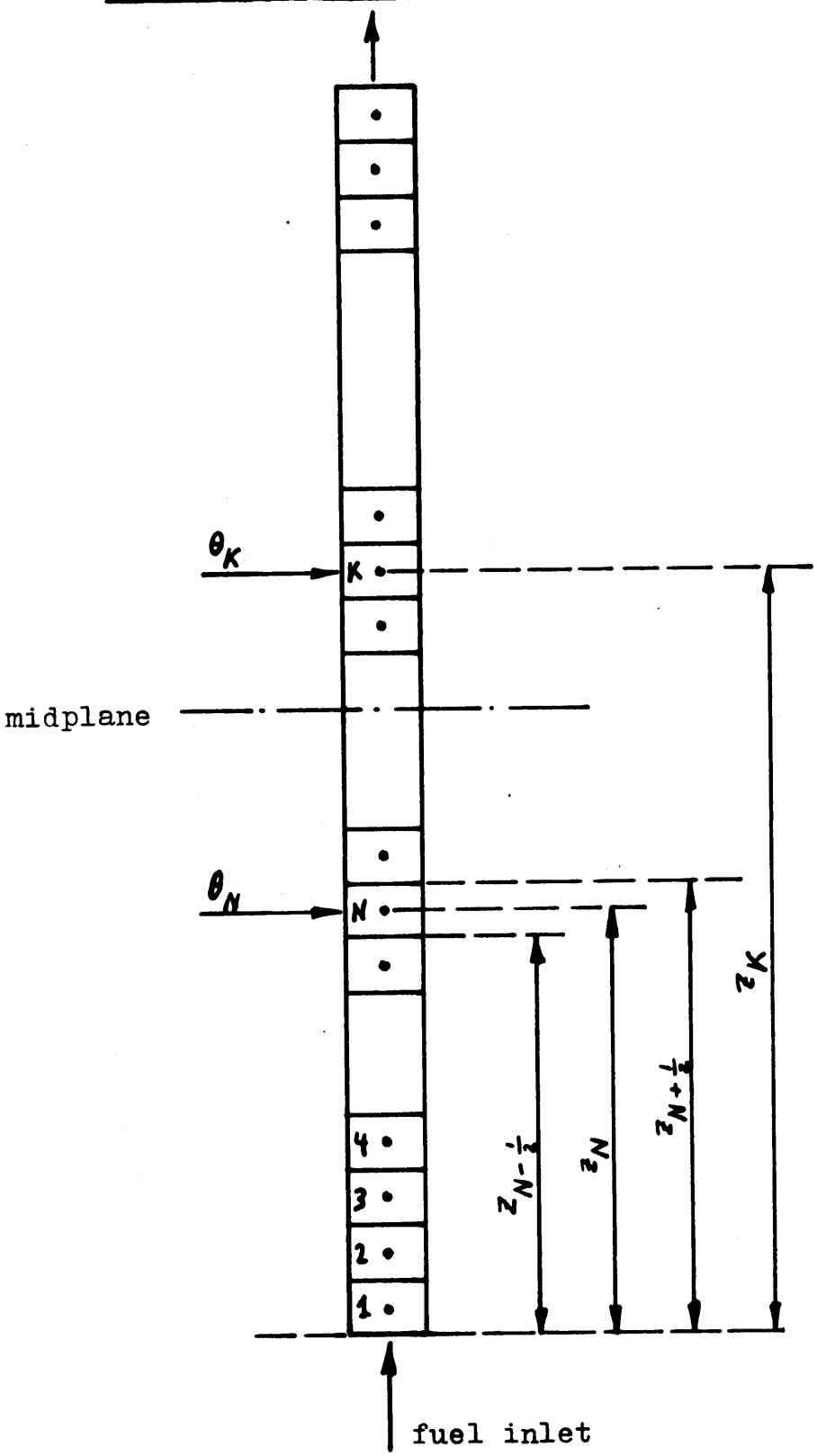

The above integral (Eq. 2.7.2) is evaluated numerically in the following way :

If z_K denotes the distance between the point K and the inlet end of the fuel channel (see Fig.II.11), the flux-time at z_K is given by

$$\theta_K = \sum_{N=1}^{K-1} [\phi_N \Delta t_N] + \frac{1}{2} \phi_K \Delta t_K \qquad (2.7.3)$$

where ϕ_N is the flux at z_N and Δt_N is the time it takes for the fuel to travel from $z_{N-\frac{1}{2}}$ to $z_{N+\frac{1}{2}}$ (Fig.II.11).

Assuming that the fission product cross sections vary as 1/v, we obtain the "2200 m/s flux-time", θ_{2K}, from the "real" flux-time, θ_K, simply by multiplying by g_w :

$$\theta_{2K} = \theta_K \, g_w \qquad (2.7.4)$$

where g_w has been defined in section 2.6. The subscript K again denotes the position of the fuel along the channel.

The total (2200 m/s) macroscopic fission product cross section at z_K is now given by

$$\Sigma_{FP2,K} = \sum_{N=1}^{K} \sigma_{FP2} (\theta_{2K} - \theta_{2N}) \Delta N_{FP,N}$$

where $\Delta N_{FP,N}$ is the number of fission products produced

during the time interval Δt_N. Inserting Eq.(2.7.1), we obtain

$$\Sigma_{FP2,K} = \sum_{N=1}^{K} \left[\sum_{i=1}^{3} y_i \sigma_i e^{-\sigma_i (\theta_{2K} - \theta_{2N})} \right] \Delta N_{FP,N}$$

which can also be written as

$$\Sigma_{FP2,K} = \sum_{N=1}^{K} \left[y_1 \sigma_1 \frac{QA_K}{QA_N} + y_2 \sigma_2 \frac{QB_K}{QB_N} + y_3 \sigma_3 \frac{QC_K}{QC_N} \right] \Delta N_{FP,N} \qquad (2.7.5)$$

where $QA_M = e^{-\sigma_1 \theta_{2M}}$

$QB_M = e^{-\sigma_2 \theta_{2M}}$

$QC_M = e^{-\sigma_3 \theta_{2M}}$

Finally, the effective macroscopic fission product cross section at z_K will be

$$\Sigma_{FP,K} = g_w \Sigma_{FP2,K} \qquad (2.7.6)$$

2.8. Spatial Considerations

The "condensed" two group diffusion equation (2.1.7) is a fourth order differential equation in ϕ :

$$D\nabla^2\phi + \frac{p_T\tau}{1-\varepsilon C_{11}}\nabla^2\left[\frac{\phi}{p_T}\left[\Sigma_a - \frac{D\nabla^2\phi}{\phi}\right]\right] = \left[\Sigma_a - \frac{\varepsilon p_T C_{10}}{1-\varepsilon C_{11}}\right]\phi$$

If the term $-\frac{D\nabla^2\phi}{\phi}$ (in the square brackets) is considered a given function of position, the equation reduces to a second order differential equation in ϕ.

In difference form, this equation can be written as

$$\underline{A}\,\underline{\phi} = \underline{B}\,\underline{\phi} \quad . \qquad (2.8.1)$$

For a total number of N mesh points in the reactor (refer to Fig.II.13), the matrix $\underline{A}$ is an N by N square matrix having five elements per row, $\underline{B}$ is an N by N diagonal matrix, and $\underline{\phi}$ is the N-dimensional flux vector.

Equation (2.8.1) is solved in a two stage iteration cycle shown in Fig.II.12. The inner iteration consists of a successive overrelaxation procedure (H2) with rescaling of the flux vector after each iterate. It computes the flux <u>shape</u>.

Fig.II.12., Simplified Flow Chart of Code

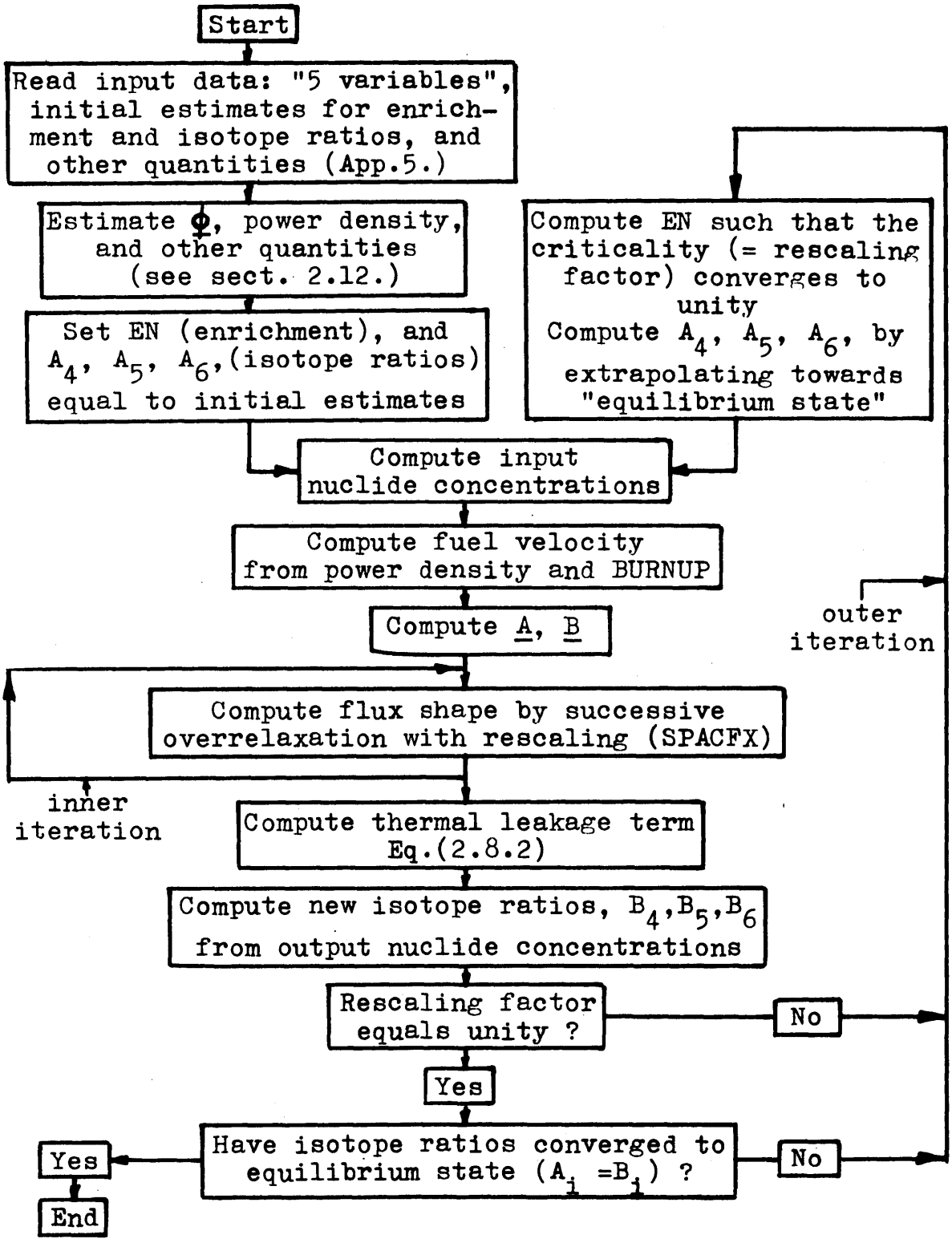

(Complete explanation of flow chart, see sect. 2.12.)

The outer iteration adjusts the fuel enrichment such that the rescaling factor in the inner iteration converges to unity, i.e., the reactor is just critical.

Also, in each outer iteration cycle, the quantity $-\frac{D\nabla^2\phi}{\phi}$ is reevaluated and fed into the elements of the matrix $\underline{A}$.

It was observed that, for reactors with blankets and reflectors, where the coefficients of the $\underline{A}$ and $\underline{B}$ matrices vary greatly from one region to another, the outer iteration may be unstable. This instability arises from a positive feedback mechanism due to the thermal leakage term $-\frac{D\nabla^2\phi}{\phi}$.

It was therefore necessary to introduce a damping factor, a, in the following way:

$$\left[\frac{-D\nabla^2\phi}{\phi}\right]^{k+1} = \frac{-D\nabla^2\phi_k}{\phi_k}\ (1-a) + \left[\frac{-D\nabla^2\phi}{\phi}\right]^{k}\ (a), \quad (2.8.2)$$

where $\left[\frac{-D\nabla^2\phi}{\phi}\right]^{k}$ is the thermal leakage term used in and held constant during the k^{th} (outer) iteration, and ϕ_k denotes the converged flux of the k^{th} (outer) iteration.

If a=0, there is no damping at all, and the procedure is the same as it was before. If a=1, the thermal leakage term stays constant, and, hence, it will always be equal to the initial estimate.

It was found that the iteration is stable for $a \geq 0.5$.

The Laplacian operator in cylindrical coordinates, with variable radial mesh spacing (see Fig.II.13), is

$$\nabla^2 u = \frac{\partial^2 u}{\partial r^2} + \frac{1}{r}\frac{\partial u}{\partial r} + \frac{\partial^2 u}{\partial z^2}$$

$$\approx \frac{\left[\frac{u_{i+1,j} - u_{i,j}}{\frac{1}{2}(g_{i+1}+g_i)}\right] - \left[\frac{u_{i,j} - u_{i-1,j}}{\frac{1}{2}(g_i+g_{i-1})}\right]}{\frac{1}{2}\left[\frac{1}{2}(g_{i+1}+g_i) + \frac{1}{2}(g_i+g_{i-1})\right]}$$

$$+ \frac{1}{r_i}\left[\frac{1}{2}\right]\left[\frac{u_{i+1,j} - u_{i,j}}{\frac{1}{2}(g_{i+1}+g_i)} + \frac{u_{i,j} - u_{i-1,j}}{\frac{1}{2}(g_i+g_{i-1})}\right]$$

$$+ \frac{1}{h^2}\left[u_{i,j+1} - 2\,u_{i,j} + u_{i,j-1}\right] \qquad (2.8.3)$$

where u represents any function of position and g_i, r_i, and h are shown in Fig.II.13.

The elements of the matrices $\underline{A}$ and $\underline{B}$ are readily evaluated from Eqns. (2.8.3) and (2.1.7).

Fig.II.13., Spatial Considerations

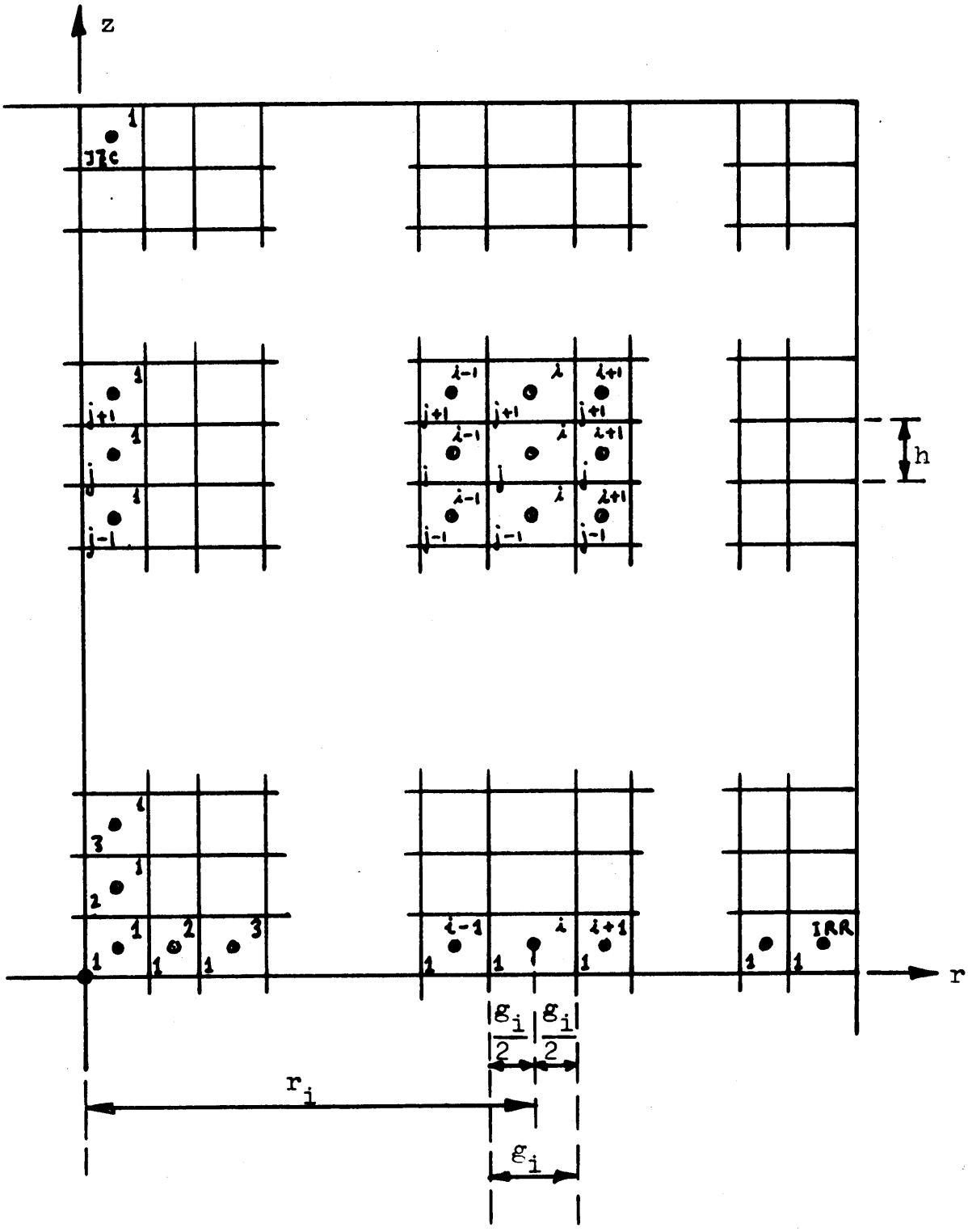

2.9. The Power Density

The power density in watts per cm^3 of reactor is proportional to n, the number of fissions per cm^3 of reactor per second. n consists of three parts :

$$n = n_{th} + n_f + n_{res} \quad . \tag{2.9.1}$$

n_{th}, n_f, and n_{res} represent the thermal, fast, and resonance fissions, respectively.

$$n_{th} = \left[N_3\sigma_{f3} + N_5\sigma_{f5}\right] \gamma_f v_{f1} \phi = C_{53}\phi \tag{2.9.1}$$

$$n_f = \frac{\eta_1 q(\varepsilon-1)}{\varepsilon(\eta_1-1)\nu_1} = \frac{\frac{q}{\phi}(\varepsilon-1)}{\varepsilon(\nu_1-1-\alpha_1)}\phi \tag{2.9.3}$$

$$n_{res} = \frac{qP_1}{\phi}\left[\frac{\langle 1-p\rangle_7}{1+\alpha_7} + p_{174}\frac{\langle 1-p\rangle_3}{1+\alpha_3} + \frac{\langle 1-p\rangle_9}{1+\alpha_9} + p_{174}\frac{\langle 1-p\rangle_5}{1+\alpha_5}\right]\phi$$

$$= \frac{qP_1}{\phi} C_{54}\phi \tag{2.9.4}$$

and, hence

$$n = \left[C_{53} + \frac{q}{\phi}\left[\frac{\varepsilon-1}{(\nu_1-1-\alpha_1)} + P_1 C_{54}\right]\right]\phi \tag{2.9.5}$$

A much more important parameter than the power density

is the "linear power" in kw per cm of fuel bundle, since this number determines the centerline temperature of the fuel.

The power density and the linear power are related by

$$(\text{power density}) = \frac{1}{A}(\text{linear power})$$

where A is the cross-sectional area of the unit cell.

2.10. The Equilibrium Cycle

As was pointed out in Chapter I., the purpose of this thesis is to investigate the characteristics of a CANDU-type reactor fueled with a mixture of ThO_2 and UO_2.

The fresh fuel which is fed continuously into the reactor core, cosists of

1. U^{233}, U^{234}, U^{235}, and U^{236} discharged from the reactor core and blanket (minus reprocessing and fabricating losses)
2. U^{233} produced by β decay of Pa^{233} which was present in the discharged fuel (optional)
3. Additional U^{235}, if necessary

} in the form of UO_2

4. Th^{232} fertile material — in the form of ThO_2

This scheme is based on the assumption that the separation of U-isotopes contained in the discharged fuel is unfeasible, and that there are no external sources of U^{233}, i.e., U^{233} is unavailable.

The blanket channels are fed with pure ThO_2.

If operation on this basis is continued for a long time, the higher uranium isotopes will build up and eventually reach their equilibrium concentrations.

It is useful to define the following quantities:

A_4 = number of atoms of U^{234} per atom of U^{233} in fresh fuel
A_5 = number of atoms of U^{235} per atom of U^{233} in fresh fuel
A_6 = number of atoms of U^{236} per atom of U^{233} in fresh fuel

The equilibrium values of these fractions are not known at the beginning. Initial estimates are therefore required. The "equilibrium state" is then approached in the following way:

For a given set of values A_4^k, A_5^k, A_6^{k*}, and a given enrichment EN^k (defined as the number of U^{233} and U^{235} atoms, divided by the total number of uranium and thorium atoms in the fresh fuel), the input nuclide concentrations are computed. Then, by using the latest converged flux shape and the current flux level, the nuclide concentration equations are solved along the fuel channel (from feed to discharge) and the output nuclide concentrations are obtained.

* The superscript k refers to the k^{th} (outer) iteration.

The entire fuel which is being discharged from the reactor (core and blanket) is then used, together with additional U^{235} makeup, if necessary, to make up a hypothetical fresh fuel having the same enrichment EN^k as the original fuel. This hypothetical fresh fuel will be characterized by certain uranium isotope ratios B_4^k, B_5^k, B_6^k.

The actual isotope ratios to be used for the feed in the $(k+1)^{st}$ iteration are then obtained from the equation:

$$A_i^{k+1} = B_i^k + x_i(B_i^k - A_i^k), \quad i=4,5,6 \qquad (2.10.1)$$

where the x_i's are extrapolation parameters used to speed up the convergence rate.

With these new isotope ratios (and with the new enrichment obtained from equation (2.12.1)), the whole cycle (see Fig.II.12.) is repeated, and the procedure is continued until, finally, in the N^{th} iteration, say, $B_i^N = A_i^N$, i=4,5,6. Clearly, this corresponds to the equilibrium state, since now, from Eq. (2.10.1),

$$A_i^{N+1} = A_i^N , \quad i=4,5,6.$$

2.11. Conversion Ratio

The following quantities are useful for the definition and evaluation of conversion ratios:

P = number of fissionable atoms produced in the reactor per unit time,

C = number of fissionable atoms consumed in the reactor per unit time,

F = number of fissionable atoms fed into the reactor per unit time,

D = number of fissionable atoms discharged from the reactor per unit time.

Obviously, $P-C = D-F$

The conversion ratio may be defined as (R1)

$$CR = \frac{P}{C} = \frac{D - F + C}{C}$$

In a thorium fueled reactor, the discharged fuel contains a considerable amount of Pa^{233} which will subsequently decay to fissionable U^{233}. If this Pa^{233} is included in the "fissionable atoms discharged from the reactor" the conversion ratio will be somewhat higher.

In addition, some of the "fissionable atoms discharged

from the reactor" will be lost in reprocessing and fabrication of new fuel. This loss may also be taken into account in the definition of the conversion ratio:

$$CR_L = \frac{P}{C + rD}$$

where r is the fraction lost in reprocessing and fabricating.

In this study, the assumption has been made that the cooling time for the spent fuel is long so that essentially all the Pa^{233} atoms are allowed to decay to U^{233} (this assumption is equivalen to setting IPADEC = 1, refer to section 2.12.). The Pa^{233} atoms are therefore included in the "fissionable atoms discharged from the reactor", and we have

$$CR = \frac{D^{23,25,13} - F^{23,25} + C^{23,25}}{C^{23,25}} \qquad (2.11.1)$$

$$CR_L = \frac{D^{23,25,13} - F^{23,25} + C^{23,25}}{C^{23,25} + rD^{23,25,13}} \qquad (2.11.2)$$

where the superscripts 23, 25, and 13 refer to U^{233}, U^{235}, and Pa^{233} respectively, and, e.g., $D^{23,25}$ is the number of atoms of U^{233} and U^{235} discharged from the reactor per unit time.

2.12. Flow Chart of Code

2.12.1. "Simplified Flow Chart"

The simplified flow chart is shown in Fig.II.12. The inner iteration computes the flux shape, as explained in sect. 2.8.

The outer iteration actually consists of two parts: the first computes the critical enrichment, and the second computes the equilibrium isotope ratios. Originally, these two iterations were done in two separate loops, the "inner" being the "enrichment-criticality loop", and the "outer" was used to find the equilibrium isotope ratios.

By combining these two iterations into a single loop, the computation time could be reduced substantially. With this new method, however, intermediate steps of the iteration do not correspond to critical reactors. This is due to the fact that the criticality depends not only on the enrichment, but also on the isotope ratios, so that a critical reactor emerges only at the end, i.e., when the isotope ratios have reached their equilibrium values.

The flux shape, on the other hand, is essentially independent of the enrichment and isotope ratios, so that, after the first few (outer) loops, the number of inner loops (SPACFX) per outer loop is very small (2 to 3).

2.12.2. Complete Flow Chart of the Code

The logic flow of the code is shown in the figure below. All symbols and names of subroutines are explained at the end of this section.

Fig.II.14., The Complete Flow Chart

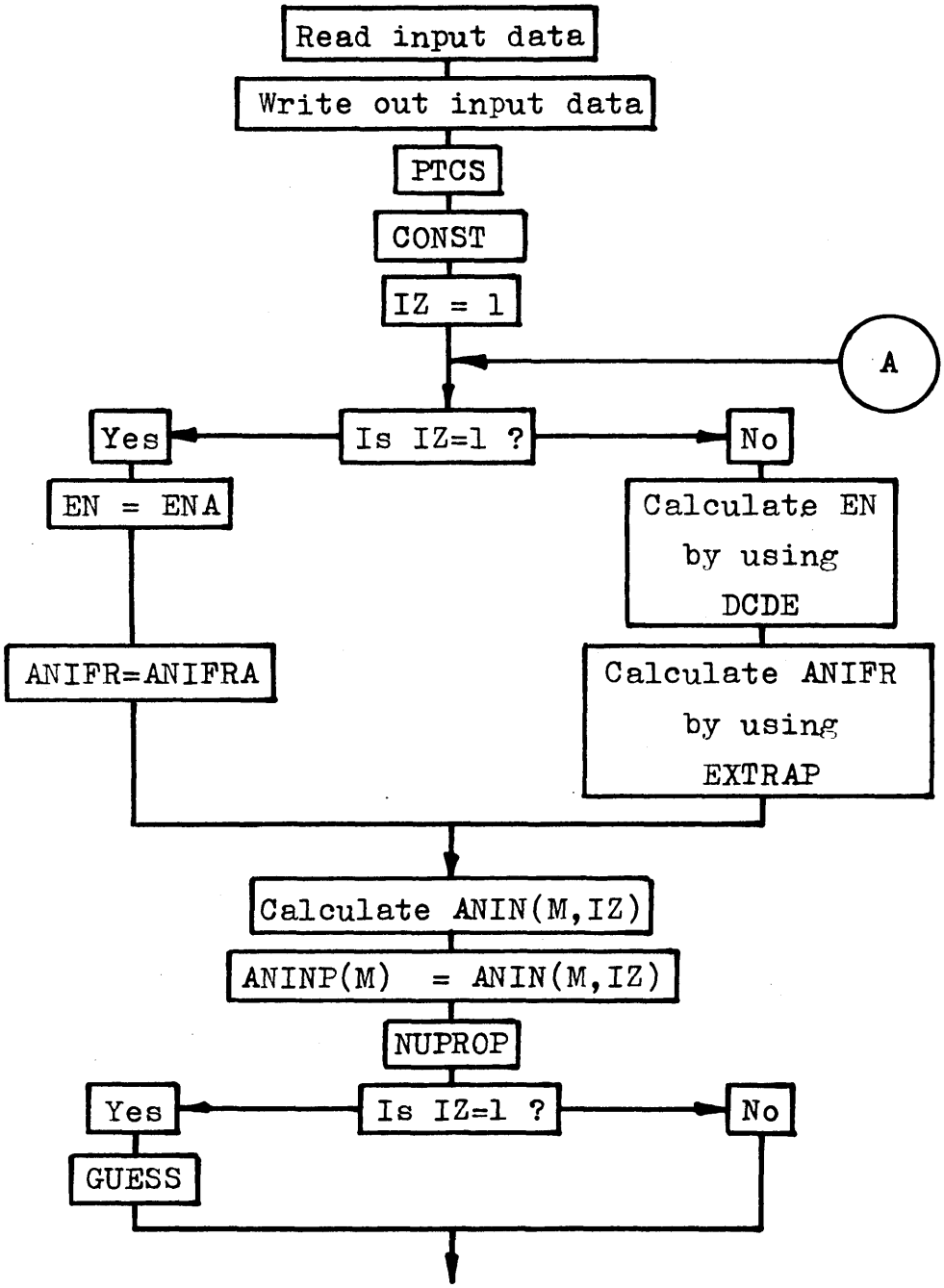

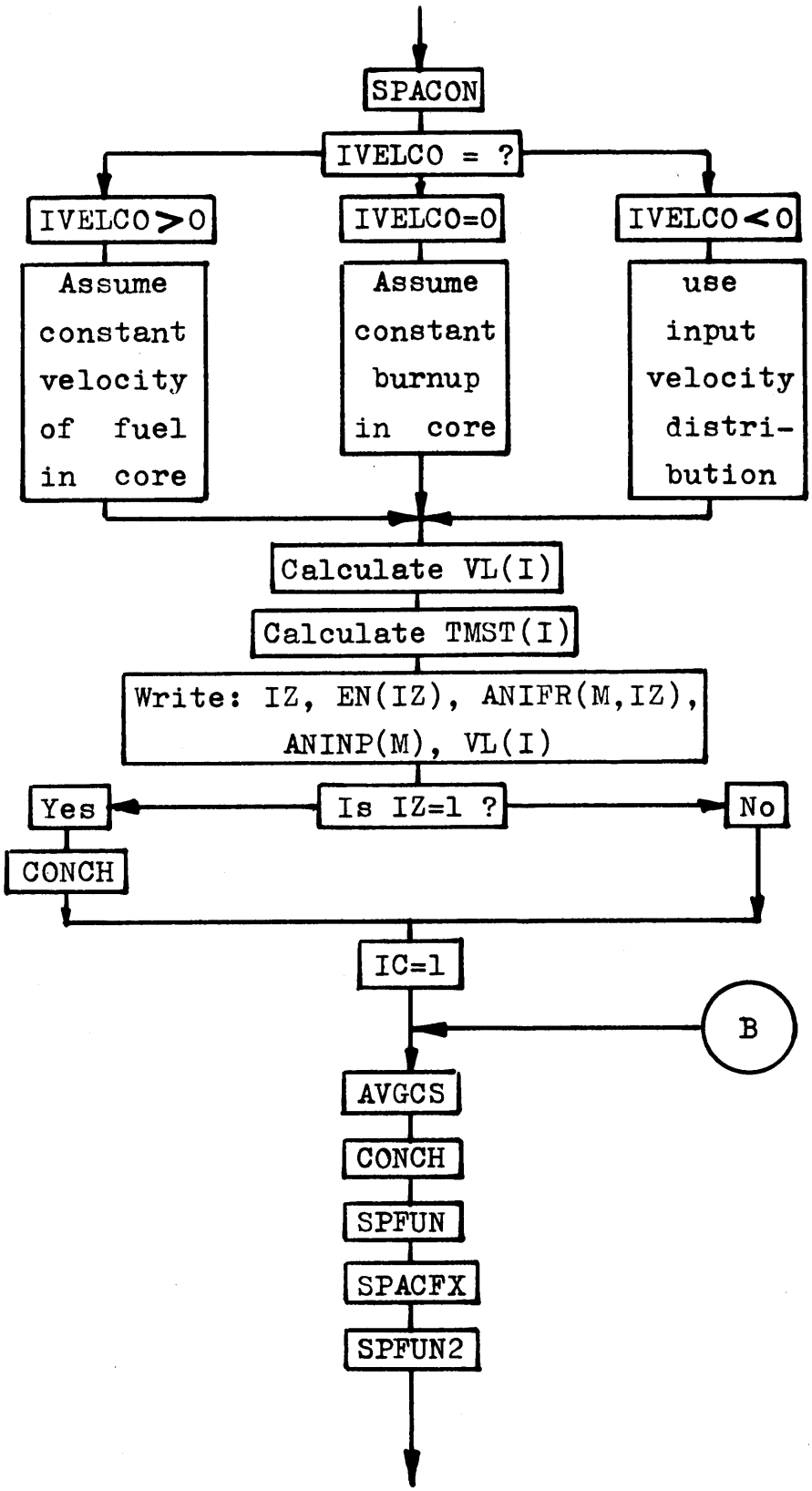
SPACON
(14)
IVELCO = ?
(15)
IVELCO>0
IVELCO=0
IVELCO<0
Assume constant velocity of fuel in core
Assume constant burnup in core
use input velocity distri-bution
(16)
Calculate VL(I)
(17)
Calculate TMST(I)
(18)
Write: IZ, EN(IZ), ANIFR(M,IZ), ANINP(M), VL(I)
(19)
Yes
Is IZ=1 ?
No
(20)
CONCH
(21)
IC=1
(22)
B
AVGCS
(23)
CONCH
(24)
SPFUN
(25)
SPACFX
(26)
SPFUN2
(27)

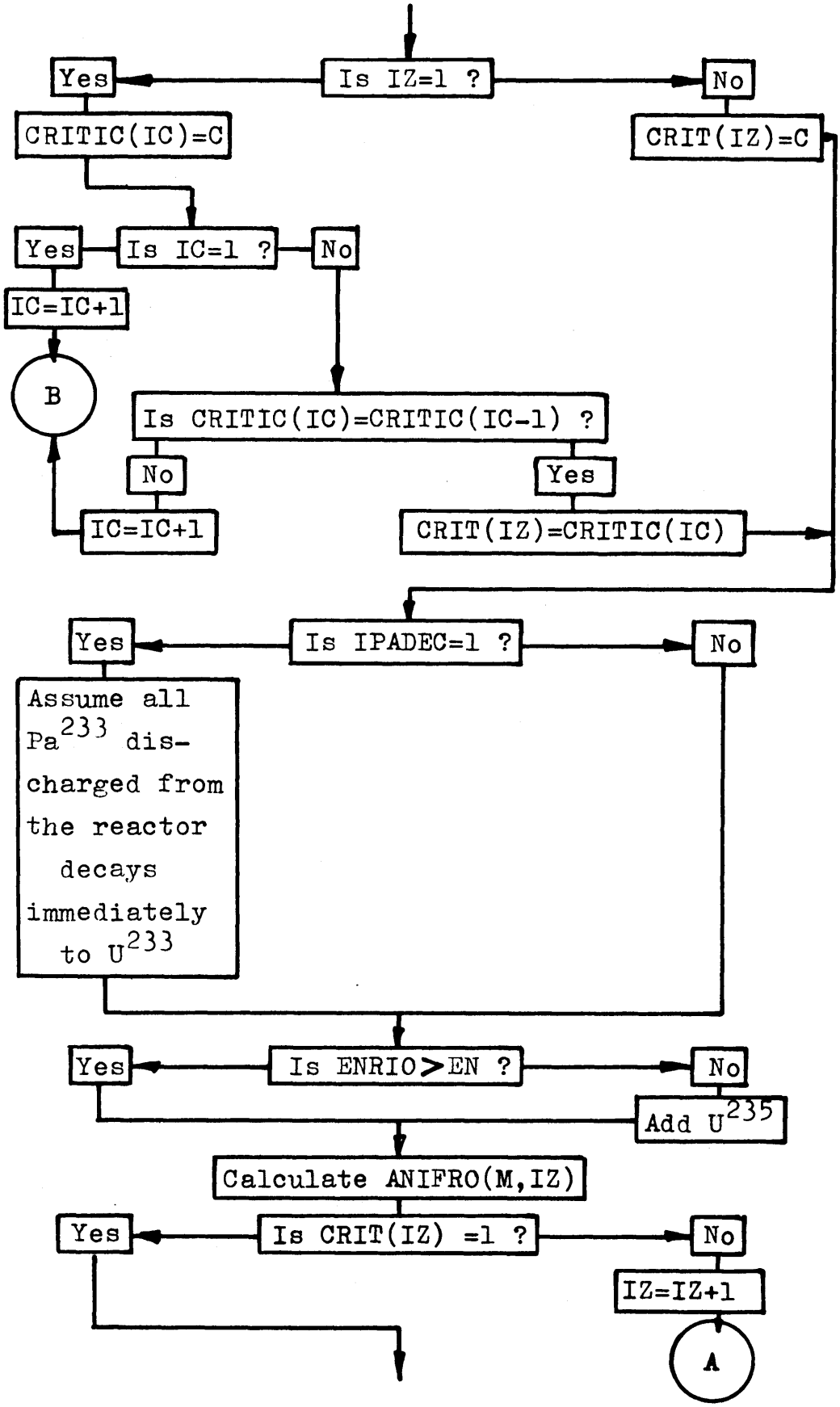
Is IZ=1 ?
Yes
No
(28)
CRITIC(IC)=C
CRIT(IZ)=C
(29)
Yes
Is IC=1 ?
No
(30)
IC=IC+1
(31)
B
Is CRITIC(IC)=CRITIC(IC-1) ?
(32)
No
Yes
IC=IC+1
CRIT(IZ)=CRITIC(IC)
(33)
Is IPADEC=1 ?
Yes
No
(34)
Assume all Pa233 discharged from the reactor decays immediately to U233
(35)
Is ENRIO>EN ?
Yes
No
(36)
Add U235
(37)
Calculate ANIFRO(M,IZ)
(38)
Is CRIT(IZ) =1 ?
Yes
No
(39)
IZ=IZ+1
(40)
A

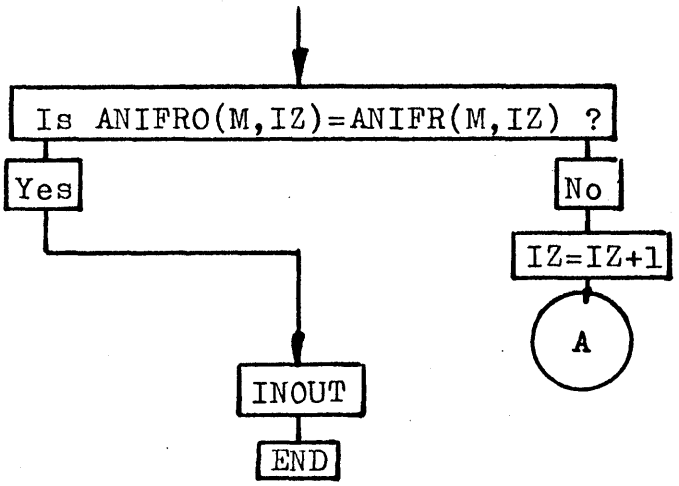

The various steps shown in the above diagram are explained below:

Step

(3) Subroutine PTCS calculates cross sections as a function of neutron energy (Eqns. 2.2.1. and 2.2.2.)

(4) Subroutine CONST supplies additional nuclear data (see Appendix 1.)

(5) IZ is the iteration parameter for the outer iteration loop.

(7) The enrichment EN is defined as the number of U^{233} and U^{235} atoms divided by the total number of uranium and thorium atoms in the fresh fuel.

If IZ=1, EN is set equal to ENA, an initial guess which is supplied as input to the code.

If IZ>1, EN is calculated from the equation

$$EN(IZ) = EN(IZ-1) + \frac{1 - CRIT(IZ-1)}{DCDE} \qquad (2.12.1)$$

where CRIT(IZ-1) is the criticality of the previous loop, and DCDE is an input parameter.

(8) The quantities ANIFR(4), ANIFR(5), and ANIFR(6) are the isotope fractions defined in section 2.10. (i.e., A_4, A_5, and A_6).

At the beginning (IZ=1) these fractions are set equal to initial estimates (ANIFRA(4), ANIFRA(5), and ANIFRA(6)).

If IZ>1, ANIFR(M) is determined from Eq. 2.10.1., where the A's are the ANIFR's and the B's are the ANIFRO's (see step (38)).

(9) ANIN(M,IZ) is the concentration of the M^{th} nuclide (in atoms per barn-cm) in the fresh fuel, in the IZ^{th} (outer) iteration. The notation is as follows:

M	nuclide
1	Th^{232}
2	Pa^{233}
3	U^{233}
4	U^{234}
5	U^{235}
6	U^{236}

First, the concentration of U^{233} is evaluated from the equation:

$$ANIN(3,IZ)=\frac{ANTHO2}{\left[1+\sum_{M=4}^{6}ANIFR(M,IZ)\right]\left[\frac{ANTHO2}{ANUO2}-1\right]+\left[\frac{1+ANIFR(5,IZ)}{EN(IZ)}\right]} \qquad (2.12.2)$$

where ANTHO2 is the number of thorium atoms per barn-cm of pure ThO_2, and ANUO2 is the number of atoms of uranium in pure UO_2. ANTHO2 and ANUO2 are calculated from the densities of the corresponding oxides (which are input numbers). (see Appendix 2.)

Then, the concentrations of U^{234}, U^{235}, and U^{236} are given by

$$ANIN(M,IZ) = ANIN(3,IZ) \times ANIFR(M,IZ) \ , \ M=4,5,6 \qquad (2.12.3)$$

and the concentration of Th^{232} is

$$ANIN(1,IZ) = ANTHO2\left[1-\frac{ANIN(3,IZ)\left[1+\sum_{M=4}^{6} ANIFR(M,IZ)\right]}{ANUO2}\right]$$

The Pa^{233} concentration in the fresh fuel is assumed to be zero:

$$ANIN(2,IZ) = 0.$$

(11) Subroutine NUPROP calculates the nuclear properties described in section 2.3.

(13) Subroutine GUESS provides initial estimates of various quantities, such as the fast non-leakage probability P_1, the thermal neutron flux ϕ, the microscopic, Wilkins-hardened cross sections σ_i, the slowing down density divided by the thermal flux, q/ϕ, and the thermal leakage, $\frac{-D\nabla^2\phi}{\phi}$.

(14) Subroutine SPACON evaluates the coefficients of the ∇^2 operator in difference form (Eq. 2.8.3).

(17) VL(I), or VL_i is the velocity of the fuel (in cm/sec) at the i^{th} radial mesh point.

(a) Core

VL_i for the core channels is evaluated in three different

ways depending on the value of the control parameter IVELCO:

If IVELCO >0, the velocity is assumed constant in all core channels, and

$$VL_i = VELOC =$$

$$\frac{CH \sum_{i=1}^{IRC} 2\pi r_i g_i \quad \frac{1}{JZC} \sum_{j=1}^{JZC} POWD_{i,j}}{3600 \times 24 \times VFL \times BURNUP \sum_{i=1}^{IRC} 2\pi r_i g_i \sum_{M=1}^{6} \frac{ANINP(M) \times ATWT(M)}{0.6025}} \qquad (2.12.4)$$

where CH is the core height, r_i and g_i are defined in Fig.II.13., and the rest of the symbols are explained in Chapter VI.

The term

$$\sum_{M=1}^{6} \frac{ANINP(M) \times ATWT(M)}{0.6025}$$

is the number of grams of Th and U per cm^3 of fuel.

If IVELCO = 0, the velocity distribution is computed in such a way that the fuel burnup, in MWD per tonne of Th and U, is constant for all core channels:

$$VL_i = \frac{CH \frac{1}{JZC} \sum_{j=1}^{JZC} POWD_{i,j}}{3600 * 24 * VFL * BURNUP \sum_{M=1}^{6} \frac{ANINP(M) * ATWT(M)}{0.6025}} \qquad (2.12.5)$$

If IVELCO < 0, an input velocity distribution, VLD_i, is used in the following way:

Since the average burnup in the core is equal to

$$BURNUP = \frac{CH \sum_{i=1}^{IRC} 2\pi r_i g_i \frac{1}{JZC} \sum_{j=1}^{JZC} POWD_{i,j}}{3600 * 24 * VFL \sum_{i=1}^{IRC} 2\pi r_i g_i VL_i \sum_{M=1}^{6} \frac{ANINP(M) * ATWT(M)}{0.6025}},$$

it follows that

$$\sum_{i=1}^{IRC} r_i g_i VL_i = \frac{CH \sum_{i=1}^{IRC} r_i g_i \frac{1}{JZC} \sum_{j=1}^{JZC} POWD_{i,j}}{3600 * 24 * VFL * BURNUP \sum_{M=1}^{6} \frac{ANINP(M) * ATWT(M)}{0.6025}}, \qquad (2.12.6)$$

and

$$VL_i = VLD_i \frac{\sum_{i=1}^{IRC} r_i g_i VL_i}{\sum_{i=1}^{IRC} r_i g_i VLD_i} \qquad (2.12.7)$$

(b) Blanket

The velocity of the fuel in the blanket channels is given in terms of the "blanket dicharge flux-time", THETAB (n/kb), which is an input parameter:

$$VL_{i_{Blanket}} = \frac{CH * \Psi_f \sum_{j=1}^{JZC} \phi_{i,j}}{JZC * THETAB * 10^{21}} \qquad (2.12.8)$$

(18) TMST(I) is the time it takes for the fuel to travel from one mesh point to the next. It is given by

$$TMST(I) = \frac{0.5 * CH}{JZC * VL(I)} \qquad (2.12.9)$$

(21) Subroutine CONCH solves the nuclide concentration equations (sect. 2.5.), calculates the macroscopic (low cross section) fission product cross section (sect. 2.7.), and determines the "six homogenized properties" as a function of position in the reactor (sect. 2.6.).

(22) IC is an iteration parameter. It is used to find the criticality CRIT(IZ) which corresponds to the enrichment EN(IZ). For IZ >1, the IC-iteration is bypassed, i.e., it is assumed that the criticality CRITIC(IC) has con-

verged to the value CRIT(IZ), which is the characteristic value for the enrichment EN(IZ), after one loop.

(23) Subroutine AVGCS computes the thermal neutron spectrum (sect. 2.2.2.), and the effective microscopic cross sections (sect. 2.2.3.).

(25) Subroutine SPFUN evaluates the coefficients of the $\underline{A}$ and $\underline{B}$ matrices (sect. 2.8.)

(26) Subroutine SPACFX computes the flux shape by a successive overrelaxation method described in sect. 2.8.

SPACFX also gives the "criticality", C, which is equal to the rescaling factor for the converged flux.

C is related to the effective multiplication factor, k_{eff} by

$$(1 - C) = \beta(1 - k_{eff}) \qquad (2.12.10)$$

where β is a constant which depends on the overrelaxation parameter used in the iteration.

(27) Subroutine SPFUN2 computes the thermal leakage term

$$C_{36} = \frac{-D\nabla^2\phi}{\phi}$$

by using the latest converged flux shape (Eq. 2.8.2.)

(34) IPADEC is a control parameter. If IPADEC = 1, all Pa^{233} discharged from the reactor is assumed to decay immediately to U^{233} (or, equivalently, the discharged fuel is allowed to cool for a very long time). If IPADEC = 0, the Pa^{233} in the discharged fuel does not decay and is separated from the uranium in reprocessing.

It is realized that both these assumptions are somewhat unrealistic. But, clearly, as far as the performance of the system is concerned, they represent an upper and a lower bound, and the true situation will lie somewhere in between.

(36) ENRIO is the feed enrichment which could be obtained by reprocessing the discharged fuel without adding U^{235} (refer to sect. 2.10.). It is given by

$$\text{ENRIO} = \frac{\text{ANINPO(3)} + \text{ANINPO(5)}}{\text{ANTHO2} + \left[1 - \frac{\text{ANTHO2}}{\text{ANUO2}}\right] \sum_{M=3}^{6} \text{ANINPO(M)}} \qquad (2.12.11)$$

For IPADEC = 0,

$$\text{ANINPO(M)} = (1\text{-ROSS}) \frac{\sum_{I=1}^{IRB} VL_I r_I g_I \text{ANOUT(M,I)}}{\sum_{I=1}^{IRC} VL_I r_I g_I}, \quad M=3,4,5,6 \qquad (2.12.12)$$

For IPADEC = 1,

$$ANINPO(3) = (1-ROSS)\frac{\sum_{I=1}^{IRB} VL_I r_I g_I (ANOUT(2,I)+ANOUT(3,I))}{\sum_{I=1}^{IRC} VL_I r_I g_I}, \qquad (2.12.13)$$

and ANINPO(4), ANINPO(5), and ANINPO(6) are the same as above (Eq. 2.12.12.).

ANOUT(M,I) is the concentration of the M^{th} nuclide in the fuel being discharged from the channel at radial position I. The notation is the same as for ANIN (see step (9)).

If ENRIO > EN, the reactor does not need any additional U^{235}, i.e., it breeds.

(37) If ENRIO < EN, the value of ANINPO(5) must be increased such that the resulting enrichment is EN. Replacing ENRIO by EN in Eq. 2.12.11., and solving for ANINPO(5) yields

$$ANINPO(5) = \frac{ANINPO(3) - EN\left[ANTHO2 + \left[1 - \frac{ANTHO2}{ANUO2}\right]\sum_{\substack{M=3 \\ M\neq 5}}^{6} ANINPO(M)\right]}{EN * \left[1 - \frac{ANTHO2}{ANUO2}\right] - 1} \qquad (2.12.14)$$

(38) The isotope fractions ANIFRO(M,IZ) ($=B_M^{IZ}$, section 2.10.) are then given by

$$\text{ANIFRO(M,IZ)} = \frac{\text{ANINPO(M)}}{\text{ANINPO(3)}} , \qquad (2.12.15)$$

$$M=4,5,6.$$

(39) Two tests are made at the end of the IZ-loop. The first is concerned with the criticality. If CRIT(IZ) is not close to unity, the parameter IZ is increased by one and steps (6) through (38) are repeated. If CRIT(IZ) satisfies the inequality

$$(1 - \text{CRDEL2}) < \text{CRIT(IZ)} < (1 + \text{CRDEL2}) \qquad (2.12.16)$$

where CRDEL2 is the "convergence criterion", an input number, the program proceeds to the second test:

(41) In order to pass the second test, the three inequalities

$$\left| \frac{\text{ANIFRO(M,IZ)} - \text{ANIFR(M,IZ)}}{\text{ANIFR(M,IZ)}} \right| < \text{ANDEL} , \quad M = 4, 5, 6 \qquad (2.12.17)$$

must be satisfied. ANDEL is the convergence criterion for the isotope fractions.

(42) If either one of the equations (2.12.17) is not satisfied, the IZ-loop is repeated.

(43) Subroutine INOUT computes (and writes out) the fuel burnup as a function of radius, the maximum burnup in the core, the average burnup in the blanket, the total power in the core, the total power in the blanket, the feed and output of each nuclide in kg/day, and the two conversion ratios defined in section 2.11.

(44) At the end, the following quantities (which are all characteristic of the "equilibrium cycle", sect. 2.10.) are printed out:

(a) Nuclide concentrations as a function of position in the reactor (CONCH),
(b) nuclear properties (NUPROP),
(c) the coefficients of the ∇^2 operator (SPACON),
(d) the thermal neutron spectrum and the microscopic Wilkins-hardened cross sections (AVGCS),
(e) the coefficients of the $\underline{A}$ and $\underline{B}$ matrices (SPFUN),
(f) the "six homogenized properties" (CONCH),
(g) the flux and power density distributions.

III. Application of Code, Results

3.1. Effects of the "Five Variables"

In this section, the results of 21 computer runs will be presented. Starting from a "standard" set of input data, only one parameter is varied at a time.

It is realized that this procedure does not give the whole picture because there may be interactions between the variables such that the individual effects do not simply add up.

Nevertheless, this type of investigation may be quite useful since it is able to show the major trends without requiring an excessive number of cases to be run.

The "standard" values of the "five variables" (see Chap.I.) are:

Blanket radius,	BR	= 255.0 cm
Fuel volume fraction,	VFL	= 0.0567
Avg. burnup in core,	BURNUP	= 10000 MWD/tonne
Max. linear power,	PDNLM	= 8.712 kw/cm
Recycle losses,	ROSS	= 2.0 %

These values correspond to the CANDU design, except for the blanket radius and the recycle losses, of course (CANDU has no blanket and does not recycle the spent fuel, in fact, it operates on a "throw-away" cycle).

In the reactor considered here, all fuel channels, including the blanket channels, have the same physical dimensions as the CANDU fuel channels. A square lattice is assumed, as in CANDU. The pitch (which is equal to 9.0 inches (22.86 cm) in the CANDU reactor) is considered a variable, here. It is related to the fuel volume fraction by

$$VFL = VFL_{CANDU} \left[\frac{pitch_{CANDU}}{pitch} \right]^2 \qquad (3.1.1)$$

where $VFL_{CANDU} = 0.0567$, and $pitch_{CANDU} = 22.86$ cm.

Similarly, the number of fuel channels in the core, n_{Ch}, (which is 306 in CANDU) can be related to the fuel volume fraction, VFL, by

$$n_{Ch} = n_{Ch,CANDU} \left[\frac{VFL}{VFL_{CANDU}} \right] \qquad (3.1.2)$$

where $n_{Ch,CANDU} = 306$. The table below gives the pitch and the number of fuel channels in the core as a function of VFL.

VFL	pitch	n_{Ch}
0.0167	42.12 cm	90
0.0267	33.31 cm	144
0.0367	28.42 cm	198
0.0467	25.19 cm	252
0.0567	22.86 cm	306
0.0667	21.08 cm	360

The pitch is assumed to be the same for core and blanket.

The following input parameters were kept constant throughout the entire investigation:

Core radius, R	= 225.61 cm
Outside radius of reflector	= 299.70 cm
Core height (= channel length), CH	= 500.40 cm
Blanket discharge flux-time, THETAB	= 0.1 n/kb
Infinite cooling time for spent fuel: IPADEC	= 1
Constant fuel velocity in core: IVELCO	= 1

The values for the core radius, the outside radius of the reflector, and the core height are taken from the CANDU reference design (Appendix 2). The control parameters IPADEC and IVELCO are explained in sect. 2.12.

The two conversion ratios given in the tables and figures below are defined in sect. 2.11.

The "transit time" of the fuel mentioned in Chap.I., is related to the fuel velocity, VL, by

$$\text{Transit time, full-power days} = \frac{\text{Core height, cm}}{3600 \times 24 \times (\text{VL, cm/sec})} \qquad (3.1.3)$$

Table III.1., Effect of Blanket Radius on Performance of Thorium Fueled CANDU Reactor

Fuel volume fraction, VFL = 0.0567 — Max. linear power = 8.712 kw/cm

Average burnup = 10000 MWD/tonne — Uranium recycle loss = 2.0 %

Outside radius of blanket, BR, cm		225.61	240.00	255.00	270.00
Core					
Enrichment, a/o U-233 + U-235 in U and Th		1.971	1.995	1.993	1.992
Atom ratio in feed	U-234/U-233, A_4	0.3893	0.3751	0.3743	0.3740
	U-235/U-233, A_5	0.4487	0.3606	0.3334	0.3237
	U-236/U-233, A_6	0.7905	0.6121	0.5610	0.5514
Fuel velocity, VL, $x10^5$, cm/sec		1.1632	0.9907	0.9861	0.9954
Power, thermal MW		752.1	643.3	638.7	643.3
Max./avg. burnup		1.303	1.525	1.547	1.543
Max./avg. power density		1.774	2.074	2.089	2.074
Max. thermal flux, ϕ, $x10^{-14}$, n/cm^2sec		1.406	1.408	1.408	1.408
Blanket					
Fuel velocity, VL_i, $x10^5$, cm/sec, radial zone	i=15	-	5.757	4.387	4.241
	i=16	-	-	2.489	2.080
	i=17	-	-	-	1.023
Power, thermal MW		0	0.3713	0.5718	0.6679
Avg. burnup, MWD/tonne		-	7.629	9.411	10.092
Total					
U-235 makeup rate, g/MWD		0.2484	0.1988	0.1834	0.1782
Conversion ratio					
in core and blanket, CR		0.8134	0.8570	0.8708	0.8756
overall, allowing for recycle losses, CR_L		0.7888	0.8300	0.8430	0.8476

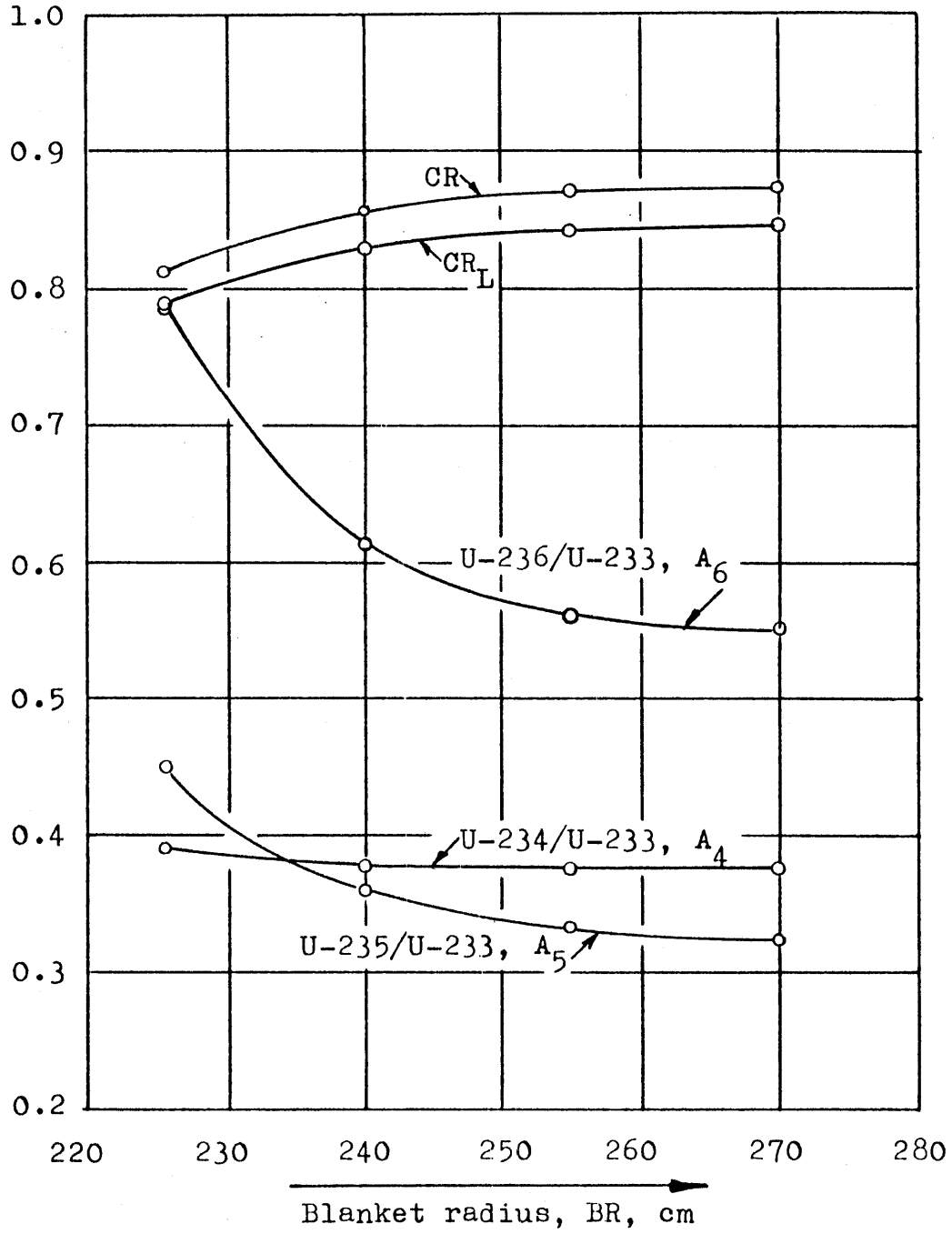

Fig.III.1., Conversion Ratio and Atom Ratios as a Function of the Outside Radius of the Blanket (see Table III.1.)

Table III.2., Effect of Fuel Volume Fraction on Performance of Thorium Fueled CANDU Reactor

Blanket radius, BR = 255.0 cm — Avg. burnup = 10000 MWD/tonne

Max. linear power, PDNLM = 8.712 kw/cm — Uranium recycle loss = 2.0 %

Fuel volume fraction, VFL	0.0167	0.0267	0.0367	0.0467	0.0567	0.0667
Core						
Enrichment, a/o U-233 + U-235 in U and Th	1.991	1.838	1.837	1.898	1.993	2.127
Atom ratio in feed: U-234/U233, A_4	0.4266	0.4177	0.4060	0.3904	0.3743	0.3561
Atom ratio in feed: U-235/U233, A_5	0.3459	0.2532	0.2520	0.2853	0.3334	0.3969
Atom ratio in feed: U-236/U233, A_6	0.8528	0.5926	0.5317	0.5525	0.5610	0.5976
Fuel velocity, VL, $x10^5$, cm/sec	0.9147	0.9413	0.9633	0.9749	0.9861	1.0122
Power, thermal MW	174.1	286.0	402.5	518.7	638.7	768.4
Max./avg. burnup	1.578	1.582	1.571	1.558	1.547	1.524
Max./avg. power density	2.257	2.197	2.145	2.118	2.089	2.042
Max. thermal flux, ϕ, $x10^{-14}$, n/cm^2sec	2.197	1.953	1.746	1.567	1.408	1.260
Blanket						
Fuel velocity, VL_i, $x10^5$, cm/sec, radial zone i=15	6.146	5.490	5.028	4.666	4.387	4.231
i=16	4.078	3.429	3.002	2.702	2.489	2.375
Power, thermal MW	0.1954	0.2952	0.3899	0.4808	0.5718	0.6672
Avg. burnup, MWD/tonne	7.326	7.942	8.483	8.963	9.411	9.717
Total						
U-235 makeup rate, g/MWD	0.2113	0.1428	0.1380	0.1569	0.1834	0.2182
Conversion ratio, in core and blanket, CR	0.8546	0.9090	0.9118	0.8946	0.8708	0.8394
Conversion ratio, overall, allowing for recycle losses, CR_L	0.8293	0.8829	0.8852	0.8675	0.8430	0.8106

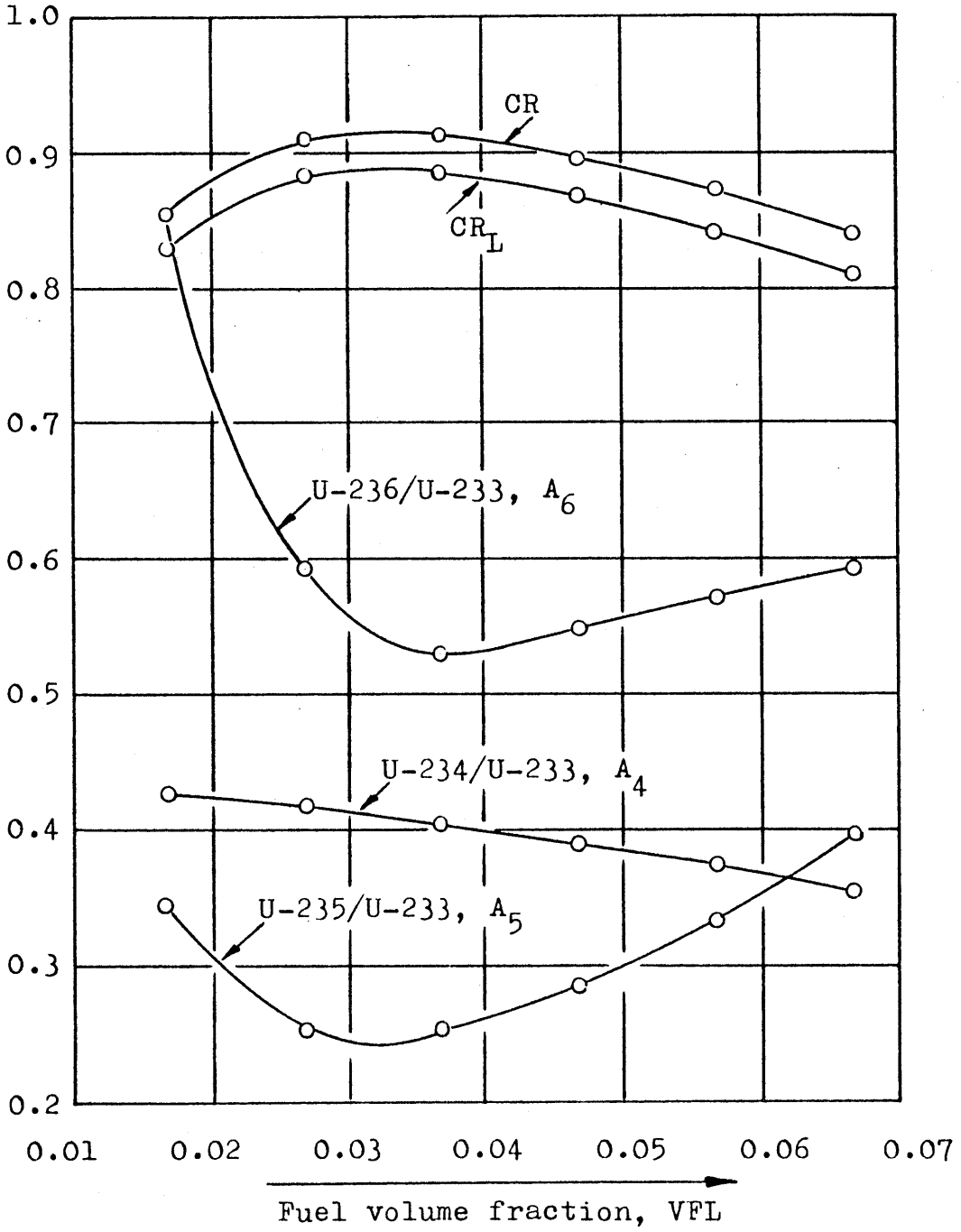

Fig.III.2., Conversion Ratio and Atom Ratios as a Function of the Fuel Volume Fraction

(see Table III.2.)

Table III.3., Effect of Average Burnup on Performance of Thorium Fueled CANDU Reactor

Blanket radius, BR = 255.0 cm — Fuel volume fraction, VFL = 0.0567

Max. linear power = 8.712 kw/cm — Uranium recycle loss = 2.0 %

Average fuel burnup in core, MWD/tonne	4000	6000	8000	10000	12000
Core					
Enrichment, a/o U-233 + U-235 in U and Th	1.793	1.862	1.927	1.993	2.063
Atom ratio in feed: U-234/U-233, A_4	0.3198	0.3461	0.3635	0.3743	0.3809
Atom ratio in feed: U-235/U-233, A_5	0.2791	0.2857	0.3070	0.3334	0.3647
Atom ratio in feed: U-236/U-233, A_6	0.3473	0.4153	0.4888	0.5610	0.6428
Fuel velocity, VL, $x10^5$, cm/sec	2.273	1.555	1.200	0.9861	0.8579
Power, thermal MW	568.1	603.4	621.4	638.7	664.7
Max./avg. burnup	1.643	1.610	1.577	1.547	1.506
Max./avg. power density	2.276	2.213	2.148	2.089	2.007
Max. thermal flux, ϕ, $x10^{-14}$, n/cm^2sec	1.421	1.414	1.410	1.408	1.407
Blanket					
Fuel velocity, VL_i, $x10^5$, cm/sec, radial zone i=15	3.843	4.016	4.202	4.387	4.663
i=16	2.169	2.272	2.381	2.489	2.647
Power, thermal MW	0.5184	0.5370	0.5547	0.5718	0.5933
Avg. burnup, MWD/tonne	9.759	9.664	9.536	9.411	9.183
Total					
U-235 makeup rate, g/MWD	0.1940	0.1787	0.1789	0.1834	0.1923
Conversion ratio, in core and blanket, CR	0.9058	0.8943	0.8822	0.8708	0.8585
Conversion ratio, overall, allowing for recycle losses, CR_L	0.8395	0.8488	0.8476	0.8430	0.8353

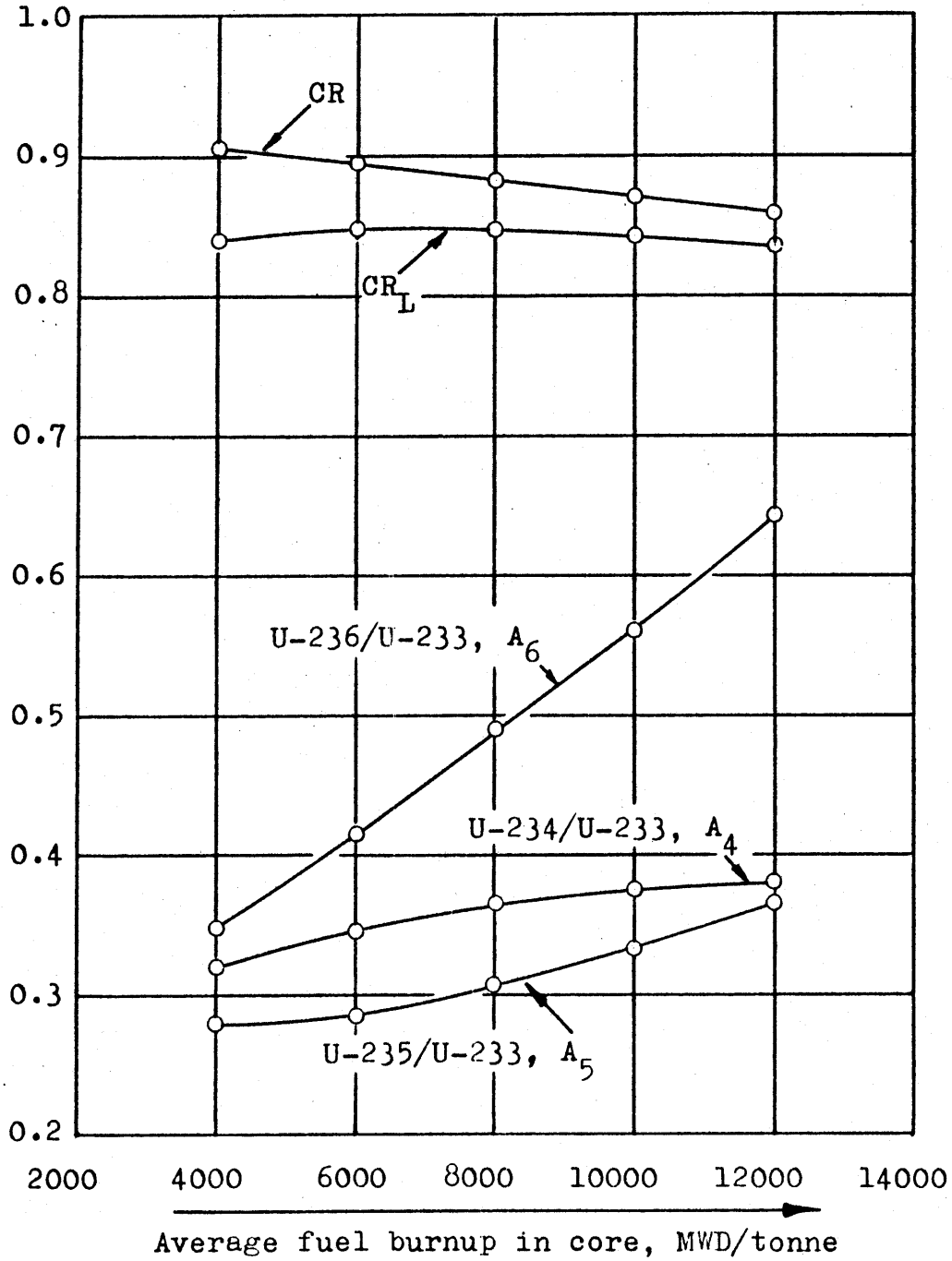

Fig.III.3., Conversion Ratio and Atom Ratios as a Function of the Average Fuel Burnup

(see Table III.3.)

Table III.4., Effect of Maximum Linear Power on Performance of Thorium Fueled CANDU Reactor

Blanket radius, BR = 255.0 cm — Fuel volume fraction, VFL = 0.0567

Average burnup = 10000 MWD/tonne — Uranium recycle loss = 2.0 %

Maximum linear power, kw/cm	4.712	6.712	8.712	10.712	12.712
Core					
Enrichment, a/o U-233 + U-235 in U and Th	1.880	1.939	1.993	2.045	2.090
Atom ratio in feed { U-234/U-233, A_4	0.3640	0.3693	0.3743	0.3788	0.3819
Atom ratio in feed { U-235/U-233, A_5	0.2804	0.3081	0.3334	0.3568	0.3761
Atom ratio in feed { U-236/U-233, A_6	0.4788	0.5165	0.5610	0.6077	0.6439
Fuel Velocity, VL, $x10^5$, cm/sec	0.5007	0.7319	0.9861	1.2706	1.5453
Power, thermal MW	323.3	473.2	638.7	820.2	998.7
Max./avg. burnup	1.600	1.578	1.547	1.512	1.495
Max./avg. power density	2.232	2.172	2.089	2.000	1.949
Max. thermal flux, ϕ $x10^{-14}$, n/cm^2sec	0.7620	1.086	1.408	1.730	2.050
Blanket					
Fuel velocity, VL_i, $x10^5$, cm/sec, radial zone i=15	2.179	3.219	4.387	5.716	7.010
i=16	1.235	1.828	2.489	3.243	3.979
Power, thermal MW	0.3506	0.4664	0.5718	0.6687	0.7519
Avg. burnup, MWD/tonne	11.620	10.456	9.411	8.447	7.742
Total					
U-235 makeup rate, g/MWD	0.1485	0.1667	0.1834	0.1999	0.2127
Conversion ratio,					
in core and blanket, CR	0.8990	0.8838	0.8708	0.8578	0.8477
overall, allowing for recycle losses, CR_L	0.8711	0.8560	0.8430	0.8300	0.8198

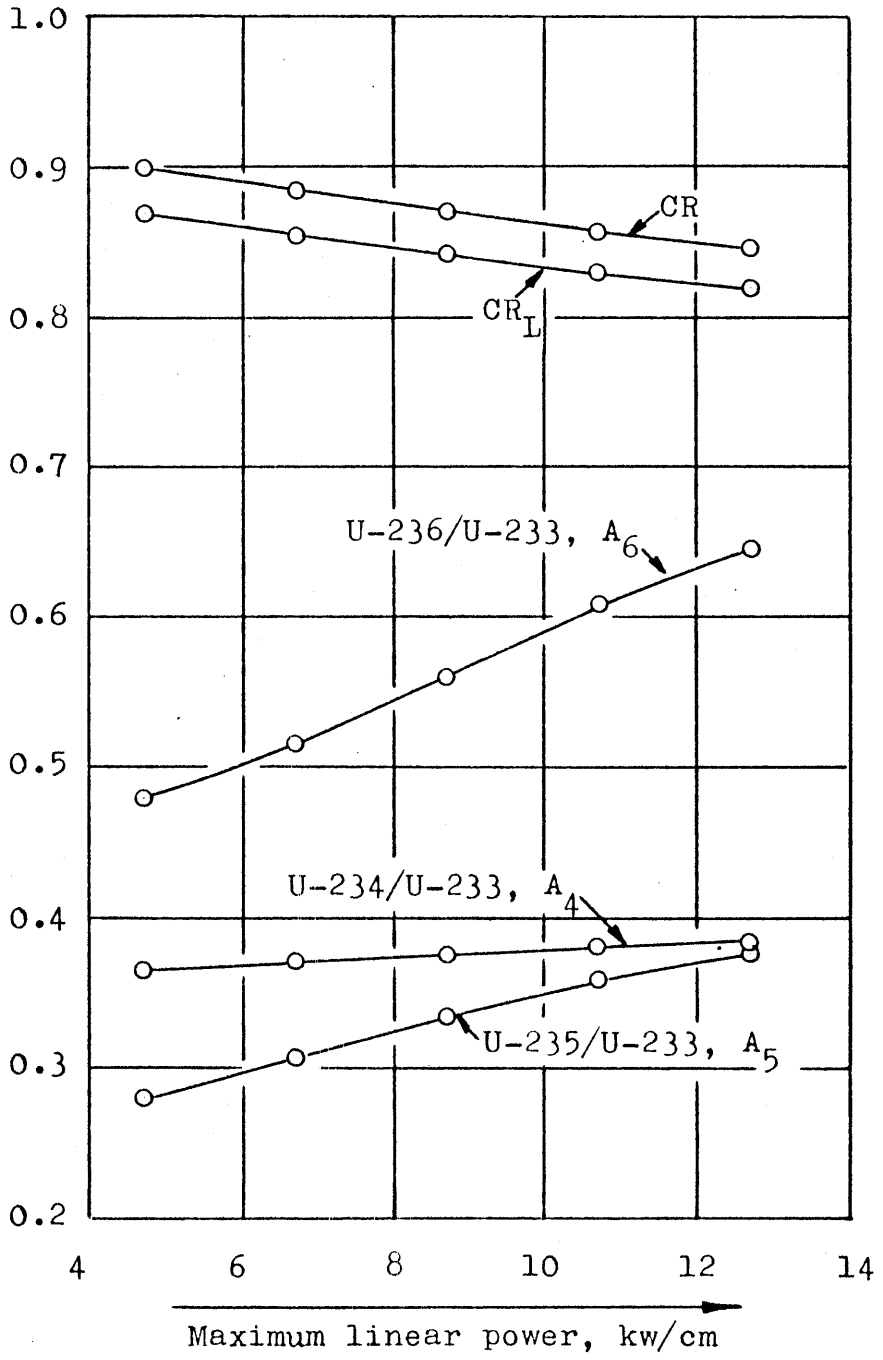

Fig.III.4., Conversion Ratio and Atom Ratios as a Function of the Maximum Linear Power (see Table III.4.)

Table III.5., Effect of Uranium Recycle Losses on Performance of Thorium Fueled CANDU Reactor

Blanket radius, BR = 255.0 cm — Fuel volume fraction, VFL = 0.0567

Average burnup = 10000 MWD/tonne — Max. linear power = 8.712 kw/cm

Uranium recycle loss, %	1.0	1.5	2.0	2.5	3.0
Core					
Enrichment, a/o U-233 + U-235 in U and Th	2.046	2.018	1.993	1.978	1.967
Atom ratio in feed: U-234/U-233, A_4	0.4008	0.3872	0.3743	0.3625	0.3538
Atom ratio in feed: U-235/U-233, A_5	0.3392	0.3352	0.3334	0.3376	0.3431
Atom ratio in feed: U-236/U-233, A_6	0.7575	0.6493	0.5610	0.5160	0.4761
Fuel velocity, VL, $x10^5$, cm/sec	1.0014	0.9934	0.9861	0.9814	0.9768
Power, thermal MW	646.9	642.4	638.7	634.6	631.9
Max./avg. burnup	1.533	1.539	1.547	1.551	1.553
Max./avg. power density	2.062	2.075	2.089	2.102	2.111
Max. thermal flux, ϕ, $x10^{-14}$, $n/cm^2 sec$	1.387	1.397	1.408	1.415	1.420
Blanket					
Fuel velocity, VL_i, $x10^5$, cm/sec, radial zone i=15	4.434	4.411	4.387	4.378	4.365
i=16	2.520	2.504	2.489	2.485	2.481
Power, thermal MW	0.5756	0.5733	0.5718	0.5709	0.5700
Avg. burnup, MWD/tonne	9.365	9.383	9.411	9.425	9.435
Total					
U-235 makeup rate, g/MWD	0.1828	0.1822	0.1834	0.1888	0.1942
Conversion ratio,					
in core and blanket, CR	0.8553	0.8642	0.8708	0.8741	0.8772
overall, allowing for recycle losses, CR_L	0.8411	0.8432	0.8430	0.8398	0.8363

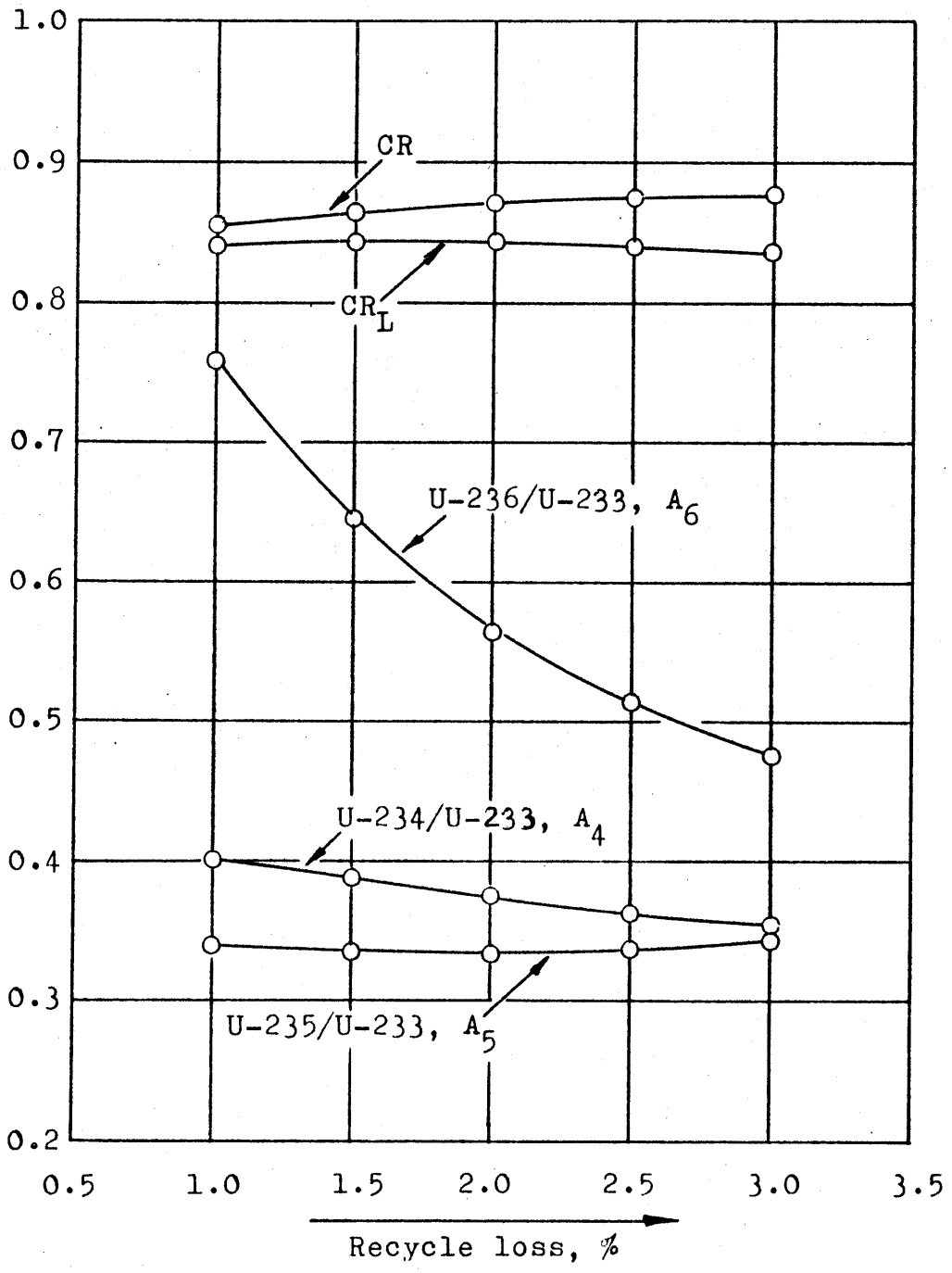

Fig.III.5., Conversion Ratio and Atom Ratios as a Function of the Recycle Loss

(see Table III.5.)

3.2. Flux Distribution

Figs.III.6. and III.7. show the radial and axial flux distributions in the "standard" reactor (refer to sect.3.1.). Fig.III.8. shows the radial flux distribution in a reactor without a blanket (BR = 225.61, Table III.1.).

3.3. Neutron Energy Spectrum

Fig.III.9. shows two flux spectra in the same reactor, one at the center of the core (Point 1, Fig.II.8.), and the other in the blanket (Point 5, Fig.II.8.). The two spectra are almost identical and, consequently, the effective cross sections (definition see sect. 2.2.3.) are essentially independent of position.

In Fig.III.10., the flux spectra of two reactors having different fuel volume fractions are compared. It is obvious that the reactor with the higher fuel volume fraction has the "harder" spectrum.

Fig.III.6., Radial Flux Distribution at Midplane of Reactor

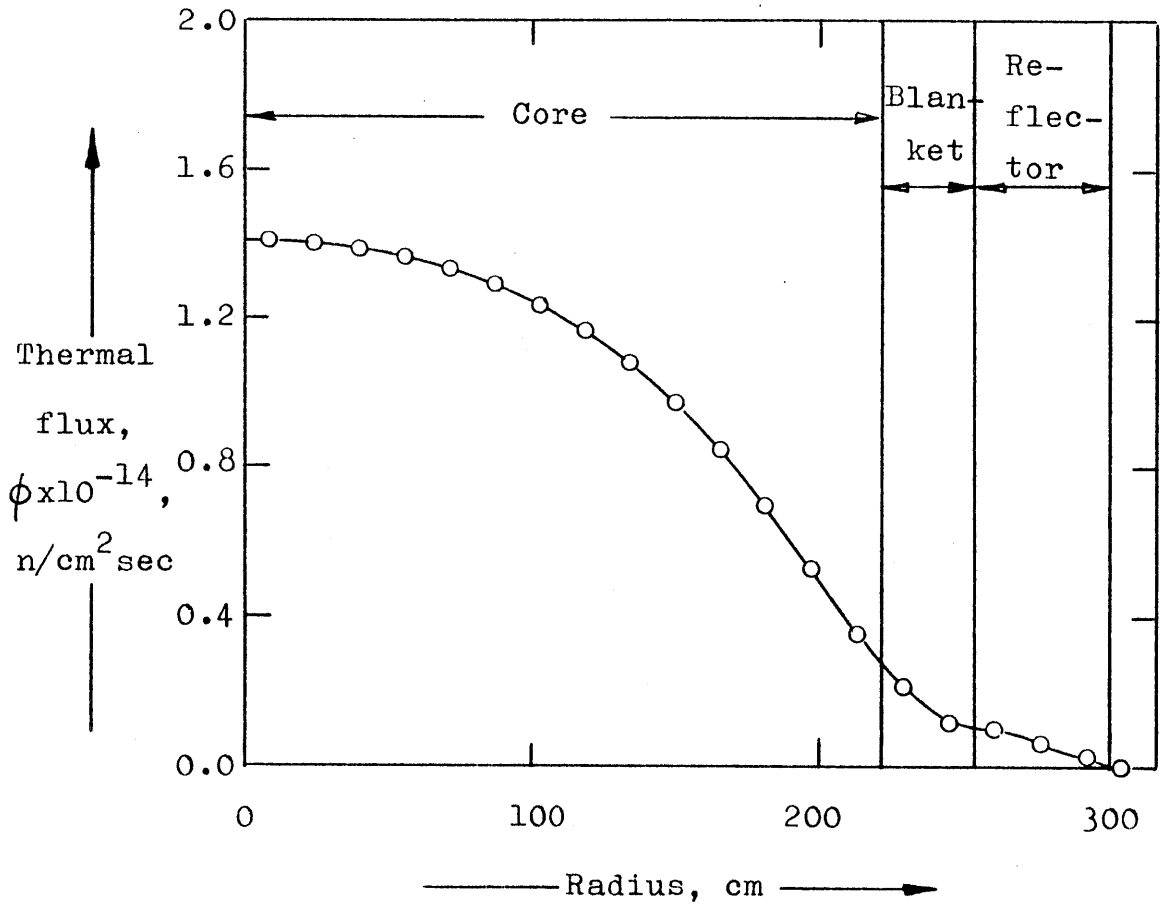

Reactor Characteristics

Core radius	= 225.61 cm
Blanket radius	= 255.00 cm
Reflector radius	= 299.70 cm
Core height	= 500.40 cm

Constant fuel velocity in core

(additional data given in Table III.1.)

Fig.III.7., Axial Flux Distribution along Center-line of Reactor

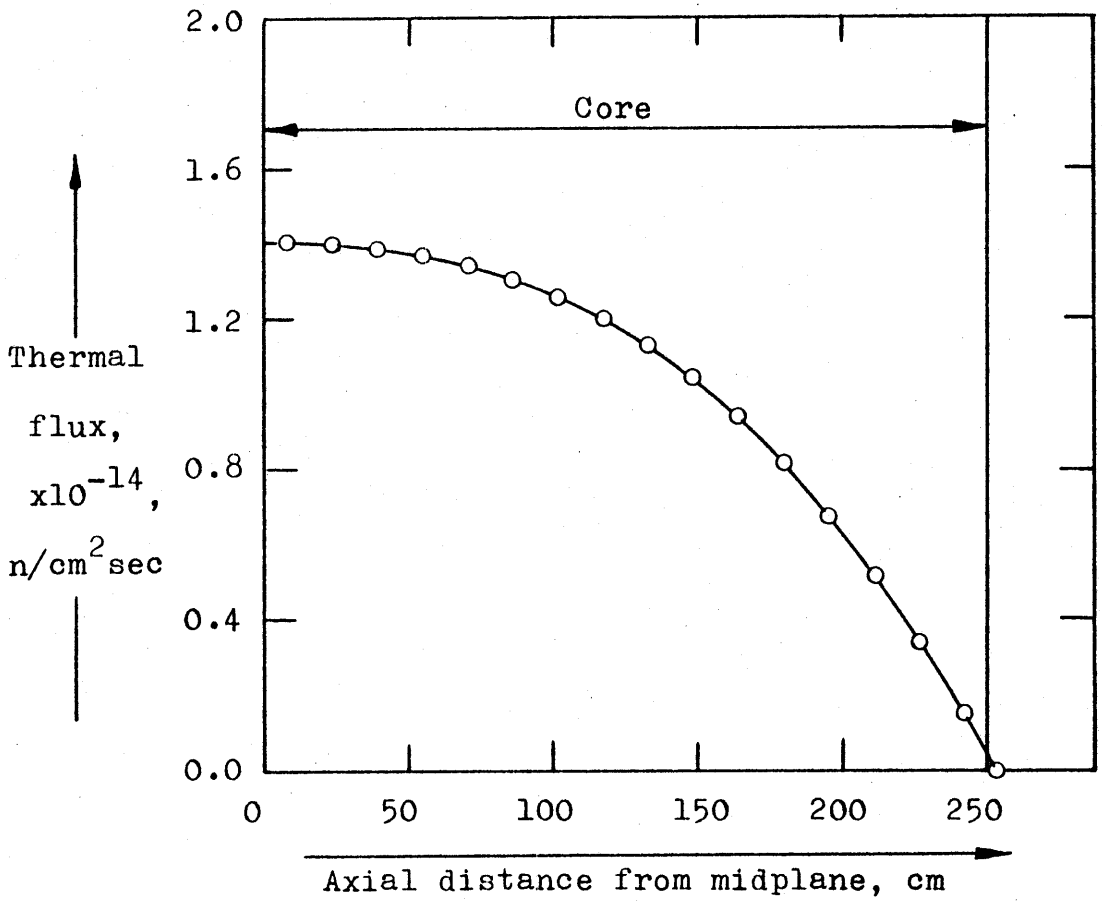

Reactor Characteristics

Core radius	= 225.61 cm
Blanket radius	= 255.00 cm
Reflector radius	= 299.70 cm
Core height	= 500.40 cm

Constant fuel velocity in core

(additional data given in Table III.1.)

Fig.III.8., Radial Flux Distribution at Midplane of Reactor

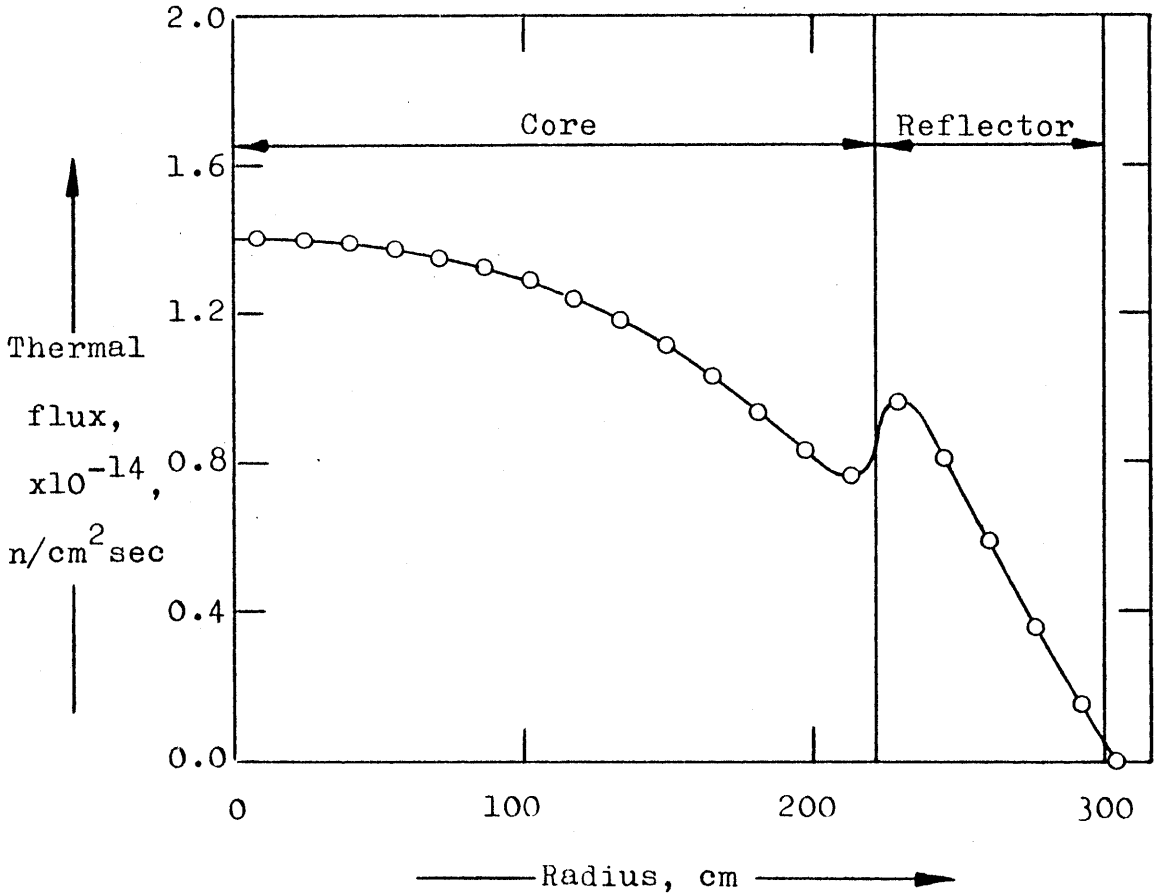

Reactor Characteristics

Core radius	= 225.61 cm
No blanket	
Reflector radius	= 299.70 cm
Core height	= 500.40 cm
Constant fuel velocity	
(additional data given in Table III.1.)	

Fig.III.9., Comparison of Flux Spectra in Core and Blanket

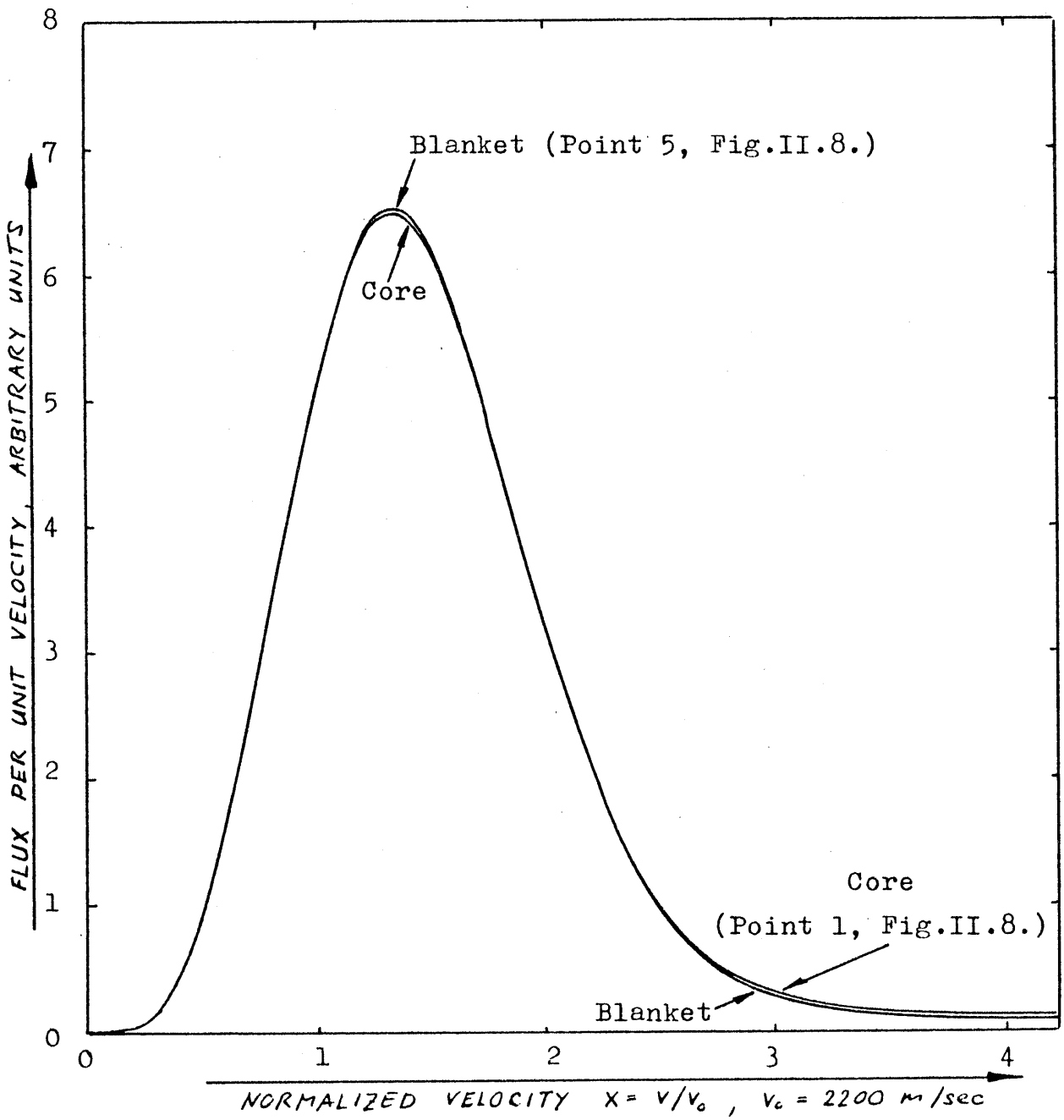

Fuel volume fraction, VFL = 0.0367

(additional data given in Table III.2.)

Fig.III.10., Comparison of Flux Spectra for two Different Fuel Volume Fractions, at Center of Core

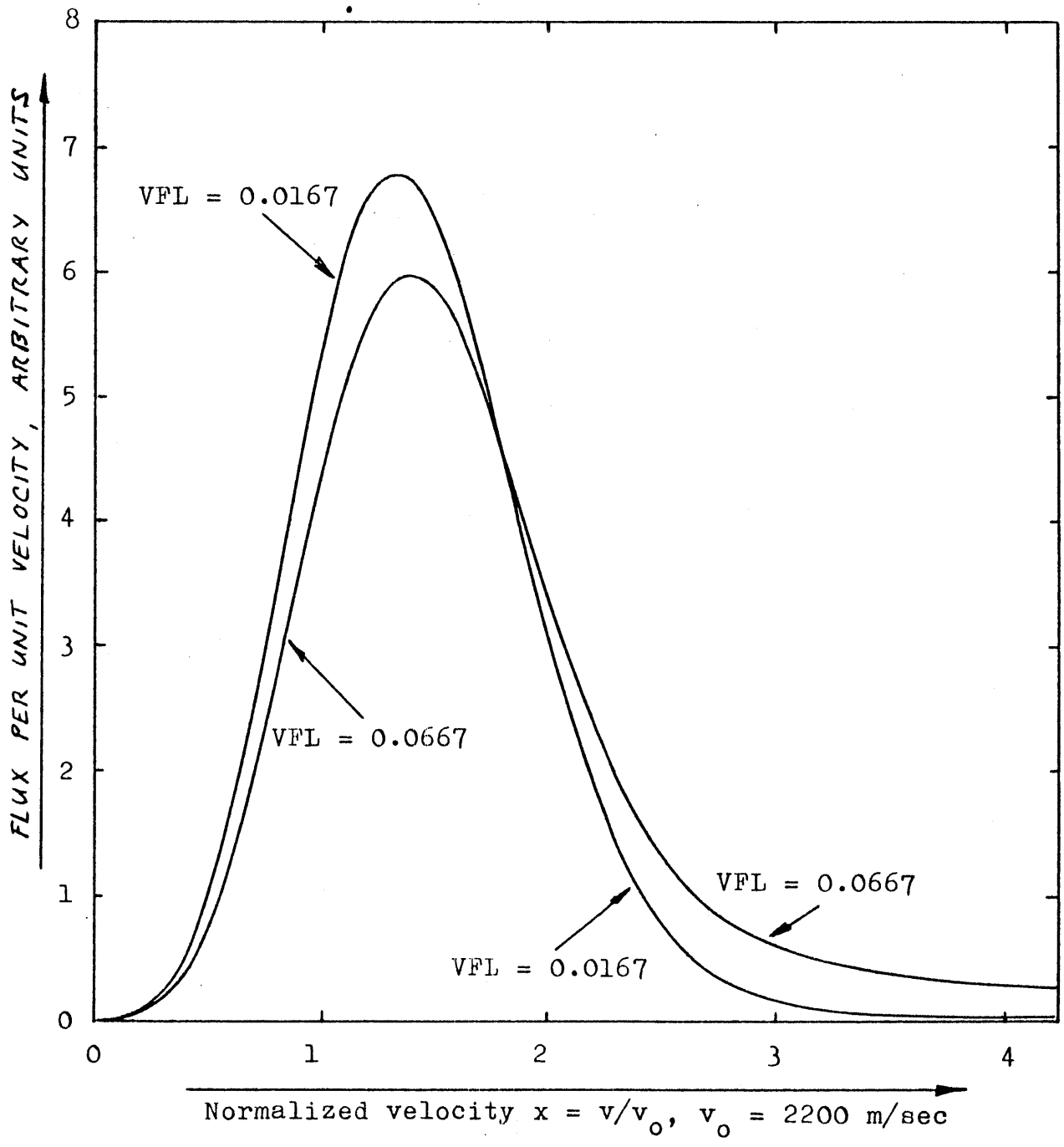

Both spectra at center of core (Point 1, Fig.II.8.)

(additional data given in Table III.2)

3.4. Nuclide Concentrations

Fig.III.11. shows the nuclide concentrations in the central fuel channel as a function of axial distance from the midplane of the reactor. The fuel moves from left to right (arrow) through the channel. The curves apply to the "standard" reactor described in sect. 3.1.

The discharge flux-time (corresponding to the right hand end of Fig.III.11.) is

$$\theta_{max} = 1.932 \text{ n/kb}$$

The input and output concentrations are given in detail in the Table below.

Table III.6., Input and Output Nuclide Concentrations in the Central Fuel Channel of the "Standard" Reactor

(in atoms/barn-cm of fuel)

Nuclide	Input	Output
Th^{232}	0.02065	0.02037
Pa^{233}	0	0.7424×10^{-5}
U^{233}	3.194×10^{-4}	3.052×10^{-4}
U^{234}	11.957×10^{-5}	12.404×10^{-5}
U^{235}	10.649×10^{-5}	5.380×10^{-5}
U^{236}	17.920×10^{-5}	18.439×10^{-5}
Np^{237}	0	6.725×10^{-6}

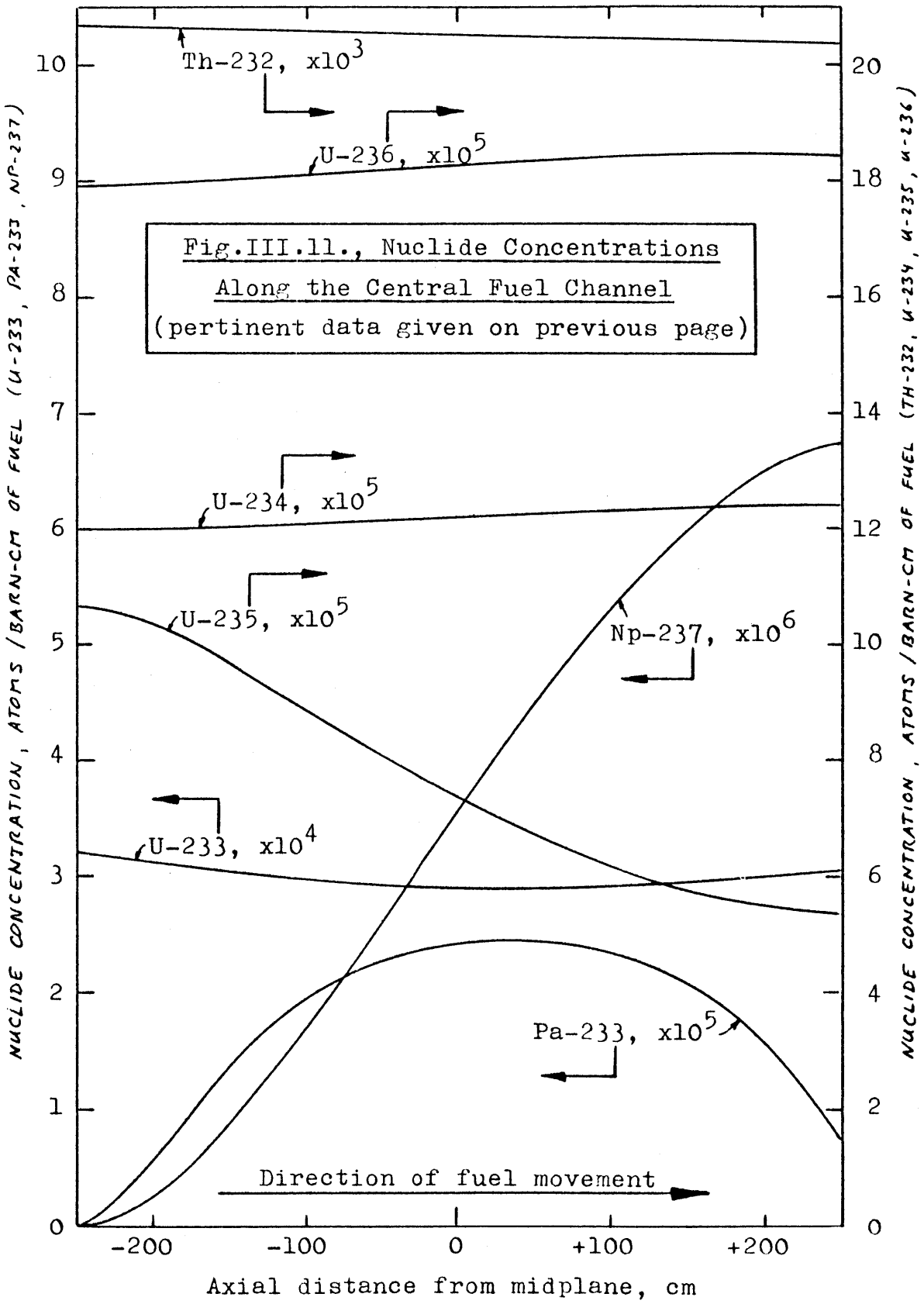

Fig.III.11., Nuclide Concentrations Along the Central Fuel Channel (pertinent data given on previous page)

Fig.III.12. shows the nuclide concentrations in one of the blanket channels (radial zone next to the core, i=15) as a function of the axial distance from the midplane of the reactor. Again, the curves represent the "standard" reactor (sect. 3.1.).

The discharge flux-time (at the right hand end of Fig. III.12.) is

$$\theta_{max} = 0.100 \text{ n/kb}$$

The input and output concentrations are given in the table below.

Table III.7., Input and Output Nuclide Concentrations in the Blanket Channel (i=15) of the "Standard" Reactor

(in atoms/barn-cm of fuel)

Nuclide	Input	Output
Th^{232}	0.021293	0.021279
Pa^{233}	0	3.437×10^{-6}
U^{233}	0	10.164×10^{-6}
U^{234}	0	4.295×10^{-8}
U^{235}	0	14.311×10^{-11}
U^{236}	0	3.189×10^{-13}
Np^{237}	0	0.971×10^{-16}

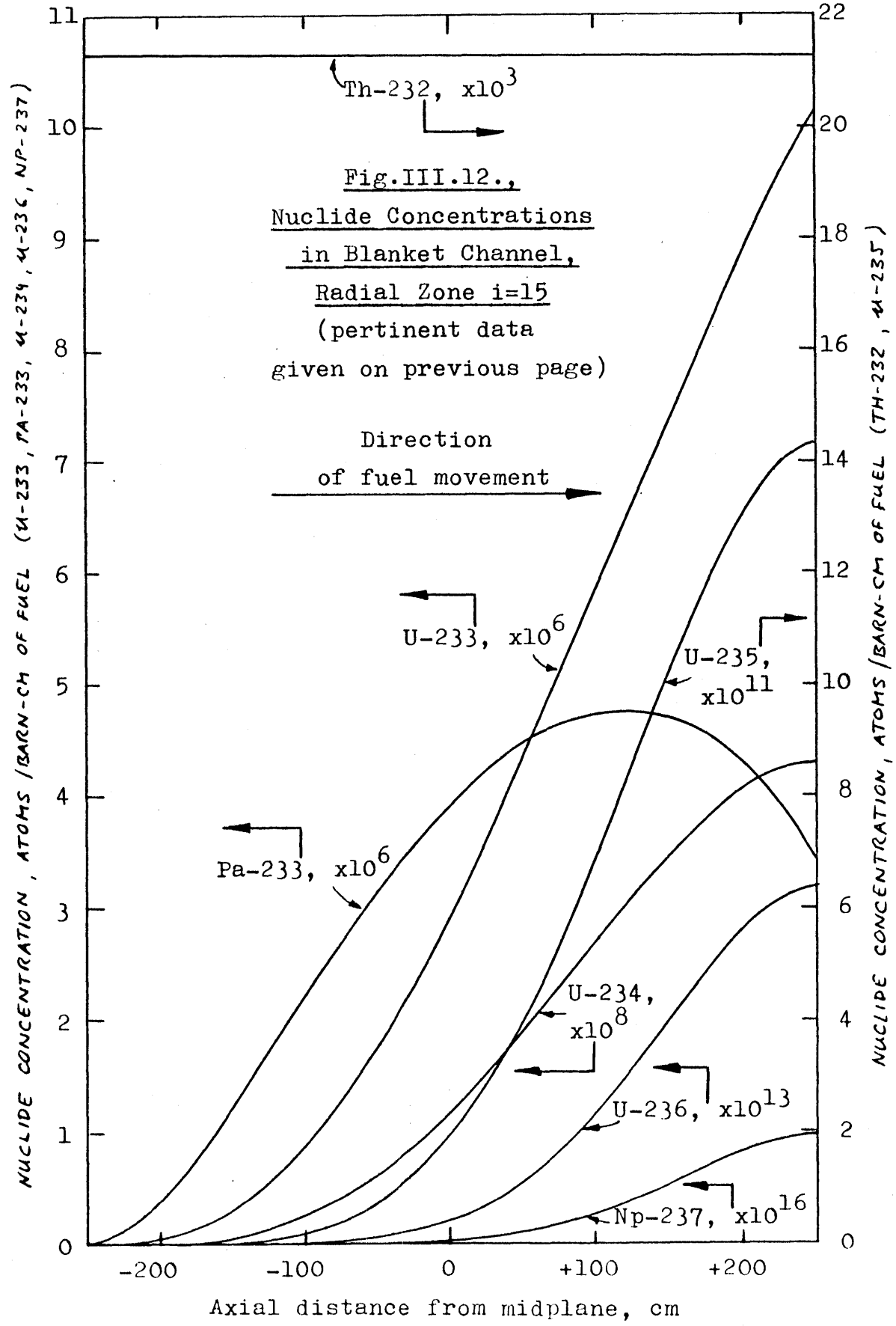
Th-232, x10^3
Fig.III.12.,
Nuclide Concentrations
in Blanket Channel,
Radial Zone i=15
(pertinent data
given on previous page)
Direction
of fuel movement
U-233, x10^6
U-235, x10^11
Pa-233, x10^6
U-234, x10^8
U-236, x10^13
Np-237, x10^16
NUCLIDE CONCENTRATION, ATOMS/BARN-CM OF FUEL (U-233, PA-233, U-234, U-236, NP-237)
NUCLIDE CONCENTRATION, ATOMS/BARN-CM OF FUEL (TH-232, U-235)
Axial distance from midplane, cm

Fig.III.13. shows the maximum atom ratio, Pa^{233}/U^{233}, in the central fuel channel as a function of the maximum thermal flux at the center of the core. The point at $\phi_{max} = 1.408 \times 10^{14}$ n/cm^{2}sec corresponds to the peak of the curve labelled "Pa^{233}" in Fig.III.11. Since the concentration of U^{233} (at the point where the atom ratio Pa^{233}/U^{233} has its maximum) varies but slightly with the flux level, it is seen that the Pa^{233} concentration is essentially proportional to the flux level.

Fig.III.13., Maximum Atom Ratio, Pa^{233}/U^{233} in Central Fuel Channel as a Function of Maximum Flux at Center of Core (refer to Table III.4.)

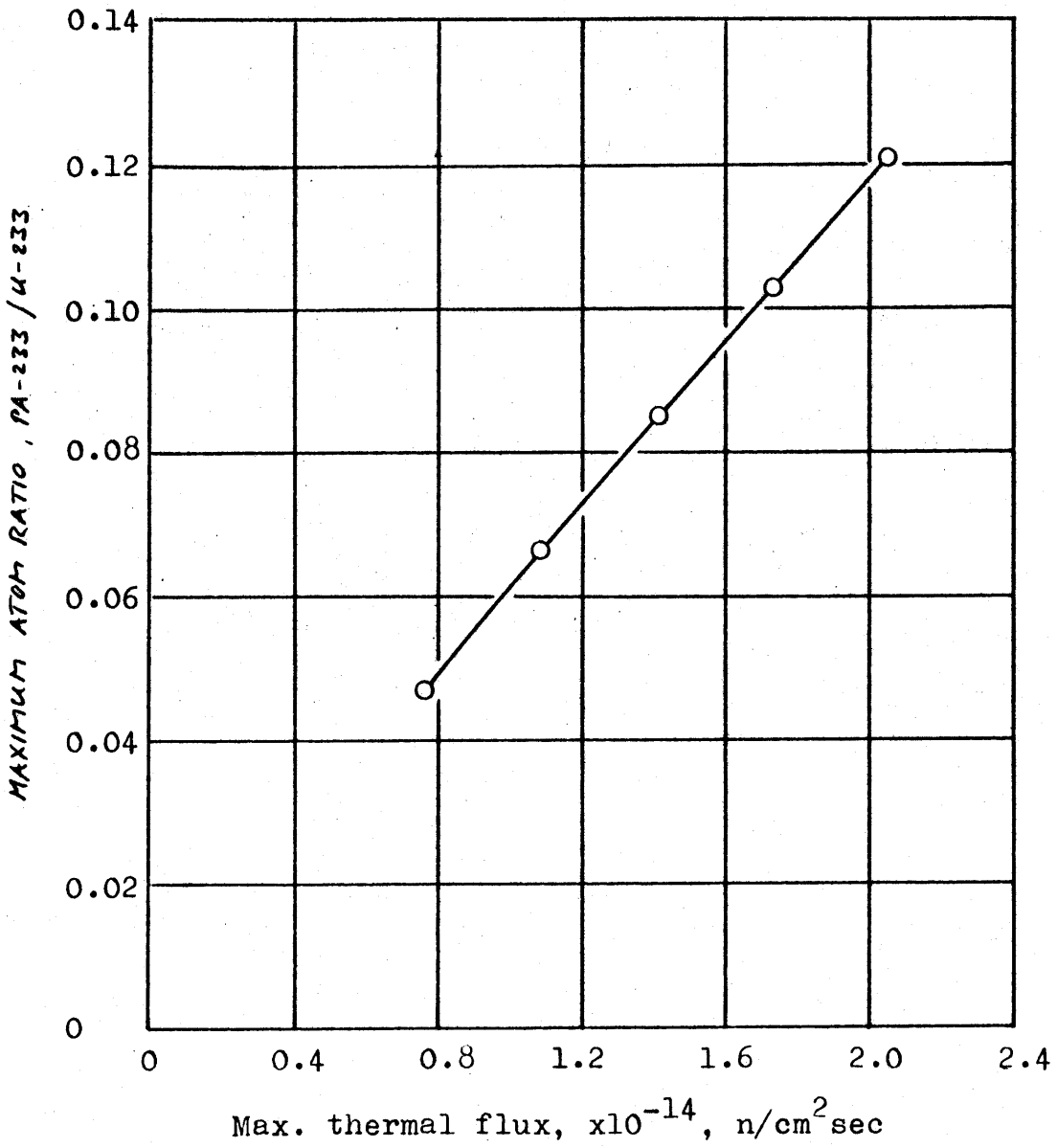

Blanket radius, BR = 255.0 cm
Fuel volume fraction = 0.0567
Average burnup = 10000 MWD/tonne
Uranium recycle loss = 2.0 %

IV. Discussion and Conclusions

The performance of the "standard" reactor (sect. 3.1.) is characterized by a disappointingly low conversion ratio (CR = 0.87). The main reason for this is the poisoning effect of the higher isotopes, especially U^{236} and Np^{237}. The equilibrium ratio of U^{236}/U^{233} in the fresh fuel is 0.56 (Table III.1.).

This high value of A_6 can be made plausible in the following way: consider a small increase in the U^{236} concentration. In order to overcome the poisoning effect due to the additional U^{236}, the U^{235} makeup rate must be increased (for CR < 1). This, in turn, leads to an increase in the rate of production of U^{236} in the reactor.

As a result of this "positive feedback", any variation in the U^{236} concentration is greatly amplified (A_6 is, in general, the most rapidly varying function in Figs. III.1. through III.5.), and, for CR < 1, the equilibrium concentration of U^{236} is much higher than one might expect.

This is, of course, strictly a consequence of the basic assumption (sect. 2.11.) that there is no U^{233} available for makeup other than that which is bred in the reactor itself, and, hence, any reactivity loss has to be compensated for by increasing the U^{235} makeup rate.

Now consider the case where all makeup consists of pure U^{233}. A system operating in this way would have a higher conversion ratio than the one using U^{235} makeup, as long as the conversion ratios of both systems are less than unity. As soon as one system has a conversion ratio greater than unity (i.e., it operates on Th^{232} feed alone), the other system must have the same conversion ratio because, now, the two systems can no longer be distinguished from one another.

Going back to the original system, we might ask ourselves whether it is at all possible to breed in a thorium fueled CANDU-type reactor.

Let us first consider the present CANDU design as described in sect. 3.1. For this reactor, the conversion ratio can be written as a function of the "five variables" in the form:

$$CR = F(BR, VFL, BURNUP, PDNLM, ROSS).$$

Assuming that there are no interactions between the variables, the function F can be approximated by

$$F(BR, VFL, BURNUP, PDNLM, ROSS) = CR_o + f_1(BR) + f_2(VFL) + f_3(BURNUP) + f_4(PDNLM) + f_5(ROSS), \quad (4.1)$$

where CR_o is the conversion ratio for "standard conditions", and each f expresses the change in conversion ratio caused by changing one of the variables from its standard value, all other variables remaining constant.

It is obvious that, if Eq. (4.1) holds, the maximum value of the function F (i.e., the maximum conversion ratio that can be achieved by varying the "five parameters") can be found by inserting the maximum values of all the f's into Eq. (4.1). These maximum f's are obtained from the data given in Tables III.1. through III.5.

For the overall conversion ratio which includes the recycle losses (see Eq. (2.11.2)), we have:

$CR_{L,o}$	= 0.8430 (Table III.1)
$f_{1,max} = CR_{L,BR=270\ cm} - CR_{L,o}$	= 0.0046 (Table III.1)
$f_{2,max} = CR_{L,VFL=0.0367} - CR_{L,o}$	= 0.0422 (Table III.2)
$f_{3,max} = CR_{L,BURNUP=6000\ MWD/tonne} - CR_{L,o}$	= 0.0058 (Table III.3)
$f_{4,max} = CR_{L,PDNLM=\ 4.712\ kw/cm} - CR_{L,o}$	= 0.0281 (Table III.4)
$f_{5,max} = CR_{L,ROSS=\ 1.5\ \%} - CR_{L,o}$	= 0.0002 (Table III.5)
$F_{max} = CR_{L,max}$	= 0.9239

The maximum conversion ratio of the reactor itself, CR_{max}, as defined by Eq. (2.11.1) is found analogously:

CR_o	= 0.8708 (Table III.1)
$f_{1,max} = CR_{BR=270\ cm} - CR_o$	= 0.0048 (Table III.1)
$f_{2,max} = CR_{VFL=0.0367} - CR_o$	= 0.0410 (Table III.2)
$f_{3,max} = CR_{BURNUP=4000\ MWD/tonne} - CR_o$	= 0.0350 (Table III.3)
$f_{4,max} = CR_{PDNLM=4.712\ kw/cm} - CR_o$	= 0.0282 (Table III.4)
$f_{5,max} = CR_{ROSS=3.0\ \%} - CR_o$	= 0.0065 (Table III.5)
CR_{max}	= 0.9863

It should be noted that this high conversion ratio (CR_{max} = 0.9863) involves a very low thermal power output (approximately 180 MW as compared to 698 MW for the CANDU reactor), and a low fuel burnup (4000 MWD/tonne).

A further increase in conversion ratio could only be achieved by introducing major changes in reactor design, such as adding an axial blanket or using a pressure vessel rather than pressure tubes and thus reducing the amount of parasitic neutron absorption.

The effect of adding an axial blanket can be estimated by assuming that the gain in conversion ratio due to a (thick) blanket is roughly proportional to the area of the core-blanket interface, i.e.,

$$\Delta CR_{\text{Axial blanket}} = \Delta CR_{\text{Radial blanket}} \frac{2\pi R^2}{2\pi RH}$$

where R and H are the radius and the height of the core, respectively, and ΔCR is the increase in conversion ratio. The result, obtained from the data in Table III.1., is:

$$\Delta CR_{\text{Axial blanket}} = (0.8756 - 0.8134) \frac{225.61}{500.40} = 0.028$$

Actually, the increase would be even greater, for the following reason: the CANDU reactor has no axial reflector so that the benefit "per unit area of core-blanket interface" is greater for the axial blanket than it is for the radial blanket.

It is clear, at this point, that in a thorium fueled reactor of the CANDU-type operating on an equilibrium cycle, breeding can only be achieved if the design is changed substantially, and if economic considerations are completely disregarded.

V. Recommendations for Future Work

5.1. Fuel Velocity Distribution

Throughout this study, it has been assumed that the velocity of the fuel in the core is the same in all channels. This implies that the fuel in the central zone will be exposed to a higher burnup than the fuel at the periphery of the core, thus leading to a certain degree of radial flux flattening. In general, the higher the ratio of maximum to average burnup, the more flux flattening can be achieved. Hence, flux flattening and "burnup flattening" are, to some extent, incompatible. However, both are highly desirable: The first reduces capital costs and the second reduces fuel cycle costs.

It is obvious that the best compromise can only be found by investigating various degrees of flux flattening, i.e., various fuel velocity distributions.

5.2. Fuel Exposure in Blanket Channels

In this study, the velocity of the fuel and, consequently, the fuel exposure in the blanket channels has been determined in such a way that the discharge flux-time was equal to a given constant (THETAB = 0.1 n/kb).

It is clear that, for a complete analysis of the system, this number should be considered a variable. It is, however,

not a very important variable. Even a large increase in THETAB would affect the overall performance of the reactor only slightly because the poisoning due to higher isotopes and fission products is very small in the blanket channels. (see Fig.III.12.).

5.3. Axial Blanket

In a reactor with a conversion ratio slightly less than unity, a small improvement on the neutron economy can lead to considerable savings in the amount of U^{235} makeup required. It has been estimated (Chap. IV.) that the addition of an axial blanket may increase the conversion ratio by as much as 0.028, or more.

A thorough investigation of this point would include analyzing reactors with radial and axial blankets of various thicknesses.

5.4. Variable Fuel Channel Geometry

In order to reduce the number of variables, the geometry of the fuel channel was fixed in this study. All channels, including the blanket channels, were assumed to be equal to the CANDU fuel channels.

Considering various cladding thicknesses, various pressure tube sizes, or even designs without pressure tubes, would show the effect of changing the amont of zirconium in the core. In addition, the rod diameter and the number

of rods per fuel bundle should be varied.

For the blanket channels, a different design should be used altogether. Due to the low power density, the rod diameter could be increased, thus leading to lower fabrication costs. In fact, the entire channel optimization would be different in the blanket from what it is in the core, and it is apparent that some heat transfer analysis is needed to determine the orders of magnitude and the ranges of the variables.

5.5. Transient Phase

All results presented in this thesis apply to the equilibrium state of a reactor which is fed with thorium and a small amount of U^{235} makeup, and which recycles its own bred U^{233} continuously. No attempt has been made to analyze the transient phase which a reactor would go through if it were started up with a charge of thorium and U^{235}. Surely, it would take many years of operation to reach the equilibrium state, and during this period, the performance of the system would change with time. It would be very interesting to see how fast (or how slowly) the equilibrium state is approached. In fact, all the important reactor characteristics should be evaluated as functions of time.

VI. Nomenclature

In this Chapter, all symbols used in the text are defined.

Text Symbol	FORTRAN Symbol	Definition
$\underline{A}$		
A	-	Area inside the "rubber band" (see sect. 8.2.2.)
$\underline{A}$	DL	Coefficient matrix for the diffusion equation in difference form (see sect. 2.8.)
A(x)	A(K)	Spectral parameter for solution of Wilkins equation (Eq.2.2.3.)
A_4	ANIFR(4)	Atom ratio U^{234}/U^{233} }
A_5	ANIFR(5)	Atom ratio U^{235}/U^{233} } in feed
A_6	ANIFR(6)	Atom ratio U^{236}/U^{233} }
a	ADDPAR	Damping factor (see Eq. 2.8.2.)
a	-	Radius of homogenized fuel rod, see Eqns. (2.3.9) and (2.3.10)
a	AL	Parameter for evaluation of thermal cross section, see Eq. (2.2.1)
ANDEL	ANDEL	Convergence criterion for atom ratios, see Eq. (2.12.17)
ANIFRA(M)	ANIFRA(M)	Initial estimate for atom ratio A_M, see sect. 2.12., step (8)

Nomenclature (continued)

Text Symbol	FORTRAN Symbol	Definition
ANIFRO(M,IZ)	ANIFRO(M,IZ)	defined in Eq. (2.12.15)
ANIN(M,IZ)	ANIN(M,IZ)	Concentration of nuclide M in fresh fuel, atoms/barn-cm of fuel, see sect. 2.12.
ANINP(M)	ANINP(M)	= ANIN(M,IZ)
ANINPO(M)	ANINPO(M)	defined in Eqns. (2.12.12) and (2.12.13)
ANOUT(M,I)	ANOUT(M,I)	Concentration of nuclide M in the fuel discharged at radial position I, atoms/barn-cm of fuel
ANTHO2	ANTHO2	Number of thorium atoms per barn-cm of pure ThO_2
ANUO2	ANUO2	Number of uranium atoms per barn-cm of UO_2
ATWT(M)	ATWT(M)	Atomic weight of nuclide M
AVGCS	AVGCS	Subroutine, see Appendix 4.
$\underline{B}$		
B_M	ANIFRO(M,IZ)	defined in Eq. (2.12.15), see also sect. 2.10.
$\underline{B}$	EL	Coefficient matrix in the diffusion equation in difference form, see sect. 2.8.

Nomenclature (continued)

Text Symbol	FORTRAN Symbol	Definition
b	-	Abbrevation for barn, Appendix 1.
b_i	B	Parameter for evaluation of cross sections as a function of energy, see Eq. (2.2.1)
BR	BR	Outside radius of blanket
BURNUP	BURNUP	Average fuel burnup in core
C		
C	DESNF	number of fissionable atoms consumed in the reactor per unit time
C	C	Criticality, see sect 2.12., step (26)
C_{10}	C10	defined by Eq. (2.6.2)
C_{11}	C11	defined by Eq. (2.6.4)
C_{36}	C36	defined in sect. 2.12., step (27)
C_{53}	C53	defined by Eq. (2.6.3)
C_{54}	C54	defined by Eq. (2.6.5)
c_i	C	Parameter for evaluation of cross sections as a function of energy, see Eq. (2.2.1)
CANDU	-	Reactor, described in Chap. I

Nomenclature (continued)

Text Symbol	FORTRAN Symbol	Definition
CH	CH	Core height
CONCH	CONCH	Subroutine, see Appendix 4.
CONST	CONST	Subroutine, see Appendix 4.
CR	CORA2	Conversion ratio of core and blanket, defined by Eq. (2.11.1)
CR_L	CORA2R	Overall conversion ratio, includes recycle losses, defined by Eq.(2.11.2)
CR_{max}	-	Maximum conversion ratio, CR, which can be obtained by varying the "five variables", see Chap. IV.
CR_o	-	Conversion ratio of the "standard" reactor, CR_o = 0.8708, see Chap. IV.
CRDEL1	CRDEL1	Criticality convergence criterion 1 (IC-loop), see Appendix 5.
CRDEL2	CRDEL2	Criticality convergence criterion 2 (IZ-loop), see Eq. (2.12.16)
CRIT(IZ)	CRIT(IZ)	Converged criticality, (outer) iteration loop IZ, see sect. 2.12.
CRITIC(IC)	CRITIC(IC)	Criticality in the IC-loop, see sect. 2.12.
CSF2	CSF2	Subroutine, see Appendix 4.

Nomenclature (continued)

Text Symbol	FORTRAN Symbol	Definition
D		
D, D_{th}	DIFFC (Core) DIFFB (Blanket) DIFFR (Refl.)	Diffusion coefficient for the thermal group, see Eqns.(2.1.5) and (2.3.12)
D_1	-	Diffusion coefficient for the fast group, see Eq. (2.1.4)
D	OUTNF	number of fissionable atoms discharged from the reactor per unit time, see sect. 2.11.
D	-	Quantity defined in Fig.VIII.1.
d	-	Diameter of fuel element, see Fig.VIII.1.
DCDE	DCDE	Criticality iteration parameter, see Eq. (2.12.1)
DELH	DELH	Axial extrapolation distance, see Appendix 2.
DELR	DELR	Radial extrapolation distance, see Appendix 2.
E		
E	ENERGY	Neutron energy, ev
E_i^o	EV	Resonance energy, see Eq. (2.2.1)

Nomenclature (continued)

Text Symbol	FORTRAN Symbol	Definition
E	-	Quantity defined in sect. 2.3.1.
EN	EN(IZ)	Enrichment, a/o $U^{233}+U^{235}$ in U and Th
e	-	Quantity defined in Fig.VIII.1.
EN(IZ)	EN(IZ)	see above
ENA	ENA	Enrichment, initial estimate, see sect 2.12., step (7).
ENRIO	ENRIO	"Output enrichment" defined by Eq. (2.12.11)
ERROR	ERROR	Flux shape convergence criterion, see Appendix 5.
EXTRAP(M)	EXTRAP(M)	= x_M, see Eq. (2.10.1)
F		
F	F	SPACFX extrapolation parameter, see Appendix 5.
F	-	Quantity defined in sect. 2.3.1.
f	-	Thermal utilization, see sect. 2.3.1.
f_1(BR)	-	CR (plotted in Fig.III.1.),minus CR_o
f_2(VFL)	-	CR (plotted in Fig.III.2.), minus CR_o
F	FEEDNF	Quantity defined in sect. 2.11.

Nomenclature (continued)

Text Symbol	FORTRAN Symbol	Definition
f_3(BURNUP)	-	CR (plotted in Fig.III.3.), minus CR_o
f_4(PDNLM)	-	CR (plotted in Fig.III.4.), minus CR_o
f_5(ROSS)	-	CR (plotted in Fig.III.5.), minus CR_o
FLF2	FLF2	Subroutine, see Appendix 4.
G		
g_i	GL(I)	Radial mesh spacing, see Fig.II.13.
g_w	SIGFAC	Ratio of effective to 2200 m/sec cross section for 1/v absorber, see sect. 2.6.
GUESS	GUESS	Subroutine, see Appendix 4.
H		
h	HL	Axial mesh spacing, see Fig.II.13.
h	-	Quantity defined in Eq. (2.5.13)
h	-	Quantity defined in Fig.VIII.1.
HALT	HALT	Subroutine, see Appendix 4.

Nomenclature (continued)

Text Symbol	FORTRAN Symbol	Definition
I		
i, I	I	Radial mesh index, see Fig.II.13.
IC	IC	Iteration parameter, defined in sect. 2.12., step (22).
IL	IL	Number of points for solution of Wilkins equation, see Appendix 5.
IP	IP	Regional index, for cross section calculation, see Fig.II.8., $1 \leq IP \leq 6$.
IPADEC	IPADEC	defined in sect. 2.12., step (34)
IPRT	IPRT	Print-out control parameter, see Appendix 5.
IRB	IRB	Number of radial mesh points in core and blanket.
IRC	IRC	Number of radial mesh points in core.
IRR	IRR	Total number of radial mesh points (core + blanket + reflector), $IRR \leq 24$
IVELCO	IVELCO	defined in sect. 2.12., step (17)
INOUT	INOUT	Subroutine, see Appendix 4.
IZ	IZ	Iteration parameter, see sect. 2.12.
J		
j, J	J	Axial mesh index, see Fig.II.13.
JZC	JZC	Number of axial mesh points (in half-core), see Fig.II.13., $JZC \leq 20$.

Nomenclature (continued)

Text Symbol	FORTRAN Symbol	Definition
K		
k	K	Index for numerical integration of the nuclide concentration equations, see sect. 2.5.2.
k	IZ	Iteration parameter for the outer iteration, see sect. 2.8.
k_{eff}	-	Effective multiplication factor, see Eq. (2.12.10).
M		
MAIN	MAIN	Main program, see sect, 2.12.
N		
N_i	ANCH	Nuclide concentration, atoms/barn-cm
N_{FP}	-	Concentration of fission products in fuel, atoms/barn-cm
n	-	Number of fissions per unit volume of reactor, per unit time
n_f	-	defined by Eq. (2.9.3)
n_{res}	-	defined by Eq. (2.9.4)

Nomenclature (continued)

Text Symbol	FORTRAN Symbol	Definition
n_{th}	-	defined by Eq. (2.9.1)
NUPROP	NUPROP	Subroutine, see Appendix 4.
P		
P	-	Number of fissionable atoms produced in the reactor per unit time, sect. 2.11.
P_1	P1	Fast non-leakage probability, defined in sect. 2.1.2.
$P(a\Sigma)$	-	Collision probability, see Eq. (2.3.9)
p_m	P(M)	Resonance escape probability, see Eq. (2.4.1)
$\langle 1-p \rangle_m$	OMPP(M)	"Resonance absorption probability", defined by Eq. (2.4.5)
p_{17}	P17	$p_1 p_2 p_7 p_9$
p_{174}	P174	$p_1 p_2 p_7 p_9 p_4 p_6$
p_T	PL	$p_1 p_2 p_7 p_9 p_4 p_6 p_3 p_5$
PDNLM	PDNLM	Max. linear power, kw/cm of channel
PHI11	PHI11	Max. thermal flux, initial estimate, see Appendix 5.
$POWD_{i,j}$	POWD(I,J)	Power density, watts/cm^3

Nomenclature (continued)

Text Symbol	FORTRAN Symbol	Definition
PRINIJ	PRINIJ	Subroutine, see Appendix 4.
PTCS	PTCS	Subroutine, see Appendix 4.
Q		
q	-	Slowing down density at fission energy see sect. 2.1.1.
QA_K	QA(K)	Quantity defined by Eq. (2.7.5)
QB_K	QB(K)	" " "
QC_K	QC(K)	" " "
q_2	-	$qP_1(p_1p_2p_7p_9)$
R		
R	CR	Core radius, cm
r	ROSS	Uranium recycle loss, see sect. 1.2.5.
r_o	-	Radius of homogenized fuel rod, see sections 2.3.1., and 8.2.2.
r_1	-	Radius of unit cell, see sect. 2.3.1.
r_i	RAD(I)	defined in Fig.II.13.
r	-	Radius of fuel element, see Fig.VIII.1.

Nomenclature (continued)

Text Symbol	FORTRAN Symbol	Definition
RI_m^∞	RI(M)	Infinite dilution resonance integral, for nuclide m, see Eq. (2.4.1)
RESPRB	RESPRB	Subroutine, see Appendix 4.
ROSS	ROSS	Uranium recycle loss, see sect. 1.2.5.
ROTHO2	ROTHO2	Density of ThO_2, g/cm^3, see Appendix 5.
ROUO2	ROUO2	Density of UO_2, g/cm^3, see Appendix 5.
RR	RR	Outside radius of reflector, see Appendix 5.
S		
SPACFX	SPACFX	Subroutine, see Appendix 4.
SPACON	SPACON	" "
SPFUN	SPFUN	" "
SPFUN2	SPFUN2	" "
T		
t	-	Time, sec, Eqns. (2.5.1) through (2.5.9)
THETAB	THETAB	Blanket discharge flux-time, see Eq. (2.12.8)
T_{D_2O}	-	defined by Eq. (2.3.16)

Nomenclature (continued)

Text Symbol	FORTRAN Symbol	Definition
TIDE	TIDE	Max. number of SPACFX loops, see Appendix 5.
TIMECK	TIMECK	Subroutine, see Appendix 4.
TMST(I)	TMST(I)	defined by Eq. (2.12.9)
U		
u	-	Arbitrary function of position in the reactor, see Eq. (2.8.3)
V		
V_i	-	Volume of i^{th} component of mixture
V_{fl}	VFL	Fuel volume fraction, see sect. 1.2.2.
v	-	Neutron velocity, see sect. 2.2.2.
v_o	-	2200 m/sec
VELOC	VELOC	Velocity of fuel in core, Eq. (2.12.4)
VL_i	VL(I)	Velocity of fuel in reactor, a function of the radial mesh index i, see sect. 2.12., step (17).
VLD_i	VLD(I)	Fuel velocity distribution, defined in sect. 2.12., step (17)

Nomenclature (continued)

Text Symbol	FORTRAN Symbol	Definition
$\underline{X}$		
x_M	EXTRAP(M)	Extrapolation parameter, see Eq.(2.10.1)
x	X	Normalized neutron velocity, v/v_o
x	-	Quantity defined in Fig.VIII.1.
$\underline{Y}$		
y_1	-	Yields of pseudo fission products, see Eq. (2.7.1)
y_2	-	
y_3	-	
y_{S91}	YSM9(1)	Yield of Sm^{149} from Th^{232} fission
y_{S92}	YSM9(2)	" " " " U^{233} "
y_{S93}	YSM9(3)	" " " " U^{235} "
y_{S11}	YSM1(1)	Yield of Sm^{151} from Th^{232} fission
y_{S12}	YSM1(2)	" " " " U^{233} "
y_{S13}	YSM1(3)	" " " " U^{235} "
y_{X1}	YXE(1)	Yield of Xe^{135} from Th^{232} fission
y_{X2}	YXE(2)	" " " " U^{233} "
y_{X3}	YXE(3)	" " " " U^{235} "

Nomenclature (continued)

Text Symbol	FORTRAN Symbol	Definition
α_i	ALPHA(I)	Epithermal capture to fission ratio, (subscript notation given in sect.2.5.1.)
β	-	Quantity defined by Eq. (2.12.10)
Γ	-	Total resonance width, Eq. (2.2.2)
Γ_a	-	Width for absorption, sect. 2.2.1.
Γ_n^o	-	Width for neutron emission, at resonance energy, sect. 2.2.1.
ε	EPSI	Fast fission factor, see sect. 2.1.1.
η_i	-	$\nu_i/(1+\alpha_i)$
θ	THETA	Flux-time, $\int \phi \, dt$, see sect. 2.7.
θ_2	THETA2	2200 m/sec- flux-time, defined by Eq. (2.7.4)
κ_o	-	Reciprocal of the diffusion length in the fuel region, see sect. 2.3.1.
κ_1	-	Reciprocal of the diffusion length in the moderator region, see sect. 2.3.1.
λ_{Pa}	PALAM	Decay constant of Pa^{233}, sect. 8.1.7.
λ_{Xe}	XELAM	Decay constant of Xe^{135}, sect. 8.1.7.
ν_1	ANU(1)	Number of neutrons per fission (Th^{232})
ν_3	ANU(2)	Number of neutrons per fission (U^{233})
ν_5	ANU(3)	Number of neutrons per fission (U^{235})

Nomenclature (continued)

Text Symbol	FORTRAN Symbol	Definition
ξ	-	Average logarithmic energy decrement, see Eq. (2.3.13)
Σ_t, Σ	-	Total macroscopic cross section of the homogenized fuel rod, above fast fission threshold
Σ_f	-	Fission
Σ_r	-	Radiative Capture
Σ_e	-	Elast. scattering
Σ_a	SIGMA	Total effective macroscopic absorption cross section of the homogenized unit cell, see Eq. (2.6.1)
$\Sigma_a(x)$	-	Total macroscopic absorption cross section of the homogenized unit cell, as a function of the normalized velocity, x, see Eq. (2.2.4)
Σ_{f3}	-	$N_3\sigma_{f3}$, effective macroscopic fission cross section of U^{233} in fuel, sect.2.1.6.
Σ_{f5}	-	$N_5\sigma_{f5}$, effective macroscopic fission cross section of U^{235} in fuel, sect.2.1.6.
Σ_{mod}	SIGMOD	Macroscopic 2200 m/sec absorption cross section of the non-fuel region, unhomogenized, see sect. 2.3.6.
$\Sigma_{s,fl}$	SGMSFL	Epithermal macroscopic scattering cross section of the fuel region, sect. 2.3.7.

Nomenclature (continued)

Text Symbol	FORTRAN Symbol	Definition
Σ_1	-	Fast macroscopic removal cross section, $\Sigma_1 = D_1/\tau$, see Eq. (2.1.4).
Σ_{FP2}	SMFP2	Macroscopic 2200 m/sec fission product cross section of fuel, see Eq. (2.7.2)
Σ_{FP}	SMFP	Effective macroscopic fission product cross section of fuel, see Eq. (2.7.6)
σ_t, σ	-	Total
σ_f	-	Fission
σ_r	-	Radiative capture
σ_e	-	Elast.scattering
σ_i	-	Inelast. scatt.
		} microscopic cross section above threshold for fast fission see sect. 2.3.2.
σ_i	SIGW	Effective microscopic cross section of nuclide i, see Eq. (2.2.5)
$\sigma(E)$	SIGX	microscopic cross section as a function of neutron energy, see Eq. (2.2.1)
$\sigma_{ai}(x)$	SIGX	microscopic cross section of nuclide i, as a function of the normalized velocity, x, see Eq. (2.2.4)
σ_{si}	-	Scattering cross section of nuclide i, see Eq. (2.3.13) and Eq. (2.3.15)
$\sigma_{tr,i}$	-	Transport cross section of nuclide i, see Eq. (2.3.12)

Nomenclature (continued)

Text Symbol	FORTRAN Symbol	Definition
σ_1	-	Cross section of pseudo fission product 1
σ_2	-	" " " " " " 2
σ_3	-	" " " " " " 3
		σ_1, σ_2, and σ_3 are 2200 m/sec cross sections, see Eq. (2.7.1)
σ_{FP2}	-	Microscopic 2200 m/sec fission product cross section, defined by Eq. (2.7.1)
$\sigma_{2200\ m/s}$	-	cross section at a neutron velocity of 2200 m/sec
τ	TAU	Fermi-age, $\tau = D_1/\Sigma_1$, see Eq. (2.3.11)
τ_{mod}	-	Fermi age of moderator, see Eq. (2.3.11)
ϕ, Φ	PHI	Thermal flux, defined by Eq. (2.2.6)
ϕ_{max}	PHI(1,1)	Maximum thermal flux in core
ϕ_1	-	Fast flux, see Eq. (2.1.4)
$\bar{\phi}_o$	-	Average flux in fuel region
$\bar{\phi}_1$	-	Average flux in moderator region
$\bar{\phi}_s$	-	Flux at surface of fuel rod
$\bar{\phi}_{cell}$	-	Average flux in the unit cell see sect. 2.3.1.
Ψ_f	PSIF	defined by Eq. (2.3.1)
Ψ_s	PSIS	defined by Eq. (2.3.2)

Nomenclature (continued)

Text Symbol	FORTRAN Symbol	Definition
Ψ_m, Ψ_{mod}	PSIM	defined by Eq. (2.3.3)
Ψ_i	-	Average flux in material i, devided by average flux in unit cell
$\Psi_{l,m}$	-	Resonance disadvantage factor, see Eq. (2.4.2)
$\overline{\xi \Sigma_s}$	SDP	Slowing down , Eq. (2.3.13)

VII. References

(A1) "Douglas Point Nuclear Generating Station", AECL-1596

(C1) Cohen, E.R., "Survey of Neutron Thermalization Theory", Proc. First United Nations Intern. Conf. on Peaceful Uses of Atomic Energy, Geneva, 1955, Vol.5, 23A, p405.

(C2) Crowther, R.L., and J.W. Weil, GEAP-2058

(C3) Craig, D.S., et al. "Long Irradiation of Natural Uranium", Proc. First Geneva Conf., 1955, vol.15, p205.

(E1) Etherington, H., "Nuclear Engineering Handbook", McGraw-Hill, 1958.

(E2) Eastwood, T.A., and R.D. Werner, "The Thermal Neutron Capture Cross Section and Resonance Capture Integral of Pa-233", Canadian Journal of Physics, 38, p751.

(G1) Goldman, D.T., and J.R. Stehn, "Chart of the Nuclides", Sixth Edition, 1961.

(G2) Glasstone, S., and M.C. Edlund, "The Elements of Nuclear Reactor Theory", D.Van Nostrand, 1952

(H1) Hildebrand, F.B., "Advanced Calculus for Applications", Prentice-Hall, 1962.

(H2) Hansen, K., Notes on Numerical Solution of Partial Differential Equations.

(H3) Hankel, R., et al., "An Evaluation of U-233 - Th Fast Breeder Power Reactors", NDA-2164-3.

(H4) Hughes, D.J., and R.B. Schwartz, "Neutron Cross Sections", BNL-325.

(K1) Kaplan, I., Notes on Reactor Theory

(N1) Neill, J.M., S.M. Thesis, MIT, 1961.

(R1) Richardson, M., Ph.D. Thesis, MIT, (in preparation)

(S1) Shanstrom, R.T., M. Benedict, and C.T. McDaniel, "Fuel Cycles in Nuclear Reactors", NYO-2131.

(S2) Smith, E.C., et al., Phys. Rev. 115, p1693, (1959).

(S3) Stuart, H., Lecture presented at the MIT Nuclear Engineering Department, 1963.

(T1) Templin, L.J., "Reactor Physics Constants", ANL-5800.

(W1) Westcott, C.H., "Effective Cross Section Values for Well-Moderated Thermal Reactor Spectra", AECL-1101, (July, 1962).

(W2) Weinberg, A.M., "Burning the Rocks", Conf. on the Physics of Breeding, Oct. 1959, Proceedings, ANL-6122.

VIII. Appendices

8.1. Appendix 1: Nuclear Data

8.1.1. Thermal Cross Sections

Nuclide or Material	Quantity	Text Reference (section)	Source
U^{233}	$\sigma_a(E)$, $\sigma_f(E)$	2.2.1.	W1
U^{235}	$\sigma_a(E)$, $\sigma_f(E)$	2.2.1.	W1
Np^{237}	$\sigma_a(E)$	2.2.1.	W1
Sm^{149}	$\sigma_a(E)$	2.2.1.	W1
Sm^{151}	$\sigma_a(E)$	2.2.1.	W1
Xe^{135}	$\sigma_a(E)$	2.2.1.	S2
Th^{232}	$\sigma_{2200m/s}$ = 7.56 b	2.2.1.	H4
Pa^{233}	$\sigma_{2200m/s}$ = 70 b	2.2.1.	H4
U^{234}	$\sigma_{2200m/s}$ = 97 b	2.2.1.	H4
U^{236}	$\sigma_{2200m/s}$ = 7 b	2.2.1.	H4
Zircaloy 2	$\sigma_{2200m/s}$ = 0.212 b	2.3.6.	A1,H4
"	σ_s = 8 b	2.3.5.	E1
"	σ_{tr} = 7.94 b	2.3.4.	E1
D_2O	$\sigma_{2200m/s}$ = 0.00225 b	2.3.6.	E1
"	σ_{tr} = 10.55 b	2.3.4.	E1
D	σ_s = 7 b	2.3.5.	E1
O	σ_s = 4.2 b	2.3.5.	E1
ThO_2	σ_{tr} = 20 b	2.3.4.	E1

8.1.2. Number of Neutrons per Fission

Nuclide	Quantity	Text Reference	Source
Th^{232}	$\nu_1 = 2.4$ (fast fission)	2.1.,2.5.	T1
U^{233}	$\nu_3 = 2.51$	2.1.,2.5.	H4
U^{235}	$\nu_5 = 2.47$	2.1.,2.5.	H4

8.1.3. Epithermal Capture to Fission Ratio

U^{233}	$\alpha_3 = \alpha_7 = 0.17$	2.1.,2.5.	S3
U^{235}	$\alpha_5 = \alpha_9 = 0.51$	2.1.,2.5.	S3

8.1.4. Infinite Dilution Resonance Integrals

Th^{232}	RI_1^∞ = 74 b	2.4.		T1
Pa^{233}	RI_2^∞ = 930 b	2.4.		E2
U^{233}	RI_3^∞ = 911 b (below 5 ev)	2.4.		T1,H4
	RI_7^∞ = 101 b (above 5 ev)	2.4.		T1,H4
	RI_{3+7}^∞ = 1012 b (total)	2.4.		T1
U^{235}	RI_5^∞ = 111 b (below 5 ev)	2.4.		T1,H4
	RI_9^∞ = 259 b (above 5 ev)	2.4.		T1,H4
	RI_{5+9}^∞ = 370 b (total)	2.4.		T1
U^{234}	RI_4^∞ = 710 b	2.4.		T1
U^{236}	RI_6^∞ = 350 b	2.4.		T1

8.1.5. Cross Sections for Th^{232} in a Fission Spectrum

fission	$\sigma_f = 0.076$ b	T1
radiative capture	$\sigma_r = 0.06$ b	
elastic scattering	$\sigma_e = 2.0$ b	
inelastic scattering	$\sigma_i = 2.6$ b	
total	$\sigma = 4.736$ b	
capture to fission ratio	$\alpha_1 = 0.79$	

8.1.6. Yields of Xe and Sm (T1)

Th^{232} fast fissions	$y(Sm^{149}) = 0.006$	
	$y(Sm^{151}) = 0.002$	
	$y(Xe^{135}) = 0.054$	
U^{233} fissions	$y(Sm^{149}) = 0.007$	
	$y(Sm^{151}) = 0.003$	
	$y(Xe^{135}) = 0.066$	
U^{235} fissions	$y(Sm^{149}) = 0.011$	
	$y(Sm^{151}) = 0.005$	
	$y(Xe^{135}) = 0.064$	

8.1.7. Decay Constants (G1)

$$\lambda(Pa^{233}) = 2.9279 \times 10^{-7} \text{ sec}^{-1}$$

$$\lambda(Xe^{135}) = 2.0927 \times 10^{-5} \text{ sec}^{-1}$$

8.1.8. Yields and Cross Sections of Pseudo Fission Products

(Data from C3, refer to section 2.7.)

Nuclide	y_1	σ_1	y_2	σ_2	y_3	σ_3
U^{233}	0.695	25	0.0976	300	-0.0089	600
U^{235}	0.852	25	0.1137	300	-0.0129	600

The corresponding values for Th^{232} are assumed to be the same as those for U^{233}. All cross sections are given in barns.

8.1.9. Various Parameters

Quantity	Text Reference	Source
Fermi-age of D_2O, τ = 123 cm^2	2.1.	E1
Thermal diffusion coefficient of D_2O, D = 0.953 cm	2.1.	E1

8.2. Appendix 2: The Reference Design

The CANDU reactor is a heavy water moderated, heavy water cooled pressure tube reactor.

The fuel consists of sintered uranium dioxide pellets. The pellets are clad in Zircaloy-2 tubes (average wall thickness = 0.0165 in (0.042 cm)) to form 0.6 in (1.522 cm) O.D. cylindrical elements 19.5 in (49.5 cm) long. Each element contains 24 pellets. The maximum diametral clearance between pellet and cladding is 0.005 in (0.013 cm).

Nineteen of these elements are assembled to make a fuel bundle held together by end supports and spaced by wire helices on the six elements of the inner ring and alternate elements of the outer ring.

There is a total number of 306 fuel channels. The channels are set on a 9 in (22.86 cm) pitch. Each channel consists of a caladria tube (inside diameter = 4.240 in (10.78 cm), minimum wall thickness = 0.049 in (0.124 cm)), a pressure tube (inside diameter = 3.250 in (8.25 cm), minimum wall thickness = 0.155 in (0.394 cm)), two end fittings and twelve fuel bundles.

The CANDU reactor has a radial reflector (reflector thickness = 74.1 cm), but no axial reflector.

More details can be found in reference A1.

In the following sections, we will reproduce that part of the information given in reference (A1) which was actually used in the calculations.

8.2.1. Gross Properties of Core

Core height	CH =	500.40 cm
Axial extrapolation distance	DELH =	4.05 cm
Extrapolated length of axial flux distribution	CH +2 DELH =	508.50 cm
Core radius	R =	225.61 cm
Outside radius of reflector	=	299.70 cm
Radial extrapolation distance	DELR =	3.60 cm
Extrapolated end-point of radial flux distribution	R + DELR =	303.30 cm
Average coolant temperature	T_{cool} =	271.0 °C
Average moderator temperature	T_{mod} =	43.3 °C

8.2.2. Geometric Properties of the Fuel Channel

The list on the following page gives the average volume of each material per unit length of unit cell. The dimensions of the entire fuel channel are considered as constant. The spacing between the channels however, is a variable,

and, hence, the moderator volume and the total volume of the unit cell are expressed in terms of VFL, the volume fraction of the fuel in the unit cell.

Fuel	29.63 cm^3/cm
Zircaloy-2 (cladding, spacer wire)	3.90 cm^3/cm
D_2O (coolant)	19.41 cm^3/cm
Zircaloy-2 (pressure tube)	11.15 cm^3/cm
Air gap	27.00 cm^3/cm
Zircaloy-2 (Calandria tube)	4.35 cm^3/cm
D_2O (moderator)	$(\frac{29.63}{VFL} - 95.44)$ cm^3/cm
Total	$(\frac{29.63}{VFL})$ cm^3/cm

The following quantities are used to calculate the "area inside the rubber band", A, and the equivalent rod radius r_o (refer to sect. 2.3.1.):

Diameter of fuel element (with cladding)	d = 1.522 cm
Maximum diameter of fuel bundle (including wire helices)	D = 8.169 cm
Spacing between elements (= thickness of wire)	e = 0.127 cm

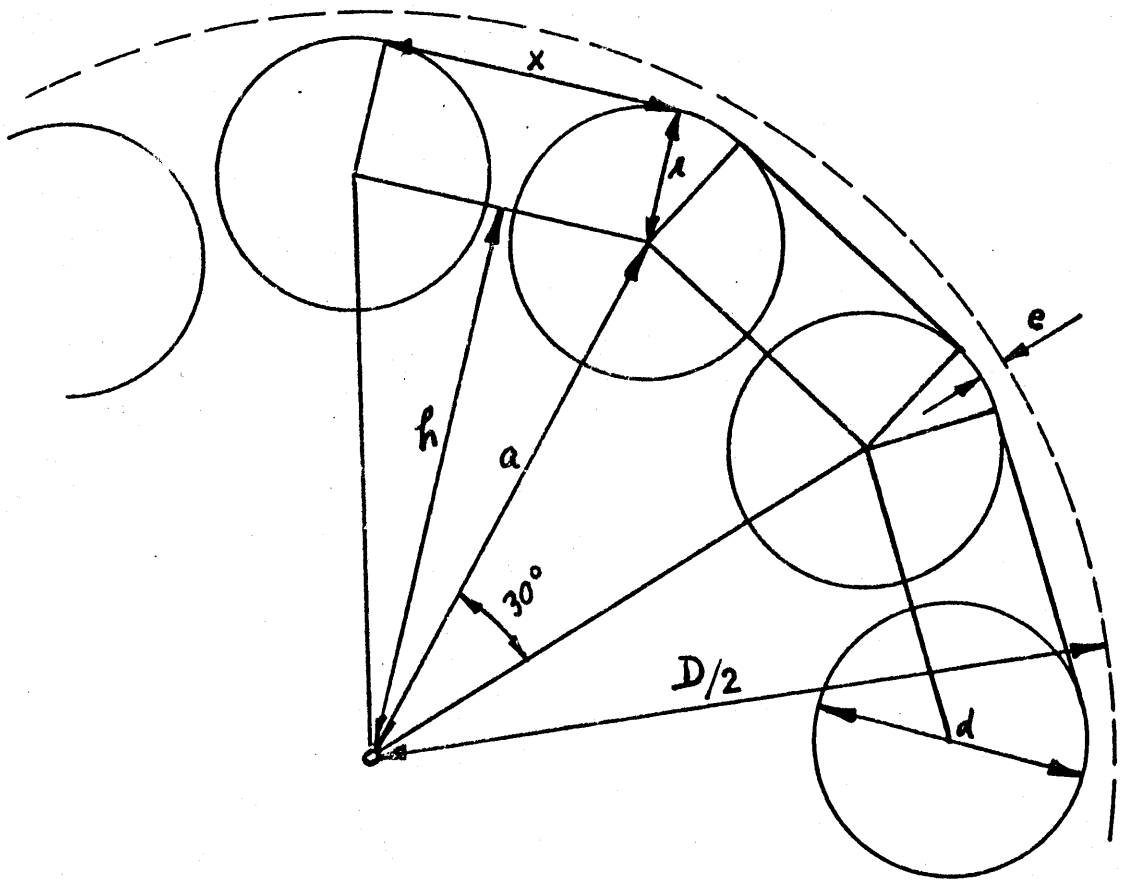

Fig.VIII.1., Geometry of the Fuel Element (19 rods)

It is seen from Fig.VIII.1. that the area A (inside the "rubber band") is given by

$$A = 6xh + 12xr + \pi r^2 \quad , \text{ or}$$

$$A = 3a^2 + 12\sqrt{2-\sqrt{3}}\, ra + \pi r^2$$

where the quantities x, h, r, and a are defined in Fig. VIII.1.

Since a = (D-d-2e)/2, and r = d/2, this last expression is easily evaluated in terms of d, D, and e. The result is:

$$A = 47.58 \text{ cm}^2$$

The equivalent rod radius is then given by

$$r_o = \sqrt{A/\pi} = 3.89 \text{ cm}$$

8.2.3. Fuel Density

The theoretical densities of UO_2 and ThO_2 are 10.96 and 9.69 gm/cm^3, respectively. The density of UO_2 in the CANDU reactor is given in (A1) as:

$$ROUO2 = 10.55 \text{ gm/cm}^3$$

which represents 96.25 % of theoretical density. The density of ThO_2 was then calculated by assuming it to be the same fraction of the theoretical density, i.e.,

$$ROTHO2 = 9.69 \times 0.9625 = 9.33 \text{ gm/cm}^3$$

8.3. Appendix 3: Calculation of $\mathcal{E}$

First, we divide the unit cell into two regions, one being inside, and the other outside the "rubber band" (Fig.II.9.). We obtain the following volumes per unit length of unit cell (see also Appendix 2.):

Inside	
Fuel	29.63 cm^3/cm
Cladding	3.90 cm^3/cm
Gap (between fuel and cladding)	0.74 cm^3/cm
Coolant	13.31 cm^3/cm
Total "inside"	47.58 cm^3/cm

Outside	
Coolant	6.10 cm^3/cm
Pressure tube	11.15 cm^3/cm
Calandria tube	4.35 cm^3/cm
Gap (between pressure tube and cal. tube)	26.26 cm^3/cm
Moderator	$(\frac{29.63}{VFL} - 95.44)$ cm^3/cm
Total "outside"	$(\frac{29.63}{VFL} - 47.58)$ cm^3/cm

Next, the homogenized macroscopic cross sections of the "fuel rod" (Eq. 2.3.10.) are evaluated for both UO_2 and

ThO_2 fuel:

Total cross section

Nuclide	N atoms per barn-cm	V cm^3/cm	σ_t barns	$NV\sigma_t$(U)	$NV\sigma_t$(Th)
U in UO_2	0.02355	29.63	4.3	3.00	
O in UO_2	0.04710	29.63	3.75	5.24	
Th in ThO_2	0.02129	29.63	4.736		2.99
O in ThO_2	0.04258	29.63	3.75		4.73
D in D_2O	0.0508	13.31	3.40	2.30	2.30
O in D_2O	0.0254	13.31	3.75	1.27	1.27
Zr	0.0429	3.90	6.20	1.04	1.04
Total				12.85	12.33

Fission cross section

Nuclide	σ_f barns	$NV\sigma_f$(U)	$NV\sigma_f$(Th)
U	0.30	0.210	
Th	0.076		0.0480
Total		0.210	0.0480

Elastic scattering cross section

Nuclide	σ_e barns	$NV\sigma_e(U)$	$NV\sigma_e(Th)$
U in UO_2	1.5	1.05	
O in UO_2	3.75	5.24	
Th in ThO_2	2.0		1.26
O in ThO_2	3.75		4.73
D in D_2O	- *)	- *)	- *)
O in D_2O	3.75	1.27	1.27
Zr	6.20	1.04	1.04
Total		8.60	8.30

Radiative capture cross section

Nuclide	σ_r barns	$NV\sigma_r(U)$	$NV\sigma_r(Th)$
U	0.04	0.0280	
Th	0.06		0.0378
Total		0.0280	0.0378

The collision probability P (Eq. 2.3.10.) is a function of $r_o\Sigma_t$. r_o is the equivalent rod radius (Appendix 2.),

*) refer to section 2.3.2.

and Σ_t is the total macroscopic (fast) cross section:

$$r_o \Sigma_t(U) = \frac{12.85 \times 3.89}{47.58} = 1.050 , \qquad P(U) = 0.6061$$

$$r_o \Sigma_t(Th) = \frac{12.33 \times 3.89}{47.58} = 0.969 , \qquad P(Th) = 0.5842$$

where the P's are taken from (K1).

Finally, with $\nu_f(U) = 2.55$, and $\nu_f(Th) = 2.4$, ε can be evaluated from Eq.(2.3.10.). The result is

$$\varepsilon\ (U) = 1.0247$$

$$\varepsilon\ (Th) = 1.0023$$

All cross sections used in this Appendix were taken from references (E1) and (T1).

8.4. Appendix 4: List of Subroutines

The following is a list of the 19 subroutines (including the MAIN program) used in the code:

Name of Subroutine	Explanation
AVGCS	sect. 2.12., step (23)
CONCH	sect. 2.12., step (21)
CONST	sect. 2.12., step (4)
CSF2	performs the integration in the numerator of Eq. (2.2.5). CSF2 is called by AVGCS.
FLF2	performs the integration in the denominator of Eq. (2.2.5). FLF2 is called by AVGCS.
GUESS	sect. 2.12., step (13)
HALT	program stop. HALT is called by WILK2 if there is no convergence in the numerical solution of the Wilkins equation, and by SPACFX if there is no convergence in the flux shape.
INOUT	sect. 2.12., step (43)
MAIN	main program, sect. 2.12.
NUPROP	sect. 2.12., step (11)
PRINIJ	prints out any two-dimensional array of numbers. Maximum array size 24 x 20.

List of Subroutines (continued):

Name of Subroutine	Explanation
PTCS	sect. 2.12., step (3)
RESPRB	calculates resonance escape probabilities from Eq. (2.4.1). RESPRB is called by CONCH.
SPACFX	sect. 2.12., step (26)
SPACON	sect. 2.12., step (14)
SPFUN	sect. 2.12., step (25)
SPFUN2	sect. 2.12., step (27)
TIMECK	prints out the time. TIMECK is called by MAIN.
WILK2	solves the Wilkins equation by a fifth order Milne method, described in (S1). WILK2 is called by AVGCS.

All subroutines mentioned in sect. 2.12. are called by the MAIN program.

8.5. Appendix 5: Operational Information

The entire code is written in FORTRAN for an IBM 7090/ 7094 computer.

8.5.1. Input data

The input data are punched on fifteen data cards. The first fourteen cards contain the floating point numbers. They are read according to FORMAT (4E15.5). The last card contains the fixed point numbers. It is read by FORMAT (19I3).

The list below gives the order and units of the various input numbers. The last column represents a typical set of input data.

Card	Text Symbol	FORTRAN Symbol	Definition	Units	Example
1	R	CR	Core radius	cm	225.61
	BR	BR	Blanket radius	cm	255.00
	-	RR	Reflector radius	cm	299.70
	DELR	DELR	Radial extrapolation distance	cm	3.60
2	CH	CH	Core height	cm	500.40
	DELH	DELH	Axial extrapolation distance	cm	4.05
	V_{fl}	VFL	Fuel volume fraction	-	0.0567

Input data (continued)

Card	Text Symbol	FORTRAN Symbol	Definition	units	Example
2	PDNLM	PDNLM	Max. linear power	kw/cm	8.712
3	BURNUP	BURNUP	Avg. fuel burnup in core	MWD/tonne	10000
	THETAB	THETAB	Blanket discharge flux-time	n/kb	0.1
	ROTHO2	ROTHO2	Density of ThO_2	g/cm^3	9.33
	ROUO2	ROUO2	Density of UO_2	g/cm^3	10.55
4	-	F	SPACFX Extrapolation parameter	-	1.25
	-	TIDE	Max. number of SPACFX loops	-	200.0
	-	ERROR	Flux shape convergence criterion	-	0.01
	a	ADDPAR	Damping factor (SPFUN2)	-	0.6
5	-	PHI11	Max. flux (initial guess)	$n/cm^2 sec$	10^{14}
	ENA	ENA	Enrichment (initial guess)	-	0.020
	DCDE	DCDE	Criticality iteration parameter	-	8.00
	ANDEL	ANDEL	Convergence criterion for atom ratios	-	0.003

Input data (continued)

Card	Text Symbol	FORTRAN Symbol	Definition	Units	Example
6	ANIFRA(4)	ANIFRA(4)	Atom ratio U^{234}/U^{233} in feed (initial guess)	-	0.37
	ANIFRA(5)	ANIFRA(5)	Atom ratio U^{235}/U^{233} in feed (initial guess)	-	0.33
	ANIFRA(6)	ANIFRA(6)	Atom ratio U^{236}/U^{233} in feed (initial guess)	-	0.54
	ROSS	ROSS	Uranium recycle loss	-	0.02
7	-	CRDEL1	Criticality convergence criterion 1 (IC-loop)	-	0.005
	CRDEL2	CRDEL2	Criticality convergence criterion 2 (IZ-loop)	-	0.00005
	x_4	EXTRAP(4)	Extrapolation parameter for atom ratio A_4	-	0.50
	x_5	EXTRAP(5)	Extrapolation parameter for atom ratio A_5	-	0.25
8	x_6	EXTRAP(6)	Extrapolation parameter for atom ratio A_6	-	3.00
	VLD_1	VLD(1)	Relative fuel velocity, radial zone i=1	-	1.0
	VLD_2	VLD(2)	Rel. fuel vel., i=2	-	1.0
	VLD_3	VLD(3)	Rel. fuel vel., i=3	-	1.0

Input data (continued)

Card	Text Symbol	FORTRAN Symbol	Definition	Units	Example
9	VLD_4	VLD(4)	Rel. fuel velocity, i=4	-	1.0
	VLD_5	VLD(5)	" " " i=5	-	1.0
	VLD_6	VLD(6)	" " " i=6	-	1.0
	VLD_7	VLD(7)	" " " i=7	-	1.0

The fuel velocity distribution is continued in the same way on cards 10 through 13 (i= 8 through 23).

14	VLD_{24}	VLD(24)	Rel. fuel velocity, i=24	-	1.0

15	IRC	IRC	Number of radial mesh points in core (IRC $\leq$ IRB)	-	14
	IRB	IRB	Number of radial mesh points in core and blanket (IRB $\leq$ IRR)		16
	IRR	IRR	Total number of radial mesh points (core+blanket+reflector) (IRR $\leq$ 24)		19
	JZC	JZC	Number of axial mesh points (JZC $\leq$ 20)		16
	IL	IL	Number of points for solution of Wilkins equation. IL must be odd and less than 50.		49

Input data (continued)

Card	Text Symbol	FORTRAN Symbol	Definition	Units	Example
15	IPADEC	IPADEC	refer to sect. 2.12.	-	1
	IVELCO	IVELCO	refer to sect. 2.12.	-	1
	-	IPRT1	Print-out control parameter for subroutine SPFUN2	-	0
	-	IPRT2	" SPACFX	-	0
	-	IPRT3	" PTCS	-	1
	-	IPRT4	" AVGCS	-	0
	-	IPRT5	" SPFUN2	-	0
	-	IPRT6	" CONCH	-	0
	-	IPRT7	" SPACON	-	0
	-	IPRT8	" CONCH	-	0
	-	IPRT9	" SPFUN	-	0
	-	IPRT10	Unused parameter	-	0
	-	IPRT11	Unused parameter	-	0
	-	IPRT12	Print-out control parameter for MAIN	-	1

8.5.2. Machine and Time Requirements

The list below gives the number of storage locations required for each subroutine (not including COMMON storage):

Subroutine	Number of locations
AVGCS	426
CONCH	2570
CONST	152
CSF2	170
FLF2	98
GUESS	592
HALT	40
INOUT	988
MAIN	2828
NUPROP	490
PRINIJ	300
PTCS	649
RESPRB	300
SPACFX	548
SPACON	421
SPFUN	397
SPFUN2	567
TIMECK	40
WILK2	493
Total	12069

The number of COMMON storage locations used is not the same for all subroutines. SPFUN2 has the largest COMMON field. It uses 10213 COMMON locations. The total number of locations used by the program is therefore:

$$12069 + 10213 = \underline{22282}$$

A typical run takes approximately four minutes on the 7094 computer. The number of IZ-loops executed during this time is usually between 18 and 24.